Novel bioplastics and biocomposites from vegetable oils

by

Phillip H. Henna

A dissertation submitted to the graduate faculty

in partial fulfillment of the requirements for the degree of

DOCTOR OF PHILOSOPHY

Major: Organic Chemistry

Program of Study Committee:
Richard C. Larock, Major Professor
John Verkade
Surya Mallapragada
Yan Zhao
Klaus Schmidt-Rohr

Iowa State University

Ames, Iowa

2008

To Kristine and my parents for everything

TABLE OF CONTENTS

LIST OF ABBREVIATIONS

AIBN	2,2’ azobisisobutyronitrile
AN	acrylonitrile
BCO	bicyclic castor oil
C_{100}LIN	100 % conjugated linseed oil
COE	cyclooctene
DCPD	dicyclopentadiene
Dil	Dilulin
DMA	dynamic mechanical analysis
DVB	divinylbenzene
Hz	hertz
GF	glass fiber
NMR	nuclear magnetic resonance
SEM	scanning electron microscopy
TGA	thermogravimetric analysis
TLC	thin layer chromatography
T_g	glass transition temperature
T_{max}	temperature of maximum degradation
T_{10}	temperature of 10 % weight loss
T_{50}	temperature of 50 % weight loss
wt. %	weight percent
υ_e	crosslinking density
% insol	percent insoluble

% ε_b	percent elongation at break
% sol	percent soluble
E'	storage modulus
σ_{max}	tensile strength
E	Young's modulus

CHAPTER 1. GENERAL INTRODUCTION

Polymeric materials have been prevalent in our everyday lives for quite a long time. Most of today's polymeric materials are derived from nonrenewable petroleum-based feedstocks. Instabilities in the regions where petroleum is drilled, along with an increased demand in petroleum, have driven the price of crude oil to record high prices. This, in effect, increases the price of petroleum-based polymeric materials, which has caused a heightened awareness of renewable alternatives for polymeric feedstocks. Cellulose, starch, proteins and natural oils have all been examined as possible polymeric feedstocks.[1]

Natural oils are commercially available on a large scale and are relatively cheap. It is projected that the U.S. alone will produce 21 billion pounds of soybean oil in the period 2008/2009.[2] Natural oils also have the advantages of inherent biodegradability, low toxicity, high purity and ready availability. Most natural oils possess a triglyceride structure as shown in Figure 1. Most natural oils have a unique distribution of fatty acid side chains, along

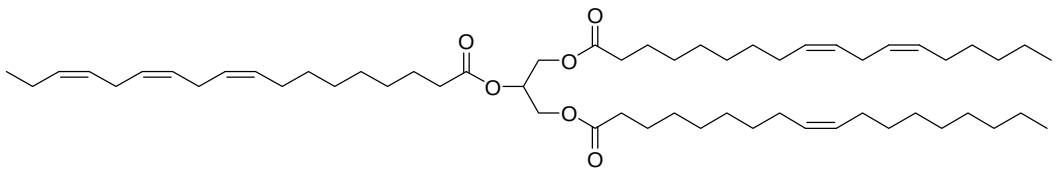

Figure 1. Molecular Structure of a Natural Oil

with varying degrees of unsaturation per triglyceride. Common fatty acid side chains in naturally occurring oils are palmitic acid (C16:0), a 16 carbon fatty acid with no unsaturation; stearic acid (C18:0), an 18 carbon fatty acid with no unsaturation; oleic acid

(C18:1), an 18 carbon fatty acid with one double bond; linoleic acid (C18:2), an 18 carbon fatty acid with two double bonds; and linolenic acid (C18:3), an 18 carbon fatty acid with three double bonds.[3] Of course, there are other fatty acids with varying degrees of unsaturation, but their abundance is usually minimal. All of the unsaturated fatty acids mentioned have naturally occurring cis double bonds, which is common for most unsaturated fatty acids.[4] In addition, the afore mentioned fatty acids have the first double bond at the position of carbon 9 (C9), followed by carbon 12 (C12), if there are two degrees of unsaturation, then at carbon 15 (C15), if there are three degrees of unsaturation. In addition, the double bonds are not in conjugation. Table 1 gives the fatty acid make-up of linseed oil.[5] It can be seen that linseed oil has an average of 6.0 double bonds per triglyceride. Its fatty acid content consists of 5.4% palmitic acid (C16:0), 3.5% stearic acid (C18:0), 19% oleic

Table 1. Fatty Acid Composition of Various Vegetable Oils

Oil	C=C Number	% Fatty Acids								
		C14:0	C16:0	C18:0	C18:1	C18:2	C18:3	C20:0	C20:1	Other
Olive	2.85	-	9.0	2.7	80.3	6.3	0.7	0.4	-	0.6
Peanut	3.37	0.1	11.1	2.4	46.7	32.0	-	1.3	1.6	4.8
Seasame	3.87	0.1	8.2	3.6	42.1	43.4	-	1.1	-	1.5
Canola	3.91	0.1	4.1	1.8	60.9	21.0	8.8	0.7	1.0	1.6
Corn	4.45	0.1	10.9	2.0	25.4	59.6	1.2	0.4	-	0.4
Soybean	4.61	0.1	10.6	4.0	23.3	53.7	7.6	0.3	-	0.4
Grapeseed	4.57	-	7.0	3.0	27.4	62.5	-	-	-	0.1
Sunflower	4.69	0.1	7.0	4.5	18.7	67.5	0.8	0.4	0.1	0.9
LoSatSoy	5.16	-	3.0	1.0	31.0	57.0	9.0	-	-	-
Safflower	5.06	0.1	6.8	2.3	12.0	77.7	0.4	0.3	0.1	0.3
Walnut	5.24	-	4.6	0.9	17.8	73.4	3.3	-	-	-
Linseed	6.24	0.2	5.4	3.5	19.0	24.0	47.0	0.6	-	0.3

acid (C18:1), 24 % linoleic acid (C18:2) and 47% linolenic (C18:3). Table 1 also gives the fatty acid composition and varying degrees of unsaturation for various other naturally-occurring natural vegetable oils.

The regions of unsaturation in natural oils allow for interesting polymer chemistry to take place. Some of this interesting polymer science, however, involves chemical modification of the regions of unsaturation. Acrylated epoxidized soybean oil (AESO) is prepared by epoxidation of the double bonds, followed by ring opening with acrylic acid. The resulting oil has both acrylate groups and hydroxyl groups. Wool and colleagues have further reacted the hydroxyl groups within the oil with maleic anhydride to produce maleated acrylated epoxidized soybean oil (MAESO).[6] The MAESO has been copolymerized with styrene free radically to produce promising thermosetting sheet molding resins. Petrović and co-workers have directly ring opened the epoxidized oil to produce polyols that produce promising polyurethanes through condensation polymerization with diisocyanates.[7]

Our group's work initially focused on direct cationic copolymerization of the double bonds or conjugated double bonds of natural oils with monomers, such as styrene and divinylbenzene, to produce promising thermosetting resins.[8] The only modification of the oils that was carried out in these studies was conjugation of the double bonds to enhance the reactivity of the oil. This work has been expanded recently with the incorporation of glass fiber to produce promising composites.[9] We have also explored thermal polymerization techniques to make novel thermosets.[10]

DISSERTATION ORGANIZATION

This dissertation is divided into four chapters. The first chapter discusses the synthesis and characterization of biobased thermosets prepared by the free radical

polymerization of conjugated linseed oil with commercially available monomers. The second chapter covers the synthesis and characterization of a chemically modified castor oil and its copolymerization with cyclooctene via ring opening metathesis polymerization (ROMP). The third chapter looks at the ROMP of a commercially available vegetable oil containing an unsaturated bicyclic moiety with dicyclopentadiene (DCPD) and characterization of the resulting materials. The fourth chapter discusses the reinforcement of a ROMP resin using short glass fibers to make composite materials.

REFERENCES

1. "*Natural Fibers, Biopolymers and Biocomposites*," Mohanty, A.K.; Misra, M.; Drzal, L.T., Eds. CRC Press, Boca Raton, 2005.
2. *World Agricultural Supply and Demand Estimate*, Office of the Chief Economist, United States Department of Agriculture, May 9, 2008.
3. Salunkhe, D.K., Chavan, J.K., Adsule, R.N., Kadam, S.S. "*World Oilseeds: Chemistry, Technology, and Utilization*", Van Nostrand Reinhold, New York 1992.
4. O'Brien, R.D. "*Fats and Oils: Formulating and Processing for Applications*", Technomic, Lancaster 1998.
5. Andjelkovic, D. D., Valverde, M.V., Henna, P.H., Li, F., Larock, R.C. *Polymer* **2005**, *46*, 9674-9685.
6. Lu, J., Khot, S., Wool, R.P. *Polymer* **2005**, *46*, 71-80.
7. Petrović, Z.S., Guo, A., Zhang, W. *J. Polym. Sci: Part A. Polym. Chem.* **2000**, *38*, 4062-4069.
8. [a] Li, F., Larock, R.C. *J. Appl. Polym. Sci.* **2001**, *80*, 658-670; [b] Li, F., Larock, R.C.

J. Appl. Polym. Sci. **2000**, *78*, 1044-1056; [c] Andjelkovic, D. D., Valverde, M.V., Henna, P.H. Li, F., Larock, R.C. *Polymer* **2005**, *46*, 9674-9685.

9. [a] Lu, Y., Larock, R.C. *J. Appl. Polym. Sci.* **2006**, *102*, 3345-3353; [b] Lu, Y., Larock, R.C. *Macromol. Mater. Eng.* **2007**, *292*, 1085-1094.

10. Li, F., Larock, R.C. *Biomacromolecules* **2003**, *4*, 1018-1025.

CHAPTER 2. BIOBASED THERMOSETS FROM FREE RADICAL COPOLYMERIZATION OF CONJUGATED LINSEED OIL

A Paper Published in Journal of Applied Polymer Science, 104, 979-985.

Phillip H. Henna, Dejan D. Andjelkovic, Petit P. Kundu, Richard C. Larock*

Department of Chemistry, Iowa State University, Ames, IA, 50011, USA

Abstract

New polymeric thermosets have been prepared from the bulk free radical copolymerization of 100% conjugated linseed oil (C_{100}LIN), acrylonitrile (AN), and divinylbenzene (DVB). Under the appropriate reaction conditions and curing sequence, 61-96 wt % of the oil is incorporated into the crosslinked thermoset. The resulting yellow transparent thermosets vary from being soft and flexible to hard and brittle. Dynamic mechanical analysis (DMA) and thermogravimetric analysis (TGA) show that these thermosets exhibit good mechanical properties and thermal stability.

Introduction

The widespread use of non-biodegradable, petroleum-based polymeric materials has raised many environmental concerns [1,2]. Demand for these nonrenewable, virtually indestructible materials is increasing, as is our dependence on crude oil. A possible remedy is to utilize natural, renewable resources as feedstocks for the preparation of plastics.

Recently, a shift in interest towards making polymeric materials prepared from readily available, renewable resources, such as cellulose [3], starch [4], proteins [5], and natural oils [6] has been seen. These biopolymers offer the advantages of low cost, ready availability from renewable natural resources, and possible biodegradability. For years, however, modified celluloses have found applications in the plastics industry [3,7]. Thus, the concept of utilizing renewable resources in plastics is not new.

Much of the work on polymeric materials derived from natural oils has involved functionalized oils. Wool et. al. and Hazer et. al. have respectively prepared a copolymer and a grafted copolymer from derivatives of soybean and linseed oils with styrene or methyl methacrylate by free radical polymerization [8,9]. Petrovic and co-workers have carried out the oxirane ring opening of epoxidized oils, followed by condensation polymerization with isocyanates to produce polyurethanes [10,11]. Our group has primarily focused on developing thermosetting resins from non-functionalized natural oils, such as soybean [12], corn [13], linseed [14], tung [15], fish [16] , and a number of other natural oils [17] via cationic, free radical, and thermal polymerizations [6,17].

Linseed oil is used widely as a drying oil for surface coatings [18]. It is a triglyceride oil composed of 4% stearic (C18:0), 19% oleic (C18:1), 15% linoleic (C18:2), and 57% linolenic (C18:3) acids with approximately 6 carbon-carbon double bonds per triglyceride [17]. The high content of linolenic acid double bonds per triglyceride makes linseed oil susceptible to free radical polymerization. Previously, our group reported the preparation of various thermosets from conjugated linseed oil, styrene, and divinylbenzene via thermal polymerization [14]. The resulting materials range from soft and rubbery materials to tough and rigid plastics.

We now wish to report that the free radical copolymerization of conjugated linseed oil (C_{100}LIN), acrylonitrile (AN), and divinylbenzene (DVB), using 2,2'-azobisisobutyronitrile (AIBN) as an initiator, produces transparent, yellow crosslinked thermosets, which range from slightly flexible to hard and brittle. These thermosets can be considered biobased, since they use as a comonomer, a natural, renewable oil.

Experimental

Materials. Regular linseed oil, provided by Archer Daniels Midland (Decatur, IL), was conjugated in our laboratory using a previously reported process [19]. The conjugation was determined to be approximately 100%. Acrylonitrile, divinylbenzene (Technical Grade – Assay 80% by GC; 20% ethylvinylbenzene), and AIBN were purchased from Aldrich Chemical Company and used as received.

Polymerization. The crosslinked polymers were prepared by bulk free radical copolymerization. The amounts of C_{100}LIN, AN, DVB, and AIBN reported are all weight percents. The ratio of AN to DVB was kept at 9:1 in all cases. The C_{100}LIN, AN, DVB, and AIBN are all weighed out and poured into a glass vial. Normally 3 gram samples were prepared. The amount of oil was varied from 30% to 75%. It was found early on that the most promising materials employed 40% to 60% oil; thus these materials were investigated most extensively. The initial oil composition was then varied in 5% increments. Enough headspace was provided between the top of the mixture and the cap of the vial to allow for any expansion or evolution of gases. The reactants were mixed thoroughly, until all of the AIBN had dissolved. Once the initiator and monomers were added, the system was cured for 12 h each at 60 ºC, 70 ºC, 80 ºC, 90 ºC, 110 ºC, and 120 ºC. This lengthy sequence was employed to minimize shrinking and cracking. After completion of the curing sequence, the

vials were broken to remove the samples. The following system of nomenclature has been adopted for simplicity; C_{100}LIN50-AN45-DVB5-AIBN1 corresponds to a polymer sample prepared from 50 wt % C_{100}LIN, 45 wt % AN, 5 wt % DVB, and 1 wt % AIBN.

Soxhlet extraction analysis. A 2 g sample of the bulk polymer was extracted for 24 h with 100 mL of refluxing methylene chloride using a Soxhlet extractor. After the extraction was complete, the resulting solution was concentrated on a rotary evaporator with subsequent vacuum drying. The soluble substances were weighed and analyzed by ^{1}H NMR spectroscopy. The insoluble materials were dried in a vacuum oven for several hours before weighing.

Characterizations. ^{1}H NMR spectroscopic analysis of the soluble substances was carried out in $CDCl_3$ using a Varian Unity spectrometer (Varian Associates, Palo Alto, CA) at 300 MHz. Cross-polarization magic angle spinning (CP MAS) ^{13}C NMR analysis of the insoluble materials remaining after Soxhlet extraction of the bulk polymers was performed using a Bruker MSL 300 spectrometer. Samples were examined at two spinning frequencies (3.2 and 3.7 kHz) in order to differentiate between actual signals and spinning side bands.

GPC analysis of the soluble materials was carried out using a Waters Breeze GPC system with a Waters 1515 pump, Waters 717-plus auto-sampler, and a Waters 2414 RI-detector using polystyrene standards for molecular weight calibration. Each sample was dissolved in THF (~2 mg/mL) and passed through a Teflon 0.2 mm filter into the sample vial. The mobile phase selected was HPLC-grade THF with a flow rate of 1 mL/min and a sample injection volume of 200 μL. The instrument was equipped with two columns (PL-Gel Mixed C 5 μm, Polymer Lab., Inc.) and heated at 40 ºC.

The dynamic mechanical properties of the bulk polymers were obtained using a Perkin-Elmer DMA Pyris-7e dynamic mechanical analyzer (Perkin-Elmer, Foster City, CA) in a three-point bending mode. The rectangular specimens made from the thermosets had dimensions of approximately 12 mm x 5 mm x 2 mm. The specimens were first cooled to -40 ºC, then heated to 200 ºC at a rate of 3 ºC/min and a frequency of 1 Hz under helium. The viscoelastic properties, namely the storage modulus E' and mechanical loss factor (damping) tan δ, were recorded as a function of temperature. Glass transition temperatures for the polymers were obtained from the peaks of the loss factor tan δ curves. Themogravimetric analysis was performed using a Perkin Elmer TGA Pyris-7 (Perkin-Elmer, Foster City, CA). Specimens having masses of approximately 10 to 15 mg were used. A temperature scan from 50 ºC to 650 ºC was performed at a heating rate of 20 ºC/min under air.

Results and Discussion

^{1}H NMR spectroscopic analysis of the oils. Figure 1 shows the ^{1}H NMR spectra of both the regular and conjugated linseed oils. The peaks from 4.1 to 4.4 ppm correspond to the four hydrogens of the methylene groups present in the glycerol moiety of the triglyceride. The peak at 2.8 ppm is observed in the spectrum of the regular linseed oil and corresponds to the methylene hydrogens between the carbon-carbon double bonds, also known as the bisallylic protons. This peak disappears upon conjugation as seen in the spectrum of the C_{100}LIN.

The conjugation is also evident in the wider range of chemical shifts for the vinylic protons (5.2-6.6 ppm) in the conjugated oil versus 5.2-5.4 ppm for the regular linseed oil. Both the regular and conjugated linseed oils are calculated by ^{1}H NMR spectroscopic analysis to have approximately 5.7 carbon-carbon double bonds per triglyceride. This degree

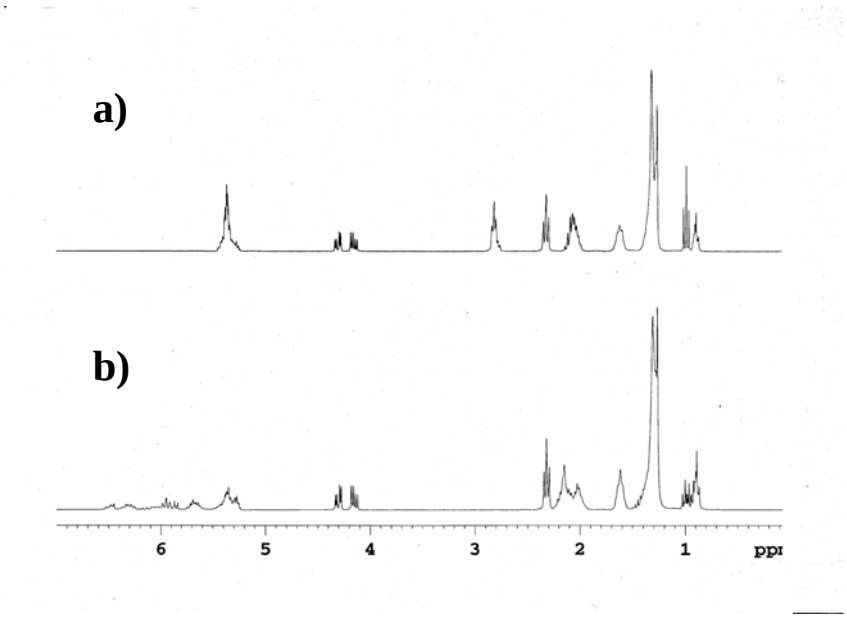

Figure 1. a) ^{1}H NMR spectra of regular linseed oil and b) 100% conjugated linseed oil.

of unsaturation is calculated by using the following equation:

$$d = (4A - B)/2B$$

where A is the integrated area of the peaks above 5.20 ppm (including the C-2 hydrogen atom of the glycerol moiety) and B is the integrated area of the peaks at 4.10-4.40 ppm [17].

By conjugating the carbon-carbon double bonds in the triglyceride side chains of natural oils, like linseed oil, their reactivity can be significantly improved [20]. It is important to note that conjugation does not change the number of carbon-carbon double bonds present in the triglyceride structure. However, the double bonds that are moved undergo a change in structure from cis to trans [21]. The percent conjugation, determined by integrating the vinylic hydrogens in the conjugated oil and taking into account the known

fatty acid composition of the oil, is approximately 100% [21]. The degree of conjugation can also be roughly estimated by identifying the absence of the bisallylic proton peak at 2.8 ppm.

Analysis of the conjugated oil in the thermosets. The polymers produced are thermosets due to crosslinking between the various carbon-carbon double bonds present in the linseed oil and divinylbenzene. They range from hard and rigid to soft and flexible materials. They are transparent, yellow, and have a slight odor. Shrinking and cracking occurred with some of the samples containing 40 and 45 wt % oil in the feed ratio. The microstructures of the bulk polymers have been investigated through Soxhlet extraction using methylene chloride as the refluxing solvent. The extracted soluble portion is an oily substance ranging from 4 to 39 wt % (Table 1).

The ^{1}H NMR spectra (Figure 2) of the soluble portions indicate that the oily substance is primarily unreacted oil. However, oligomers or low molecular weight components of polyacrylonitrile may also be present. They would probably appear in the same region as the saturated hydrogens of the oil. The weak peaks in the vinylic region (5.2-6.5 ppm) indicate that the extracted oils are more saturated than the original oil. The samples prepared using 40% to 60% oil, range from hard and rigid to soft and flexible. The increasing amounts of unreacted oil seen with the systems having the greater oil content appear to act as a plasticizer causing the change in properties.

Further elucidation of the extracts, carried out by gel permeation chromatography (GPC), indicates the presence of three components of varying molecular weights (MW) (Figure 3).

Table 1. Properties of Various Thermosets

Sample Composition	% Soluble[a]	% Insoluble[b]	T_g (°C)
C_{100}LIN40-AN54-DVB6-AIBN1	**4**	**96**	**101**
C_{100}LIN45-AN49.5-DVB5.5-AIBN1	**4**	**96**	**93**
C_{100}LIN50-AN45-DVB5-AIBN1	**8**	**92**	**80**
C_{100}LIN55-AN40.5-DVB4.5-AIBN1	**20**	**80**	**72**
C_{100}LIN60-AN36-DVB4-AIBN1	**39**	**61**	**60**

[a] % Soluble represents any component or material extracted from the crosslinked thermoset.
[b] % Insoluble is the crosslinked thermoset that remains behind after extraction.

Table 1. Continued

Sample Composition	v_e[c] (mol/m^3)	Storage Modulus 25 °C (Pa)	T_{max}[d] (°C)
C_{100}LIN40-AN54-DVB6-AIBN1	**6879**	**1.62×10^9**	**432**
C_{100}LIN45-AN49.5-DVB5.5-AIBN1	**4910**	**1.07×10^9**	**435**
C_{100}LIN50-AN45-DVB5-AIBN1	**3429**	**7.15×10^8**	**456**
C_{100}LIN55-AN40.5-DVB4.5-AIBN1	**3128**	**4.28×10^8**	**464**
C_{100}LIN60-AN36-DVB4-AIBN1	**1549**	**1.60×10^8**	**476**

[c] Crosslinking densities obtained from the equation $E' = 3\nu_e RT$ using the storage modulus values at 40 °C above the glass transition temperature.[d] Temperature of maximum degradation.

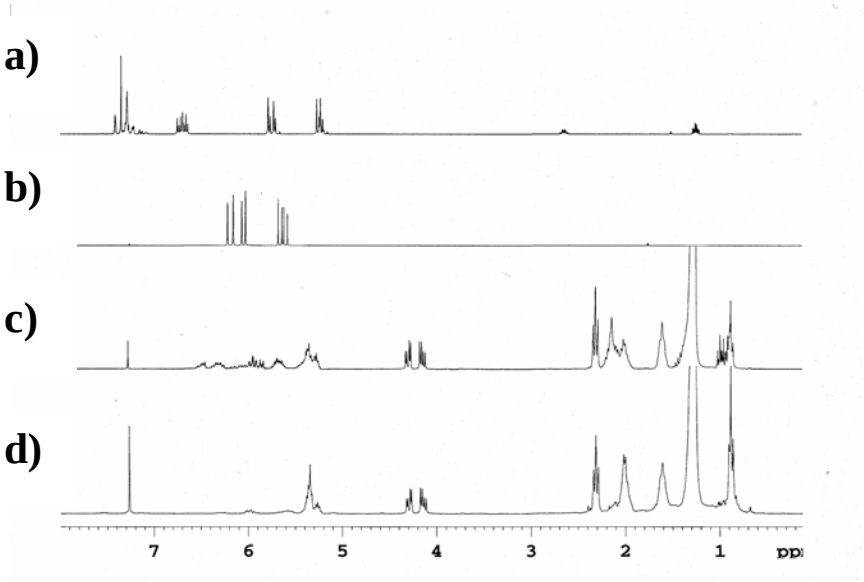

Figure 2. ^{1}H NMR spectra of a) DVB, b) AN, c) C_{100}LIN , and d) the soluble portion of C_{100}LIN50-AN45-DVB5-AIBN1.

Thus, peaks A, B, and C correspond to molecular weights of approximately 380, 1300, and 2600 g/mol, respectively. Analysis of C_{100}LIN indicates that peak B corresponds to the molecular weight of the triglyceride. However, the actual molecular weight of linseed oil is around 880 g/mol. Differences in hydrodynamic volume between the polystyrene standards used for calibration and the oil are responsible for the discrepancy [22]. Peak C appears to correspond to a dimer of the triglyceride, while peak A is some lower molecular weight component, perhaps oligomers of polyacrylonitrile, since the peak height is proportional to the concentration of AN monomer in the original composition.

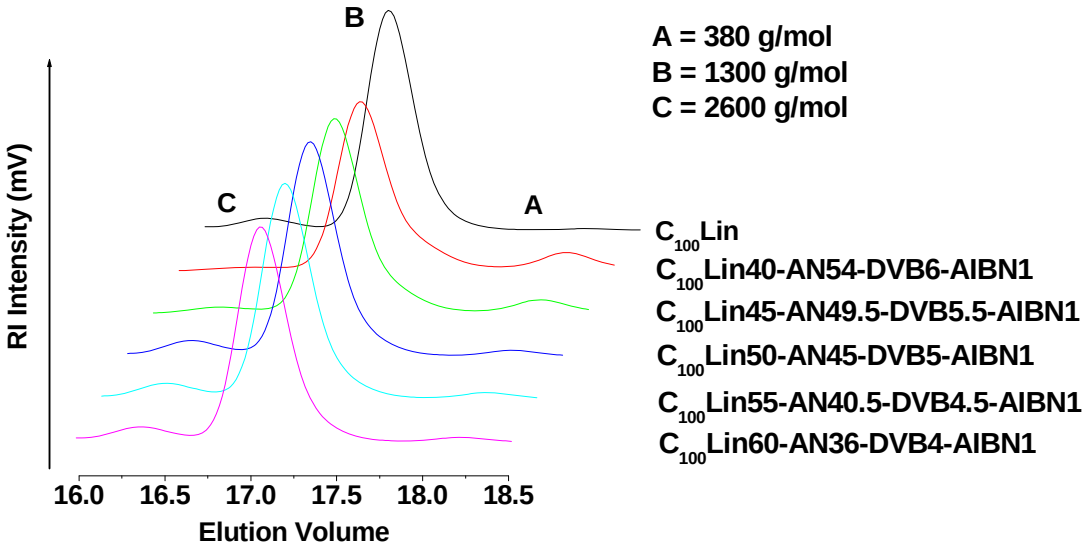

Figure 3. GPC analysis of the soluble extracts

The insoluble crosslinked substances remaining after extraction correspond to 61 to 96% of the original thermoset material (Table 1). These samples are highly crosslinked and are insoluble in THF and CH_2Cl_2. The absence of DVB peaks in the ^1H NMR spectrum of the soluble components (Figure 2) indicates that the DVB crosslinker has been completely incorporated into the crosslinked network. As the amount of DVB is increased in the original composition, an increase in the yield of crosslinked polymer is also seen. This is also consistent with the extraction results mentioned above (Table 1).

Solid state ^{13}C NMR analysis was carried out on the insoluble crosslinked materials. Figure 4 shows the presence of the triglyceride carbonyl (C=O) at 170 ppm. Carbon-carbon double bonds (C=C) from either the oil or the DVB are seen at approximately 135 ppm. The cyano group (CN) carbon associated with the acrylonitrile is buried under the carbon-carbon double bond signals around 135-140 ppm. The aromatic signal associated with the DVB is

also buried under the carbon-carbon double bond signals. Thus, it can be concluded from both the ^{1}H and solid state ^{13}C NMR that the bulk polymer structure is a crosslinked polymer network retaining free (unreacted) oil that is more saturated than the oil employed in the feed. The more saturated free oil may be due to either triglyceride molecules that are dimerized as

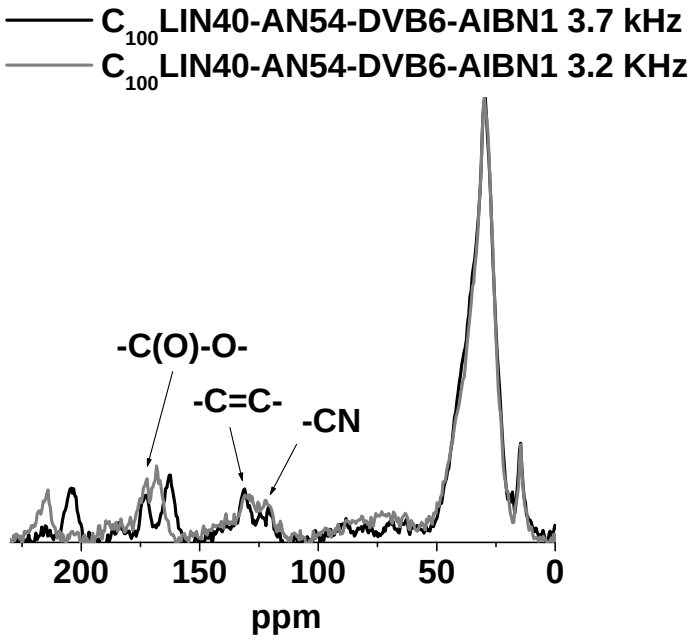

Figure 4. Solid state ^{13}C NMR spectra of the insoluble portion after extraction of C_{100}LIN40-AN54-DVB6-AIBN1

evidenced by GPC analysis and/or triglyceride molecules that are more highly saturated and cannot therefore be incorporated into the thermoset as easily.

Dynamic mechanical analysis. The dynamic mechanical analysis (DMA) results in Figure 5 show the temperature dependence of the loss factor tan δ for the various compositions investigated. All of the compositions give a single tan δ peak indicating that the C_{100}LIN-

AN-DVB systems possess a single homogeneous phase at the molecular level. This tan δ peak is a primary relaxation peak, which corresponds to the glass transition (T_g), and is a result of the micro-Brownian motion of the amorphous chains of the thermoset [23]. The data in Figure 5 and Table 1 indicate that as the amount of oil in the original composition increases, along with an increase in the amount of unreacted oil in the thermoset, the T_g values decrease from about 101 ºC to 60 ºC. As mentioned earlier, the unreacted oil can act as a plasticizer, allowing more flexibility between the chains, which results in the material having lower T_g values.

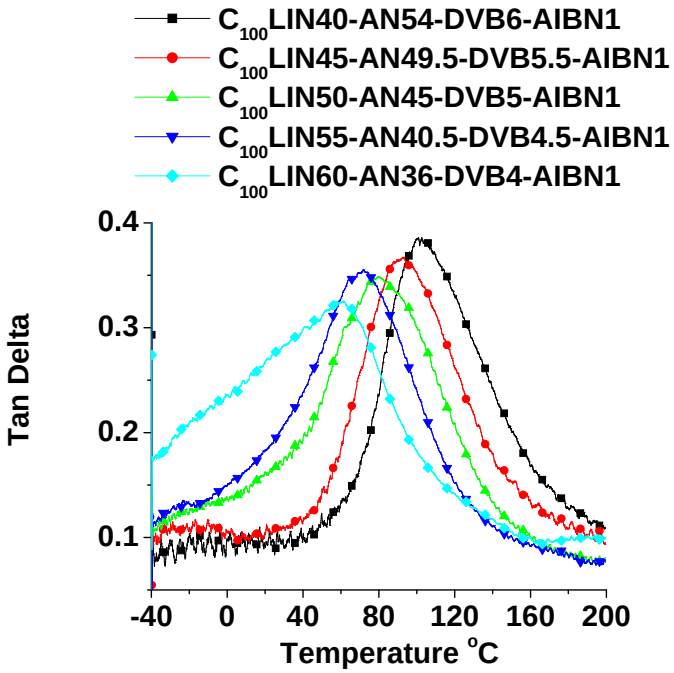

Figure 5. Tan delta graphs obtained by dynamic mechanical analysis for non-extracted samples

DMA analysis also shows how the crosslinking density plays a role in the T_g. The experimental crosslinking density has been calculated according to the kinetic rubber theory of elasticity [24,25] using the following equation:

$$E' = 3\upsilon_e RT$$

where E' is the storage modulus at T_g + 40 ºC in the rubbery plateau, υ_e is the crosslinking density, R is the gas constant, and T is the absolute temperature in Kelvin. The data in Table I indicate that as the amount of DVB is decreased, the crosslinking density also decreases. This decline in T_g is seen because less crosslinking results in greater segmental mobility when compared to systems with higher crosslinking. This means lower temperatures are needed for initiation of the segmental motion of the polymer chains.

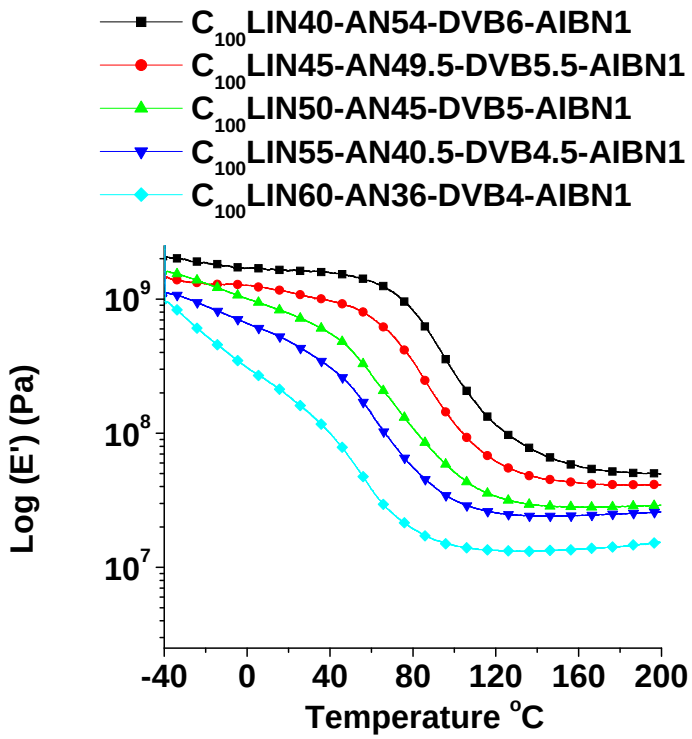

Figure 6. Storage modulus from dynamic mechanical analysis for non-extracted samples

The storage modulus E' of the different compositions plotted against temperature is shown in Figure 6; the room temperature values are given in Table 1. The table shows that increasing the amount of oil from 40% oil in the original composition (C_{100}LIN40-AN54-DVB6-AIBN1) to 60% oil (C_{100}LIN60-AN36-DVB4-AIBN1) results in a decrease in the storage modulus. Since the storage modulus is the ability of a material to return or recover from an applied force [26], the data correlates nicely with the samples possessing higher DVB content and crosslinking densities (those with 40% and 45% oil in the original composition) having higher storage modulus values than the samples with less DVB and lower crosslinking densities [27].

Thermogravimetric analysis. The thermogravimetric analysis (TGA) data is shown in Figure 7 and Table I. The thermal decomposition of these materials can be divided into three

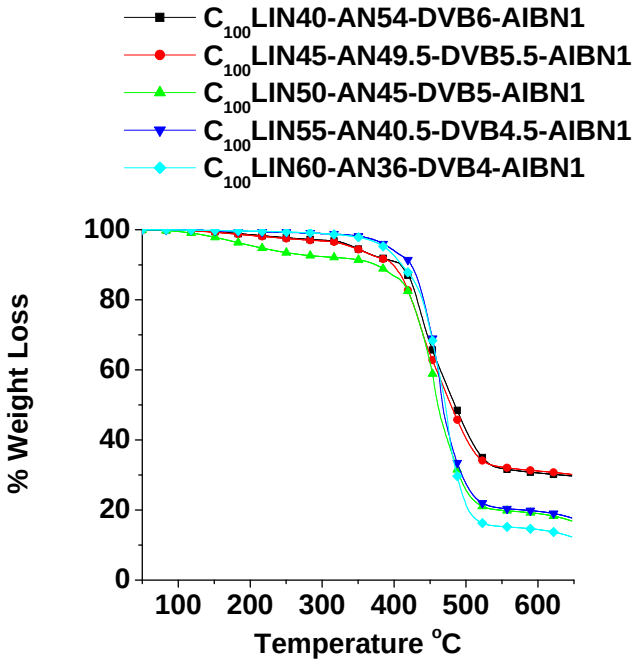

Figure 7. Percent weight loss of samples obtained by thermogravimetric analysis

stages. The first stage is from 50 ºC to 400 ºC and corresponds to degradation of the soluble components (*i.e*. oil) in the thermoset. The second stage from 400 ºC to 525 ºC represents decomposition of the bulk crosslinked thermoset. This region is where the maximum degradation of the material occurs. The third stage from 525 ºC to 650 ºC corresponds to oxidation of the char.

The temperature of maximum degradation (T_{max}) (Table I) in the second stage increases as the oil content goes from 40% oil in the feed ratio to 60%. This is interesting, since the samples with more oil in the feed composition have lower crosslinking densities than those with less oil in the feed composition. This trend is opposite to that seen with the cationic polymerizations of natural oils carried out in our group previously [28]. However, the samples C_{100}LIN55-AN40.5-DVB4.5-AIBN1 and C_{100}LIN60-AN36-DVB4-AIBN1 may have so much unreacted oil (Table 1) that all of it may not degrade in the first stage of the thermal degradation. This means that the unreacted oil, which still has unsaturation as evidenced by the ^{1}H NMR spectrum of the soluble materials, might undergo further curing during thermogravimetric analysis, resulting in enhanced thermal stability.

Conclusions

The free radical polymerization of 100% conjugated linseed oil, AN, and DVB initiated by AIBN gives thermosets that are transparent and yellow, and range from hard and brittle to soft and rubbery. Extraction analysis reveals that not all of the oil is incorporated into the thermoset. Dynamic mechanical analysis (DMA) shows that the unreacted oil and the crosslinking density affect the glass transition temperature and storage modulus. From thermogravimetric analysis (TGA) it can be seen that these samples are thermally stable up to 150 ºC, and that the bulk thermoset does not degrade until temperatures that slightly exceed

400 ºC. The range of properties attained with these materials makes them suitable for applications where petroleum-based polymers are currently used. Even though these thermosets contain monomers obtained from petroleum, they represent a significant step towards a more biobased plastic.

Acknowledgments

The authors gratefully acknowledge Archer Daniels Midland, the Illinois-Missouri Biotechnology Alliance, and the USDA for their financial support. We would like to thank Dr. Paul Bloom from Archer Daniels Midland for the donation of linseed oil, and Dr. Fumikiko Kondo from Kawaken Fine Chemicals for the rhodium(III) chloride used to conjugate the linseed oil. Finally, we thank Dr. Surya Mallapragada from the Department of Chemical Engineering, Dr. Vladimir Tsukruk from the Materials Science and Engineering Department, and Dr. Jay-lin Jane from the Department of Food Science and Human Nutrition at Iowa State University for the use of their facilities.

References

1. Bisio, A.L.; Xanthos, M.; How to manage plastics wastes: Technology and market opportunities; Hanser Publishers: New York, 1995.
2. Mustafa, M.; Plastics waste management: Disposal, recycling, reuse; Marcel Dekker: New York, 1993.
3. Toriz, G.; Gatenholm, P.; Seiler, B.D.; Tindall, D. In Natural fibers, biopolymers and biocomposites. Mohanty, A.K.; Misra, M.; Drzal, L.T., Eds.; CRC Press: Boca Raton, 2005, Chap.19.

4. Chiou, B.; Glenn, G.M.; Imam, S.H.; Inglesby, M.K.; Wood, D.F.; Orts,W.J. In Natural fibers, biopolymers and biocomposites, Mohanty, A.K.; Misra, M.; Drzal, L.T., Eds.; : CRC Press; Boca Raton, 2005, Chap. 20.
5. Zhang, J.; Jiang, L.; Zhu, L.; Jane, J.; Mungara, P. Biomacromolecules 2006, 7, 1551.
6. Li, F.; Larock, R.C. In Natural fibers, biopolymers and biocomposites. Mohanty, A.K.; Misra, M.; Drzal, L.T., Eds.; CRC Press: Boca Raton, 2005, Chap. 23.
7. Mohanty, A.K.; Misra, M.; Drzal, L.T.; Selke, S.E.; Harte, B.R.; Hinrichsen, G. In Natural fibers, biopolymers and biocomposites. Mohanty, A.K.; Misra, M.; Drzal, L.T., Eds.; CRC Press: Boca Raton, 2005, Chap. 1.
8. Can, E.; Kusefoglu, S.; Wool, R.P. J Appl Polym Sci 2001, 81, 69.
9. Cakmakli, B.; Hazer, B.; Tekin, I.O.; Kizgut, S.; Kosal, M.; Menceloglu, Y. Macromol Biosci 2004, 4, 649.
10. Petrovic, Z.S.; Guo, A.; Zhang, W. J Polym Sci, Part A: Polym Chem 2000, 38, 4062.
11. Petrovic, Z.S.; Zhang, W.; Zlatanic, A.; Lava, C.C.; Ilavskyy, M. J Polym Environ 2002, 10, 5.
12. Andjelkovic, D.D.; Li, F.; Larock, R.C. In Feedstocks for the future: Renewables for the production of chemicals and materials. Bozell, J.J.; Patel, M.K., Eds.; American Chemical Society Symposium Series: Washington DC, 2006, Chap. 6.
13. Li, F.; Hasjim, J.; Larock, R.C. J Appl Polym Sci 2003, 90, 1830.
14. Kundu, P.P.; Larock, R.C. Biomacromolecules 2005, 6, 797.
15. Li, F.; Larock, R.C. Biomacromolecules 2003, 4, 1018.
16. Li, F.; Marks, D.W.; Larock, R.C.; Otaigbe, J.U. Polymer 2000, 41, 7925.

17. Andjelkovic, D.D.; Valverde, M.; Henna, P.; Li, F.; Larock, R.C. Polymer 2005, 46, 9674.

18. Salunkhe, D.K.; Chavan, J.K.; Adsule, R.N.; Kadam, S.S. World oilseeds: Chemistry, technology and Utilization; Van Nostrand Reinhold: New York, 1991.

19. Larock, R.C.; Dong, X,; Chung, S.; Reddy, C.; Ehlers, L.E. J Am Oil Chem Soc 2001, 78, 447.

20. Marc, L.G. Organic chemistry; Addison-Wesley: Reading, MA, 1984.

21. Andjelkovic, D.D.; Min. B.; Ahn, D.; Larock, R.C. J. Agric Food Chem 2006, 54, 9535.

22. Andjelkovic, D.D.; Larock, R.C. Biomacromolecules 2006, 7, 927.

23. Murayama, T. Dynamic mechanical analysis of polymeric materials; Elsevier: Amsterdam, 1978.

24. Flory, P.J. Principles of polymer chemistry; Cornell University Press: Ithaca, NY, 1953.

25. Ward, I.M. Mechanical properties of solid polymers; Wiley Interscience: London, 1971.

26. Menard, K.P. Dynamic mechanical analysis: A practical introduction; CRC Press: Boca Raton, 1999.

27. Li, F.; Larock, R.C. J Polym Sci Part B: Polym Phys 2000, 38, 2721.

28. Li, F.; Larock, R.C.. J Appl Polym Sci 2001, 80, 658.

CHAPTER 3. RUBBERY THERMOSETS BY THE RING OPENING METATHESIS POLYMERIZATION OF A FUNCTIONALIZED CASTOR OIL

A paper published in Macromolecular Materials and Engineering, 2007, 292, 1201-1209.

Phillip H. Henna and Richard C. Larock

Department of Chemistry, *Iowa State University*, *Ames*, *IA*, *50011*, *USA*

Abstract

Rubbery thermosets prepared by the ring opening metathesis polymerization (ROMP) of a modified castor oil, containing norbornene moieties, and cyclooctene have been synthesized and characterized. The thermosets range from 55 to 85 wt.-% oil and are flexible, slightly transparent, and have a sand-like hue. Extraction analysis shows that increasing the concentration of the modified castor oil in the feed ratio results in an increase in the extracted (unreacted or oligomeric) components in the final thermoset. All of the specimens have glass transition temperatures near or below 0 ºC and have tan delta values above 0.3, making some of them candidates for damping materials. Thermogravimetric analysis reveals that all of the specimens have temperatures of maximum degradation (T_{max}) around 500 ºC. DMA and TGA analysis on solvent-extracted specimens show that the presence of the soluble fractions helps to plasticize the materials and give added thermal stability.

Introduction

Recent instabilities in the price of crude petroleum have caused many to look for renewable alternatives.[1] The production of ethanol from cellulosic sources is one area

receiving much attention.[2] However, another fast growing research field is the use of renewable resources, such as cellulose, proteins, and vegetable oils to produce polymeric materials suitable as replacements for petroleum-based plastics.[3]

The use of vegetable oils as renewable feedstocks for the chemical industry offers a wide array of possibilities and applications.[4] In recent years, vegetable oils have been used as co-monomers to produce a wide range of polymeric materials. Our group has focused mainly on the cationic,[5] free radical,[6] and thermal polymerization[7] of regular and conjugated oils. Other groups have focused on functionalizing oils, which are then polymerized either free radically[8] or through condensation polymerization.[9]

Ring opening metathesis polymerization (ROMP) generates polymers from strained cycloalkenes through carbon-carbon double bond cleavage and subsequent reconnection of the vinylic carbons.[10] The ROMP of a wide variety of cyclic monomers has been reported.[11] Triglyceride oils have also been shown to undergo olefin metathesis with alkenes to produce various polymeric materials.[12] Olefin cometathesis allows for two different sets of carbon-carbon double bonds to be cleaved and the olefinic fragments then connected to each other. However, to our knowledge there have been no reports on the ROMP of triglyceride oils functionalized with strained unsaturated ring systems. In this work, a series of new polymeric materials have been prepared from a functionalized castor oil and cyclooctene by ROMP, and their structure/property relationships and thermal/mechanical properties have been determined by NMR spectroscopy, thermogravimetric analysis (TGA), and dynamic mechanical analysis (DMA).

Experimental

Materials. Castor oil, Grubbs catalyst (second generation), triethylamine (99%) and potassium bromide (FT-IR grade, ≥ 99%) were obtained from Aldrich Chemical Company (Milwaukee, WI) and used without further purification. Bicyclo[2.2.1]hept-5-ene-2,3-dicarboxylic anhydride (> 95%) was obtained from Fluka (St. Gallen, Switzerland) and used as received. Cyclooctene (95%) (COE) was obtained from Acros (Geel, Belgium) and used as received. Toluene (ACS certified) and methylene chloride (ACS certified, stabilized with amylene) were both obtained from Fisher (Fair Lawn, NJ) and were used as received.

Preparation of the bicyclic castor oil derivative (BCO). To 110 g (0.120 mol) of castor oil in a 500 mL roundbottom flask was added 51 g (0.311 mol) of bicyclo[2.2.1]hept-5-ene-2,3-dicarboxylic anhydride and then 31 g (0.310 mol) of triethylamine. The addition of these reagents was done in a fume hood and no precautions were taken to remove any residual moisture. The reaction was stirred for 24 h at 65 ºC. The resulting oil was diluted with methylene chloride, washed several times with dilute hydrochloric acid, and dried over magnesium sulfate. After removal of the solvent, a viscous yellow/orange oil was obtained in almost quantitative yield.

Polymerization. A typical polymerization procedure follows: 50 mg (5.9×10^{-5} mol) of Grubbs second generation catalyst is weighed into a 20 mL glass vial in a glovebox. Outside of the glovebox, the appropriate amount (weight percent) of functionalized castor oil (BCO) is added to the catalyst. This is followed by adding the appropriate amount (weight percent) of cyclooctene (COE) on top of the oil. The nomenclature used throughout the manuscript is as follows: a specimen containing 55 weight percent BCO and 45 weight percent COE is written as BCO55COE45. This mixture is then mixed with a spatula and, if need be, with a

stir bar. In all cases, 10 g of BCO plus COE have been employed. The mixtures were cured in a programmable oven for 12 h at 65 ºC, and then 12 h at 100 ºC. The resulting thermosets are rubbery and slightly transparent with a tan hue. Small particles of undissolved catalyst could be seen in these thermosets when using 50 mg of catalyst.

^{1}H NMR spectroscopy. ^{1}H NMR spectroscopy of the soluble portions was carried out in $CDCl_3$ using a Varian spectrometer (Palo Alto, CA) at 400 MHz.

IR. Infrared spectroscopy of the insoluble portions was carried out on a Mattson Galaxy Series FTIR 3000 instrument (Madison, WI) using a KBr pellet.

Dynamic Mechanical Analysis. Dynamic mechanical analysis (DMA) has been carried out on a Perkin-Elmer DMA Pyris-7e dynamic mechanical analyzer. Specimens were cut into rectangular shapes 3.5 mm thick, 5 mm deep and 12-15 mm long. The method used equilibrated the specimen for 1 minute at -70 ºC before ramping the temperature from -70 ºC to 100 ºC at a heating rate of 3 ºC/min and a frequency of 1 Hz using helium as a gas. The viscoelastic properties, namely the storage modulus and tan delta, have been obtained.

Thermogravimetric Analysis. Thermogravimetric analysis (TGA) of the specimens has been carried out using a Perkin-Elmer TGA Pyris-7 thermogravimetric analyzer. Specimens of approximately 10 mg were heated from 50 ºC to 650 ºC at a heating rate of 20 ºC/min using air as a gas.

Extraction Analysis. Extractions were performed using a soxhlet extractor. A 2.5 gram polymer specimen was extracted by refluxing it in 100 mL of methylene chloride for 24 h.

Results and Discussion

Synthesis and Characterization of BCO. The BCO was synthesized by simple esterification of castor oil by the commercially available bicyclic anhydride

bicyclo[2.2.1]hept-5-ene-2,3-dicarboxylic anhydride, and the structure of the oil determined. Figure 1 shows the ^{1}H NMR spectra of both regular castor oil and BCO. Integration of the methine hydrogen (A) at 3.6 ppm for castor oil reveals that castor oil has approximately 2.6 hydroxyl groups per triglyceride, which correlates with what is found in the literature.[13]

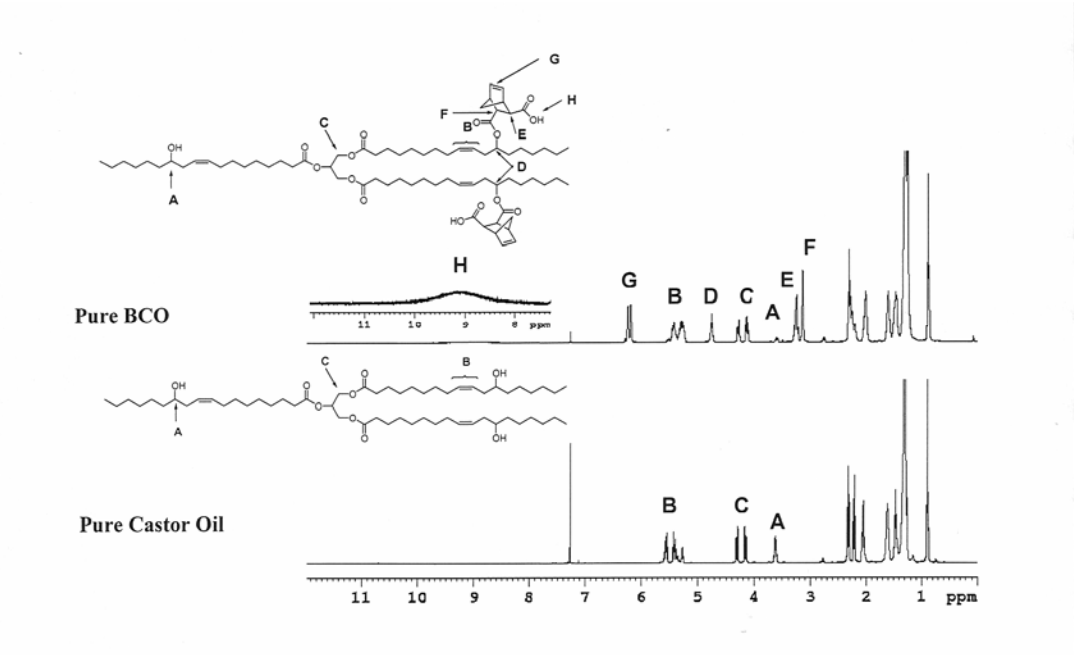

Figure 1. Structures and ^{1}H NMR Spectra of Pure Castor Oil and Pure BCO

Upon reaction with bicyclo[2.2.1]hept-5-ene-2,3-dicarboxylic anhydride, the methine peak at 3.6 ppm present in the BCO diminishes substantially and a new peak appears at 4.75 ppm (D) corresponding to the new methine hydrogen peak adjacent to the ester carbonyl. In addition to this, the presence of new peaks at 3.1 and 3.3 ppm (E and F, respectively) along with the appearance of the bicyclic vinylic protons at 6.3 ppm (G) and the carboxylic acid proton around 9.1 ppm (H) indicate formation of the anticipated BCO (Figure 2). Integration of the methine hydrogen peak adjacent to the ester carbonyl at 4.75 ppm (D) and the bicyclic

vinylic protons at 6.3 ppm (G) indicate there are approximately 2.4 bicyclic moieties per triglyceride. ^{13}C NMR spectra for both the pure castor oil and the BCO have been obtained. Figure 2 shows two additional peaks in the carbonyl region for the BCO corresponding to the carboxylic acid (A) and ester carbonyl (B) carbons of the bicyclic moiety.

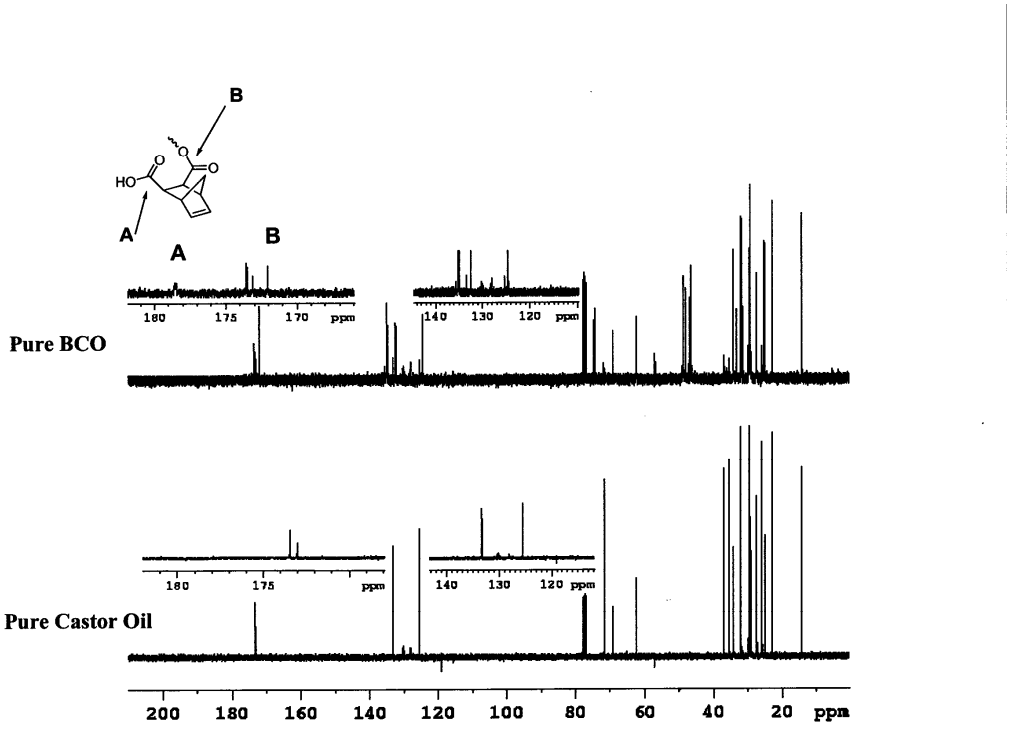

Figure 2. ^{13}C Spectra of Pure Castor Oil and Pure BCO

Optimization of the Catalyst Concentration. The determination of the optimum catalyst concentration for the cometathesis of BCO and COE was first examined. Catalyst concentrations varying from 0.125 up to 4 wt.-% were investigated using the composition BCO50COE50. As the catalyst concentration increased, the specimens became much darker in color, from light maroon to dark burgundy, and less translucent. Gelation for all specimens

took place within approximately 15 minutes at 65 ºC with the exception of the 4 wt.-% specimen that gelled within 10 minutes at room temperature.

Table 1 gives some of the extraction data for the resulting thermosets with varying amounts of initiator.

Table 1. Extraction Data for Various Catalyst Concentrations

Catalyst (wt.-%)	% sol	% insol
0.12	**21**	**79**
0.25	**10**	**90**
0.50	**2**	**98**
1.0	**3**	**97**
2.0	**4**	**96**
4.0	**12**	**88**

As the catalyst content is increased, the percent soluble material, the non-crosslinked or oligomeric component, decreases from 21% soluble material at 0.125 wt.-% catalyst to 4% soluble material when using 2 wt.-% catalyst. However, with 4 wt.-% catalyst, the soluble component increases to 12%. It is possible that this concentration of catalyst induces the formation of cyclic oligomers or metathesis products involving the carbon-carbon double bonds of the fatty acid side chains causing less incorporation into the thermoset and a higher soluble component.

Figure 3 shows the ^{1}H NMR spectra of the extracts for all of the catalyst concentrations investigated. All of the extracts have prominent peaks around 1.25 ppm, 1.95 ppm, and 5.35 ppm, which correspond to portions of the unreacted triglyceride or fatty acid segments. However, the extract may also contain oligomers of the castor oil and/or cyclooctene that could be buried within these peaks or whose presence is too small to easily detect. Figure 3 also shows the presence of peaks around 2.3 ppm and 6.95 ppm for all

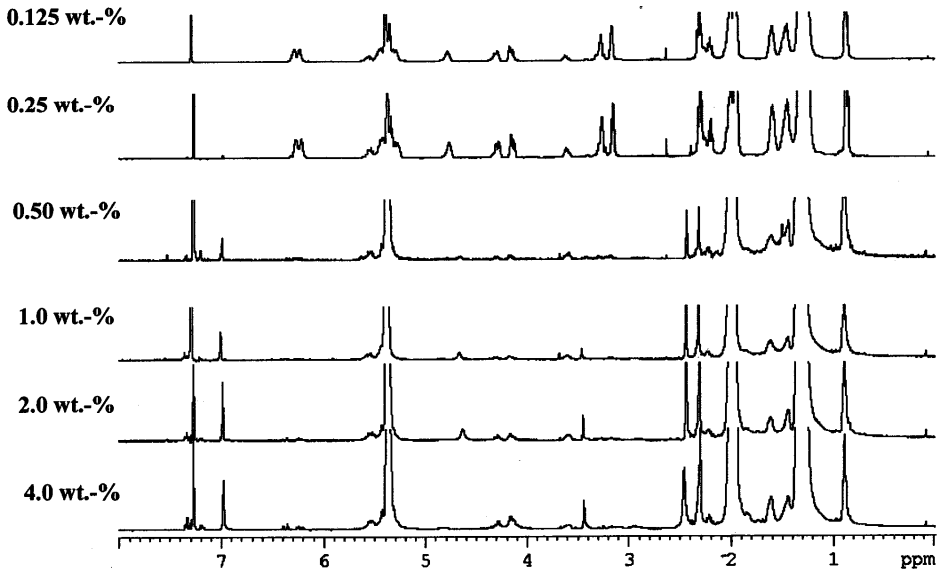

Figure 3. ^{1}H NMR Spectra of the Extracts for Various Catalyst Concentrations

concentrations of the catalyst, except 0.125 wt.-%. The ^{1}H NMR spectrum of the pure Grubbs 2nd generation catalyst (not shown) reveals that these peaks are that of residual catalyst.

Specimens with 0.125 and 0.25 wt.-% of catalyst seem to have more unreacted or oligomeric BCO as evidenced in Figure 3 by the methylene hydrogens at 4.1 ppm and 4.3 ppm, which correspond to the glycerol moiety in the triglyceride, along with the vinylic hydrogens at 6.2 ppm, which correspond to the norbornene unit of the BCO. As the catalyst concentration increases, these BCO peaks diminish substantially, indicating that there is less unreacted BCO in the extract and more in the crosslinked network.

The goal was to find a concentration of catalyst that was relatively low, effective in polymerizing the monomers, and could be used when higher oil concentrations were employed in the thermoset. Since 0.125 and 0.25 wt.-% had a larger presence of unreacted

norbornene units in the extract, these concentrations of catalyst were considered too low, especially when higher concentrations of BCO were to be used in the thermoset. Thus 0.5 wt.-% was chosen for the "optimum" concentration of catalyst to be used for all of the subsequent specimens to be examined.

Extraction Analysis. Initially, a series of compositions was prepared that varied from 55 to 100 wt.-% of the oil in increments of 10 wt.-%. However, after the curing of the thermosets was complete, the specimens with 95 and 100 wt.-% BCO oil did not gel. Therefore, only compositions with 55 to 85 wt.-% oil were analyzed. Their extraction analysis, DMA, and TGA data are shown in Table 2.

Table 2. DMA, TGA and Extraction Analysis of BCO/COE Samples. Values in Parenthesis Indicate Analysis Done on Solvent Extracted Material

Specimen	T_g (°C)	crosslink density (mol/m^3)	tan delta	T_{max} (°C)	% sol	% insol
BCO55COE45	**1 (35)**	**288**	**0.39**	**504 (466)**	**5**	**95**
BCO65COE35	**-9 (1)**	**185**	**0.53**	**500 (474)**	**4**	**96**
BCO75COE25	**-14 (10)**	**166**	**0.80**	**503 (475)**	**11**	**89**
BCO85COE15	**-13**	**111**	**0.93**	**504 (474)**	**20**	**80**

In looking at the extraction data, it can be seen that the soluble, non-crosslinked or oligomeric component increases as the concentration of BCO in the initial feed composition increases. The ^{1}H NMR spectral data suggest that the extracts are composed of unreacted BCO, oligomers of polycyclooctene (polyCOE), or oligomers of BCO plus cyclooctene (Figure 4). As the amount of oil increases in the initial feed of the thermoset, the methylene peaks at 4.1 and 4.3 ppm and the norbornene peaks at 6.3 ppm increase in intensity, indicating that less BCO is incorporated into the thermoset. The decline in intensity of these peaks with the BCO concentrations of 55 and 65 wt.-% and the larger presence of peaks with

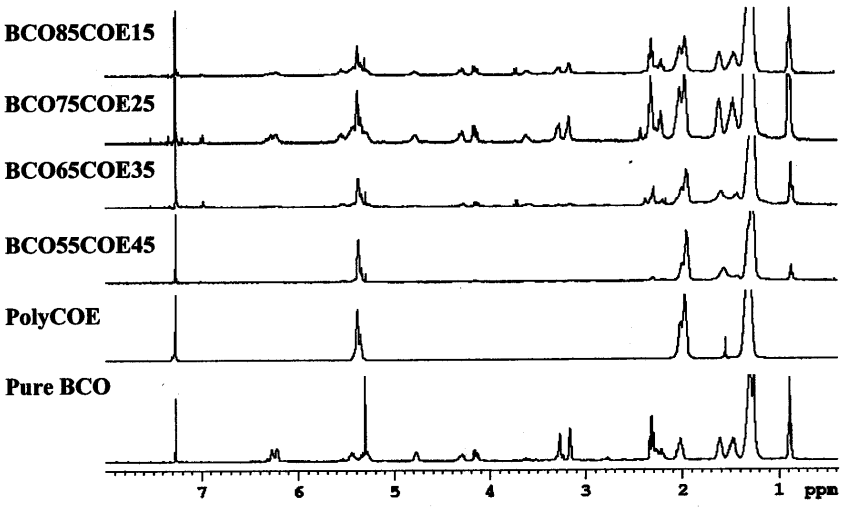

Figure 4. ^{1}H NMR Spectra of the Monomers and Extracts

chemical shifts around 1.25, 2.0 and 5.35 ppm suggest that these compositions may have a greater presence of polycyclooctene or oligomers thereof. This is seen in the corresponding soluble portions reported in Table 2.

When comparing the reactivities of norbornene and cyclooctene, the highly strained norbornene unit has a greater reactivity than the cyclooctene.[14] However, the BCO possessing a norbornene-like moiety does not undergo ROMP unless a certain concentration of cyclooctene is present. A most likely reason for this is viscosity. BCO alone is highly viscous, and if copolymerized when COE is present in only low concentrations, the system is still quite viscous. This decreases the mobility of the BCO monomer resulting in a lower reactivity and less incorporation into the thermoset.[15] In fact, when pure BCO was polymerized with the Grubbs catalyst in the presence of a roughly equal wt.-% of toluene to

decrease the viscosity, the oil-toluene mixture gelled within minutes at 65 ºC. The specimen obtained was a hard rubber. These results suggest that the high viscosity of pure BCO is responsible for the lack of gelation. The reactivity of the BCO may also be slowed by the fatty acid chains, which could hinder coordination between the catalyst and the norbornene moiety of the BCO.

Figure 5 shows the FTIR spectra for the insoluble component from the BCO85COE15 sample, pure BCO and pure polyCOE. The peaks around 2900 cm^{-1} correspond to the aliphatic hydrogens of both the fatty acid chains of the BCO and the cyclooctene-derived portions of the thermoset. Peaks around 1150 cm^{-1} due to the C-O single bonds present in the ester groups in the glycerol and the bicyclic moieties in the insoluble BCO85COE15 and pure BCO samples are clearly absent in the polyCOE. As seen in Figure

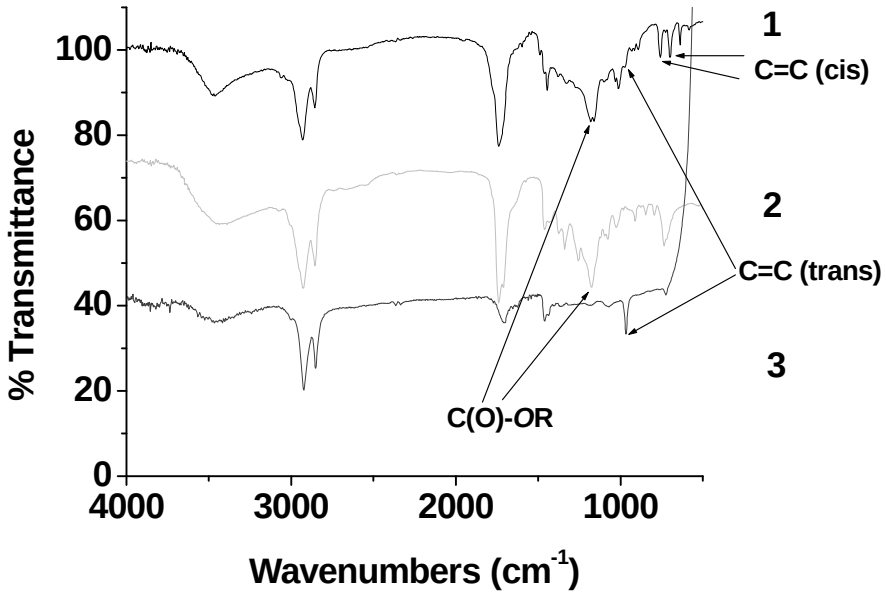

Figure 5. IR Spectra for (1) the Insoluble Portion of BCO85COE15, (2) Pure BCO, and (3) PolyCOE

5, peaks due to the olefinic and aliphatic regions of the insoluble BCO85COE15 material, pure BCO and polyCOE all appear in the same region, so trying to find peaks corresponding to the cyclooctene portions in the insoluble BCO85COE15 is difficult. But, at 970 cm^{-1} a large peak from the polyCOE and a shoulder peak from the insoluble BCO85COE15 can be seen, indicating cyclooctene incorporation. This peak, which is not present in the pure BCO, can perhaps be attributed to a trans double bond in the metathesized backbone of the insoluble thermoset. However, the backbone of the crosslinked network contains not only trans double bonds. Between 675 cm^{-1} and 750 cm^{-1}, there are two C-H stretches that arise when a cis double bond is present. Although these peaks could conceivably be due to the cis double bonds present in the fatty acid side chains, the fact that they don't exactly align with analogous peaks in the IR spectrum of pure BCO suggests that the crosslinked polymer network is composed of both cis and trans double bonds.

Dynamic Mechanical Analysis. DMA analysis for the various compositions studied is shown in Table 2 and Figure 6. The glass transition values (T_g), determined by the temperature associated with the maximum peak height for tan delta, range from about 1 ºC to -14 ºC. As the BCO content increases, the glass transition temperature decreases. This is due to both an increase in the soluble portion, which can act as a plasticizer, and to the increase in the flexible triglyceride molecule in the backbone of the crosslinked polymer.[16] Both result in an increased flexibility of the thermoset as the BCO content increases. In addition to this, the decreased crosslink density (Table 2) associated with the increase in the concentration of the BCO oil allows for greater segmental mobility of the polymer chains, giving a lower glass transition temperature.

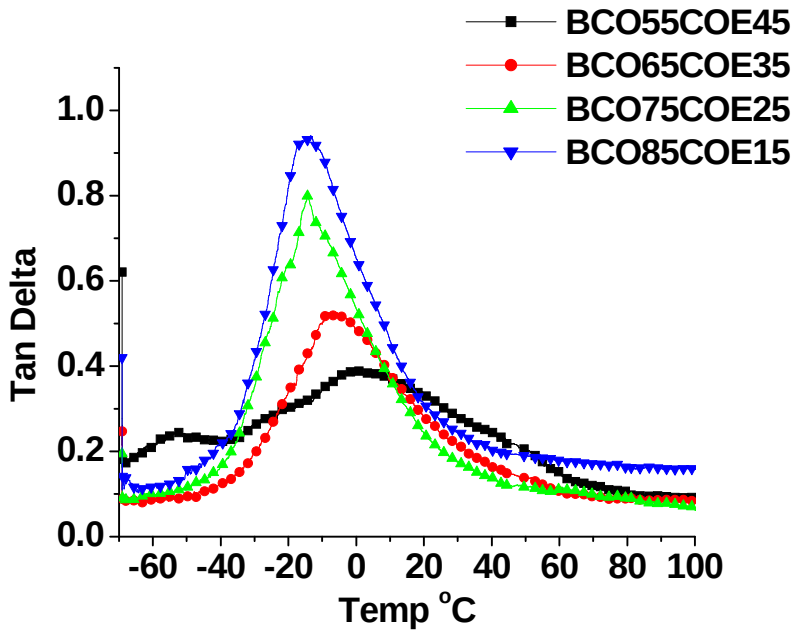

Figure 6. Dynamic Mechanical Analysis of the BCO/COE Thermosets

The homopolymerization of cyclooctene yields a polymer whose T_g is less than - 60 ºC. [17] It has been shown in the literature that the copolymerization of cyclooctene with a norbornene derivative can result in dramatic increases in the T_g, depending on the ratio of cyclooctene and norbornene.[18] This is apparently due to the presence of the rigid norbornene monomer, which is known to give higher T_g materials. In the BCO/COE thermosets, the rigidity of the norbornene-like moiety coupled with the crosslinking ability of the BCO (discussed later) yield higher T_g materials when compared to pure polycyclooctene.

The crosslink densities have been calculated 40 ºC above their T_g, using the rubber theory of elasticity.[20,21] The following equation was used:

$$E' = 3\upsilon_e RT$$

in which E' (Pa) is the storage modulus at T_g + 40 ºC in the rubbery plateau, υ_e is the crosslinking density, R is the gas constant 8.31 J/mol*K and T is the absolute temperature in Kelvin at T_g +40 ºC. From Table 2 it can be seen that as the amount of oil in the feed ratio of the thermosets increases, the crosslink densities decrease from 288 to 111 mol/m^3. This is interesting, because the BCO oil is the crosslinker in these thermosets. However, since the thermosets with greater amounts of BCO oil have also greater amounts of unreacted oil (crosslinker), lower crosslinking densities are observed.

Also shown in Table 2 are the tan delta values for the thermosets. All of the samples have a tan delta greater than 0.3. The 75 wt.-% and 85 wt.-% BCO specimens have tan delta values above 0.3 over a temperature range of approximately 60 ºC, making these particular materials attractive in damping applications.[19] It can be seen that increases in the BCO concentration result in increasing tan delta values. This is expected, since these specimens are more rubbery and flexible, allowing for better damping. In addition to this, except for the BCO55COE45 material, all other materials have single tan delta curves indicating no phase separation. The BCO55COE45 material appears to have possible phase separation as evidenced by a small peak around -50 ºC, indicating a polyCOE rich phase, and a larger peak around 1 ºC, which corresponds to both BCO- and COE- rich phases.

As mentioned earlier, the soluble fraction or unreacted oil present in these polymers can serve as a plasticizer, which can help soften the thermoset and lower the glass transition temperature. A plasticizer is typically a high boiling, oily organic liquid (usually an ester) that helps to soften the material and lower the glass transition temperature.[22] Plasticizers can also be organic solvents or even water. We wanted to explore how much of a role the soluble fraction (plasticizer) plays in the final properties of the thermoset. Therefore, DMA analysis

was carried out on the extracted samples. However, it should be noted that solvent-extracted samples swell significantly during the extraction process and, after removal of the solvent and the soluble components, the resulting samples may contain small voids and cracks. Also, when larger amounts of oil are used (i.e. 75 and 85 wt.-%) the solvent-extracted thermosets become quite weak and can fall apart easily. Because of this, we could not obtain DMA data for the BCO85COE15 sample. Nonetheless, we still went ahead with the DMA analysis for the other three samples.

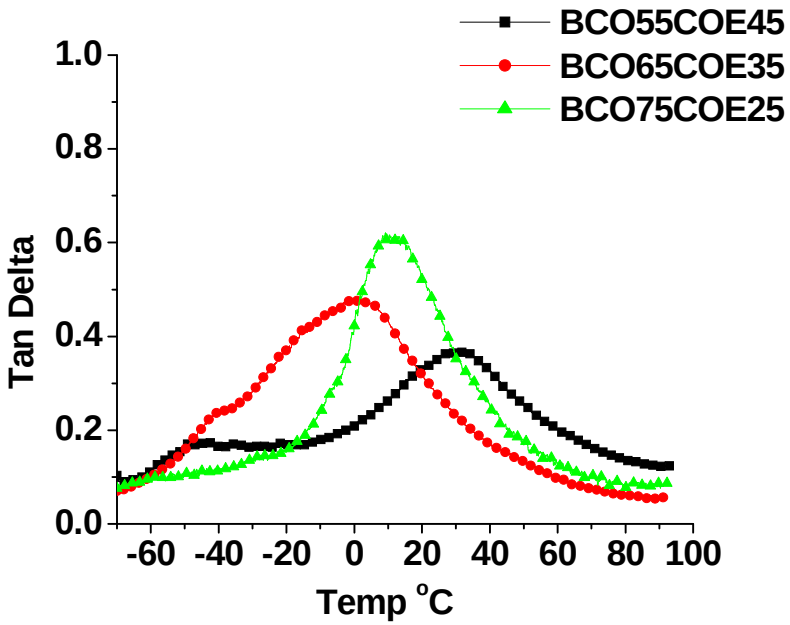

Figure 7. Dynamic Mechanical Analysis of the Solvent-Extracted BCO/COE Thermosets

Figure 7 and the values in parentheses in Table 2 show the DMA results obtained for the solvent-extracted thermosets. It can be seen for the 55 wt.-% BCO sample the T_g increases from 1 ºC to 35 ºC, for the 65 wt.-% BCO sample the T_g increases from -9 ºC to 1 ºC, and for the 75 wt.-% BCO sample the T_g increases from -14 ºC to 10 ºC. This indicates

that the role of the soluble fraction or unreacted oil is that of a plasticizer, since these specimens follow the expected trend of plasticized materials.[23]

Further proof that the free fatty acid chains incorporated in the crosslinked thermoset act as plasticizers is evident from analysis of the DMA data. The solvent-extracted 65 wt.-% BCO and 75 wt.-% BCO samples have much lower T_g's (1 ºC and 10 ºC, respectively) than the solvent-extracted 55 wt.-% BCO sample (T_g = 35 ºC). This lower T_g can be attributed to the higher content of free fatty acid chains incorporated into the crosslinked network for the 65 wt.-% BCO and 75 wt.-% BCO, which can internally plasticize these materials and lower the T_g of the thermosets.

When comparing the solvent-extracted and non solvent-extracted T_g's in Table 2, the effect of the soluble fraction as a plasticizer looks to be much greater for the 55 wt.-% BCO sample than for the 65 wt.-% BCO and 75 wt.-% BCO samples. Perhaps the lower content of free fatty acid chains incorporated into the crosslinked network of the 55 wt.-% BCO results in less internal plasticization from these free fatty acid chains, yielding a larger plasticization impact by the soluble fraction. When comparing the 65 wt.-% and 75 wt.-% solvent extracted T_g's it can be seen that the 65 wt.-% has a lower T_g than the 75 wt.%, even though it has less oil. At this point in time we cannot offer any valid explanation for this. Thus, from the solvent-extracted DMA analysis, we can conclude: 1) that the soluble fraction or unreacted oil does indeed plasticize the oil; and 2) that the free fatty acid chains incorporated into the crosslinked polymer network also act as plasticizers.

Thermogravimetric Analysis. Table 2 and Figure 8 shows the TGA analysis data obtained from the thermosets,. Figure 8 shows that the BCO/COE thermosets, pure BCO and polycyclooctene are all thermally stable below 200 ºC in air. There are three stages of

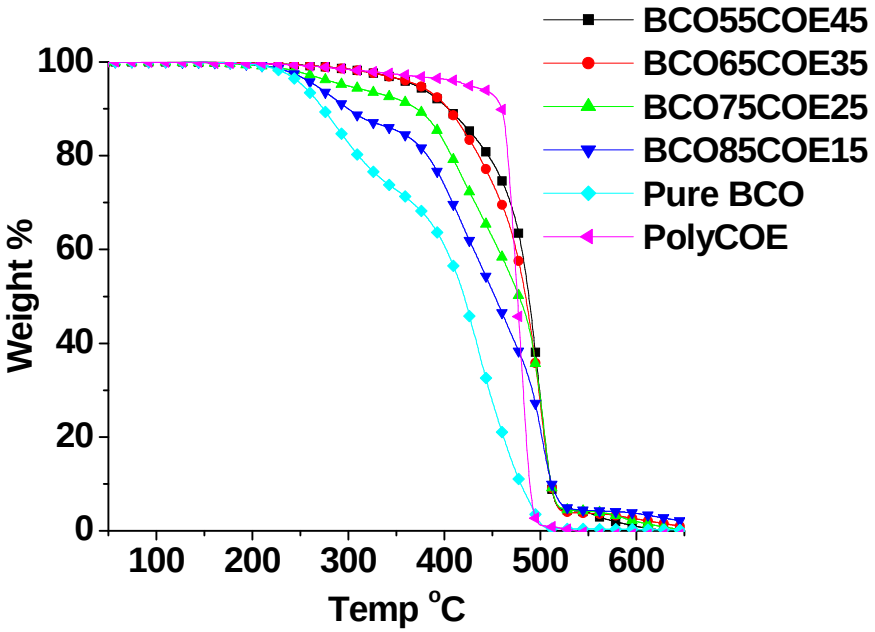

Figure 8. Thermogravimetric Analysis of the BCO/COE Thermosets, Pure BCO, and PolyCOE

decomposition associated with these thermosets. Stage I represents the decomposition of some of the soluble components and is evident from 50 to 400 ºC. Interestingly, the BCO85COE15 curve is similar to that of pure BCO in the region below 400 ºC, which may be due to the fact that this sample contains such a large amount of oil (reacted and unreacted). Stage II represents the main chain degradation of the crosslinked network and appears in the region from 400 ºC to 500 ºC. Stage III (500 ºC to 650 ºC) represents degradation of the char that remains behind.

The T_{max} (temperature of maximum degradation) values are summarized in parentheses in Table 2 and in Figure 9, which shows the results obtained from the solvent-extracted specimens. These thermosets follow a four stage degradation curve. The smaller

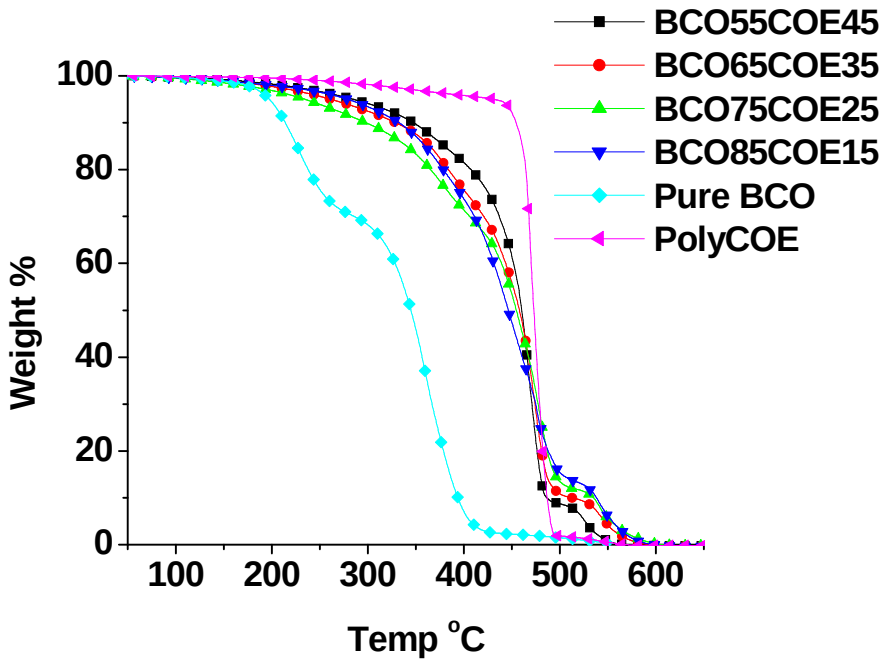

Figure 9. Thermogravimetric Analysis of the Solvent-Extracted BCO/COE Thermosets, Pure BCO, and PolyCOE

step at 500 ºC may be related to residual soluble portions remaining behind in the solvent-extracted thermoset, which could indicate that our extraction time of 24 hours may not remove the entire soluble portion. Table 2 shows that the solvent-extracted specimens have T_{max} values around 470 ºC and the non-extracted specimens have T_{max} values around 500 ºC. The greater thermal stability associated with the non-extracted specimens indicates that the soluble fraction does play a role in enhancing the thermal stability.

Regardless of the specimen composition, it has been found that all of the non-extracted specimens have approximately the same T_{max} values, around 500 ºC, and all of the solvent-extracted specimens have T_{max} values around 470 ºC. The reasons for this are not exactly clear, but may be attributed to thermal crosslinking during stage I or at the beginning

of stage II of the residual double bonds remaining behind in the metathesized thermoset. The effect of this may be that all of the thermosets have roughly the same enhanced thermal stability, or perhaps the cyclooctene portions of the thermoset play the deciding factor in the thermal stability of the final thermosets. Indeed, from both Figures 8 and 9, it is seen that the homopolymer of cyclooctene (polyCOE) degrades at a relatively high temperature (T_{max} 475 ºC), which may ultimately influence the thermal properties of the final thermoset.

Conclusions

We have been able to synthesis and copolymerize a functionalized castor oil (BCO) with cyclooctene (COE) by ROMP. Rubbery thermosets, which are transparent with a light tan hue possessing 55 to 85 wt.-% oil, have been prepared. The catalyst concentration determined to be most effective in this study was 0.5 wt.-%.

The glass transition temperatures of the BCO/COE thermosets range from 1 ºC to -14 ºC, well below ambient temperatures. Tan delta values are above 0.3, making some of these materials attractive as damping materials. DMA analysis of the extracted specimens shows that the soluble portions and the free fatty acid chains incorporated into the crosslinked polymer networks act as plasticizers due to lower T_g's.

TGA analysis shows that all of the samples are thermally stable below 200 ºC. All of the solvent-extracted samples have T_{max} values around 470 ºC and the non-extracted samples have T_{max} values around 500 ºC. The higher T_{max} values associated with the non-extracted materials indicate that the soluble fraction helps to enhance the thermal stability of the samples. The reasons for the various BCO/COE compositions having similar T_{max} values is suggested to be related to thermal crosslinking of the metathesized double bonds in the

thermosets, or the thermal stability of the COE portions in the network, as evidenced by the relatively high T_{max} for polyCOE.

Acknowledgments

The authors gratefully acknowledge the Illinois-Missouri Biotechnology Alliance and the Grow Iowa Values Fund for funding this research. Also, we thank Dr. Surya Mallapragada from the Department of Chemical and Biological Engineering for the use of her thermal analysis equipment.

References

[1] "*Feedstocks for the Future: Renewables for the Production of Chemicals and Materials*", ACS Symposium Series 921; J.J. Bozell, M.K. Patel, Eds.; American Chemical Society: Washington D.C., 2006.

[2] J. Johnson, *Chem. Eng. News* **2006**, *84* (35), 16.

[3] [3a] J. Zhang, L. Jiang, L. Zhu, J. Jane, P. Mungara, *Biomacromolecules* **2006**, *7*, 1551; [3b] Y. Wang, X. Cao, L. Zhang, *Macromol. Biosci.* **2006**, *6*, 524; [3c] For a review see: *Natural Fibers, Biopolymers, and Biocomposites*; Mohanty, A.K., Misra, M., Drzal, L.T., Eds.; CRC Press Taylor and Francis, Boca Raton 2005.

[4] U. Biermann, W. Friedt, S. Lang, L. Wilfried, G. Machmüller, J.O. Metzger, M. Rüsch gen Klaas, H.J. Schäfer, M.P. Schneider, *Angew. Chem. Int. Ed*. **2000**, *39*, 2206.

[5] [5a] F. Li, R.C. Larock, *J. Appl. Poly. Sci.* **2001**, *80*, 658; [5b] F. Li, M.V. Hansen, R.C. Larock, *Polymer* **2001**, *42*, 1567; [5c] F. Li, R.C. Larock, *J. Poly. Environ*. **2002**, *10*, 59; [5d] D.D. Andjelkovic, M. Valverde, P. Henna, F. Li, R.C. Larock, *Polymer* **2005**, *46*, 9674.

[6] [6a] P.H. Henna, D.D. Andjelkovic, P.P. Kundu, R.C. Larock, *J. Appl. Poly. Sci*. **2007**,

104, 979; [6b] M.S. Valverde, D.D. Andjelkovic, P.P. Kundu, R.C. Larock, to be submitted.

[7] [7a] F. Li, R.C. Larock, *Biomacromolecules* **2003**, *4*, 1018; [7b] P.P. Kundu, R.C. Larock, *Biomacromolecules* **2005**, *6*, 797.

[8] [8a] B. Cakmakli, B. Hazer, I.O. Tekin, S. Kizgut, M. Kosal, Y. Menceloglu, Y. *Macromol. Biosci*. **2004**, *4*, 649; [8b] J. LaScalla, R.P. Wool, *Polymer* **2005**, *46*, 61.

[9] [9a] Z.S. Petrović, Z. Wei, I. Javni, *Biomacromolecules* **2005**, *6*, 713; [9b] A. Zlatanić, Z.S. Petrović, K. Dušek, *Biomacromolecules* **2002**, *3*, 1048.

[10] K.J. Ivan, J.C. Mol, "*Olefin Metathesis and Metathesis Polymerization*", Academic Press, San Diego 1997.

[11] [11a] C.W. Bielawski, R.H. Grubbs, *Prog. Polym. Sci.* **2007**, *32*, 1; [11b] B.M. Novak, R.H. Grubbs, *J. Am. Chem. Soc*. **1988**, *110*, 960; [11c] M.A. Hillmyer, W.R. Laredo, R.H. Grubbs, *Macromolecules* **1995**, *28*, 6311.

[12] [12a] M.D. Refvik, R.C. Larock, Q. Tian, *J. Am. Oil Chem. Soc.* **1999**, *76*, 93; [12b] Q. Tian, R.C. Larock, *J. Am. Oil Chem. Soc.* **2002**, *79*, 479; [12c] S. Warwel, F. Brüse, C. Demes, M. Kunz, M. Rüsch gen Klass, *Chemosphere* **2001**, *43*, 39; [12d] J. Patel, S. Mujcinovic, W.R. Jackson, A.J. Robinson, A.K. Serelis, C. Such, *Green Chemistry* **2006**, *8*, 450.

[13] T. Eren, S. Çolak, S.H. Küsefoglu, *J. Appl. Poly. Sci*. **2006**, *100*, 2947.

[14] "*Handbook of Metathesis Volume 3- Applications in Polymer Synthesis*"; R.H. Grubbs, Ed.; Wiley-VCH: Weinheim, Germany, 2003.

[15] G.G. Odian, "*Principles of Polymerization*", Wiley-Interscience, Hoboken 2004.

[16] D.D. Andjelkovic, R.C. Larock, *Biomacromolecules* **2006**, *7*, 927.

[17] L. Morbelli, E. Eder, P. Preishuber-Pflügl, F. Stelzer, *J. Mol. Catal. A.* **2000**, *160*, 45.

[18] T. Hino, N. Inoue, T. Endo, *J. Poly. Sci. A.* **2005**, *43*, 6599.

[19] F. Li, R.C. Larock, *Polym. Adv. Technol.* **2002**, *13*, 436.

[20] P.J. Flory, "*Principles of Polymer Chemistry*", Cornell University Press, Ithaca 1953.

[21] I.M. Ward, "*Mechanical Properties of Solid Polymers*", Wiley Interscience, New York 1971.

[22] A.S. Wilson, "*Plasticisers: Principles and Practice*", The University Press, Cambridge, 1995.

[23] "*Sound and Vibration Damping with Polymers"*, ACS Symposium Series 424; R.D. Corsaro, L.H. Sperling, Eds.; American Chemical Society: Washington D.C., 1990.

CHAPTER 4. NOVEL THERMOSETS OBTAINED BY ROMP OF A FUNCTIONALIZED VEGETABLE OIL AND DICYCLOPENTADIENE

A Paper to be Published in Journal of Applied Polymer Science

Phillip Henna and Richard C. Larock*

Department of Chemistry Iowa State University Ames, IA 50011

Abstract

New polymeric thermosetting resins prepared by the ring opening metathesis polymerization (ROMP) of a commercially available vegetable oil derivative, Dilulin, and dicyclopentadiene (DCPD) have been prepared and characterized. A thorough characterization of the modified oil itself has been carried out to elucidate its structure. Grubbs second generation catalyst has been used to effect the ROMP of the strained unsaturated norbornene-like rings in the commercial oil. Dynamic mechanical analysis of the thermosetting resins reveals that glass transition temperatures from 36 ºC to -29 ºC can be obtained when the proper ratio of oil and DCPD is employed. Thermogravimetric analysis reveals that these resins have very similar temperatures of maximum degradation (T_{max} values). Extraction analysis indicates that all samples have at least a 20 % soluble fraction and that the soluble fraction is composed of oligomers, unreacted triglyceride oil or both. The effect of the soluble fraction as a plasticizer has also been explored.

Introduction

A recent increased interest in the production of plastics and rubbers from renewable and sustainable feedstocks has been driven by high and unstable petroleum prices and

uncertainties as to how long our petroleum supply can last. While a great deal of attention has been focused on the production of ethanol from cellulosics[1] and biodiesel from vegetable oil,[2] increasing research has been directed towards biobased materials and plastics from these and other renewable resources.[3]

Vegetable oils are a very promising renewable feedstock for polymer synthesis as either the triglyceride oil itself or derivatives thereof.[4] Previous work has focused on either condensation[5] or free radical[6] polymerization to produce thermosetting resins. Our group has investigated cationic,[7] free radical,[8] thermal[9] and more recently ring opening metathesis polymerization (ROMP)[10] of vegetable oils or derivatives thereof to produce a variety of thermosetting resins.

ROMP constructs polymers by cleavage of the olefinic portions of strained ring systems that are then reconnected with olefinic portions of another ring system. Figure 1

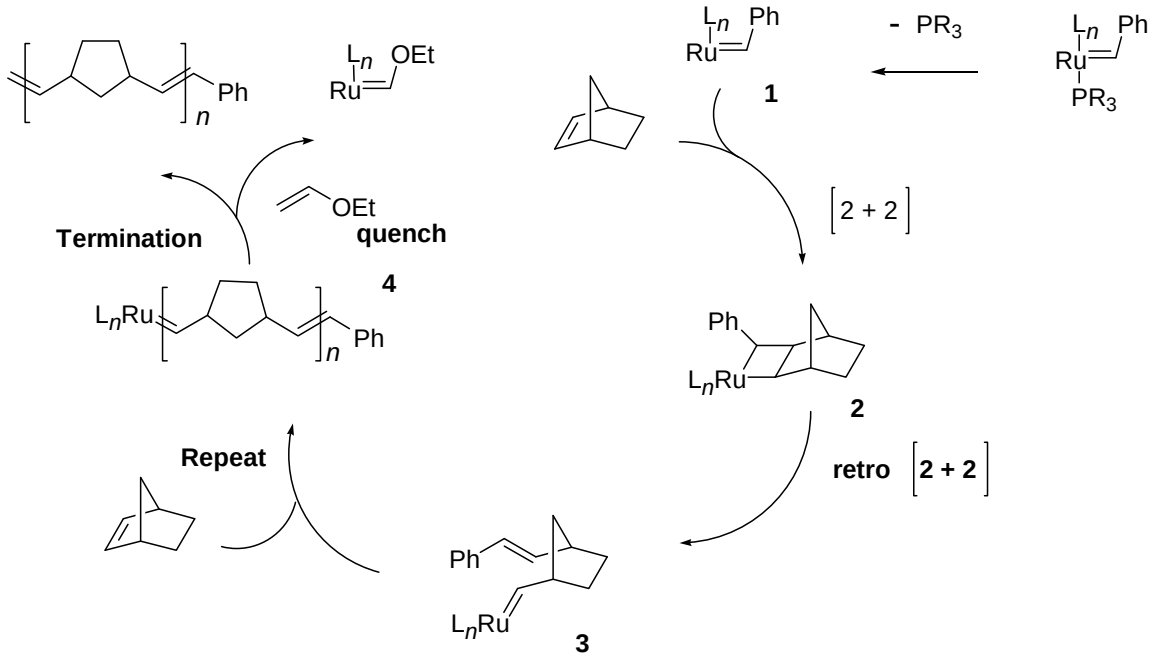

Figure 1. Generalized Mechanism of ROMP

shows a generalized ROMP mechanism. First, the phosphine ligand dissociates from the precatalyst (step 1). The resulting 14 electron transition metal complex undergoes a [2 + 2] cycloaddtion with the cyclic monomer to give a metallacyclobutane intermediate (step 2), which then undergoes [2 + 2] cycloreversion to give the ring opened product (step 3). This process continues until the ruthenium carbine is quenched with ethyl vinyl ether, which terminates the polymerization (step 4).[11] While much has been reported on the ROMP of various cyclic systems,[12] to our knowledge, our work on the ROMP of a functionalized castor oil containing a bicyclic moiety (BCO) and cyclooctene is the first report of the ROMP of a triglyceride oil.[10] One disadvantage of this particular system is that castor oil is not readily available. In addition to this, the BCO needs to be synthesized. Dilulin is a commercially available vegetable oil derivative prepared by heating dicyclopentadiene (DCPD) and linseed oil, which contains an unsaturated norbornene-like bicyclic moiety.[13] We now wish to report the synthesis and characterization of unique rubbery materials by the ROMP of Dilulin and DCPD.

Experimental

Materials. Dilulin was obtained from Cargill (Minneapolis, MN). Dicyclopentadiene (> 95%) was purchased from Alfa Aesar (Ward Hill, MA). Methylene chloride stabilized with amylene and ethyl acetate was supplied by Fisher (Fair Lawn, NJ). Grubbs second generation catalyst and potassium bromide (FT-IR grade ≥ 99%) were obtained from Sigma-Aldrich (Milwaukee, WI). Unless otherwise stated, all reagents were used as received.

Recrystallization of Grubbs second generation catalyst. To improve the solubility of the olefin metathesis catalyst with the Dilulin and DCPD, the Grubbs catalyst was subjected to a freeze-drying process similar to that found in the literature.[14] We used a modified procedure

in which 0.5 g of catalyst in a small beaker is dissolved in 10 mL of benzene and placed in liquid nitrogen for 5 min. The beaker is then removed from the liquid nitrogen and a Kim-Wipe was placed around the top of the beaker, which was then placed in a vacuum oven overnight. This process gives a quantitative yield of crystals that are much larger than the original material and possess a higher surface area.

Polymerization. A typical 5 g polymerization was carried out as follows: to a 20 mL vial is added 12.5 mg (0.25 wt %) of the recrystallized Grubbs second generation catalyst. To this was added the appropriate amount (in wt %) of Dilulin, which was stirred in with the catalyst. Then the appropriate amount (in wt %) of DCPD was added. Samples ranging from 50 wt % up to 100 wt % oil were prepared. Bulk polymerization was affected by stirring at room temperature for a few minutes and then pouring the reaction mixture into a 55 mm petri dish. The samples are cured in an oven for 1 h at 65 ºC and post-cured for 3 h at 150 ºC. All of the samples gelled, resulting in transparent, amber rubbers. For larger scale polymerizations (25 g), the resin was poured into a mold made of two 6 x 8 inch glass plates separated by a 1/8 inch rubber gasket and clamped with paper binder clamps. The nomenclature adopted for these thermosets is as follows: a sample with 50 wt % Dilulin and 50 wt % DCPD is identified as Dil50DCPD50.

Soxhlet Extraction. All materials have been characterized by soxhlet extraction as follows. A 2-3 gram sample was cut into a rectangular shape. The sample was placed into a cellulose thimble (Whatman), which was subsequently placed into a soxhlet extractor equipped with a 250 mL round bottom flask containing 100 mL of methylene chloride and a stir bar. A condenser was placed on top of the extractor and the sample refluxed (~ 60 ºC) for 24 h. Evaporation of the solvent yielded an oily residue (extract), which was dried for 24 h at an

elevated temperature in a vacuum oven alongside the insoluble crosslinked portion. Both the extract and the insoluble portion were then weighed and analyzed further.

Purification of Dilulin. A 55 mm diameter buchner funnel with Whatman number 1 filter paper was fitted atop a 250 mL filter flask connected to a water aspirator vacuum. Twenty five mL of hexanes was passed through the funnel to wet the filter paper. Then silica gel was poured onto the wet filter paper to a height of approximately 1.5 inches and then leveled. Another piece of filter paper was placed on top of the silica gel. Fifty mL of hexanes was poured through the flash column, followed by 1 g of Dilulin dissolved in 10 mL of hexanes. An additional 150 mL of hexanes was poured through to elute the DCPD or oligomers. The vacuum was removed and the filter flask was quickly emptied. Then another 100 mL of hexanes was passed through while pulling a vacuum. TLC showed no spot indicating DCPD or oligomers after addition of the 100 mL of hexanes. The oil was eluted by placing another 250 mL flask onto the flash column and pulling a vacuum. Approximately 200 mL of ethyl acetate was passed through the flash column. TLC showed no spot indicating oil after addition of the 200 mL of ethyl acetate. Each solvent fraction was put into a pre-weighed roundbottom flask and placed onto a rotary evaporator. After all of the solvent was removed, the flasks were placed in a vacuum oven for a few hours. After weighing each fraction, it was found that Dilulin contains approximately 95% of the desired oil and approximately 5% of unreacted DCPD or oligomers thereof. The ratio of each of these, however, may vary from one batch of Dilulin to another.

Polymer Characterization. ^{1}H NMR spectroscopic analysis of the extract (soluble portion) was performed in $CDCl_3$ using a Varian spectrometer (Palo Alto, CA) at 400 MHz. FT-IR analysis of the oils and insoluble portions were carried out on a Mattson Galaxy Series FTIR

3000 instrument (Madison, WI). For the oils, a salt plate was the dispersing medium. For the insoluble portions, the samples were ground into a powder, mixed with KBr and pressed into a pellet. The insoluble portions were also analyzed with cross-polarization/magic angle spinning ^{13}C NMR on a Bruker AV600 spectrometer (Bruker America, Billerica). The samples were examined at two spinning frequencies (3.2 and 3.8 kHz) to differentiate between the actual and spinning sidebands. Dynamic mechanical analysis (DMA) was recorded on a TA Instruments (New Castle, DE) Q800 DMA using a film/fiber tension mode and single cantilever mode. For the film/fiber mode, the specimens were cut into rectangular shapes approximately 24 mm in length, 10 mm wide and 1.5 to 2 mm thick. DMA multi-frequency strain analysis was employed with an oscillation amplitude of 20 micrometers, a static force of 0.01 N and a force track of 300%. Samples were cooled and held isothermally for 3 minutes at -60 ºC before the temperature was increased at 3 ºC/min to 100 ºC. The single cantilever mode samples were about 30 mm long, 15 mm wide and 3 mm thick. DMA multi-frequency strain analysis with an oscillation amplitude of 15 micrometers was employed. Thermogravimetric analysis of the specimens was carried out on a TA Instruments (New Castle, DE) Q50 TGA. Samples were scanned from 50 ºC to 650 ºC in air with a flow rate of 20 mL/min.

Results and Discussion

Characterization of Dilulin. Dilulin is synthesized by the presumed Diels-Alder reaction between the double bonds of linseed oil and cyclopentadiene formed by cracking DCPD at high temperature and pressure[13] (Figure 2). Thin layer chromatography (TLC) of Dilulin using 20:1 hexane:ethyl acetate reveals that the oil is a mixture of two components; one with a low R_f (0.16) and the other with a high R_f (0.74). The more polar low, R_f material is the

Dilulin itself. The less polar, high R_f material consists of residual or copolymers thereof.

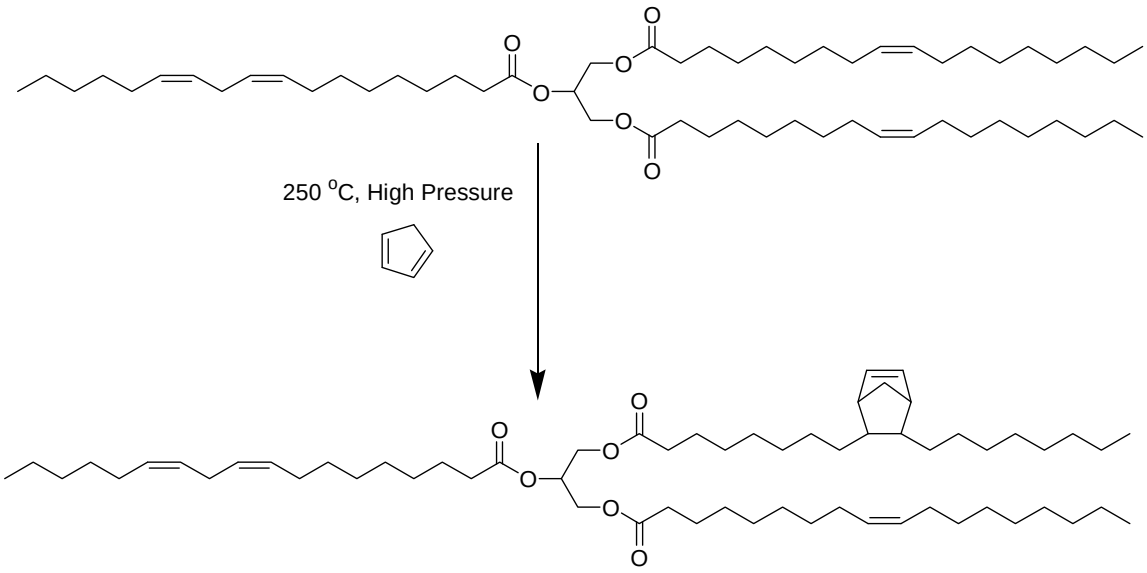

Figure 2. Diels-Alder Reaction Between Linseed Oil and Cyclopentadiene

Separation of Dilulin into the oil and residual DCPD was carried out on a flash silica gel column. It was found that the low R_f fraction consists of approximately 95% of Dilulin and that the high R_f portion contains approximately 5% Dilulin. FT-IR and ^{1}H NMR spectral analysis of the "purified Dilulin" provided results essentially identical to those of the non-purified Dilulin (mentioned next); therefore, only characterization of the non-purified Dilulin will be discussed.

A representative structure of Dilulin has been determined by ^{1}H NMR spectroscopy. Figure 3 shows both the structures and ^{1}H NMR spectra for Dilulin and regular linseed oil. Regular linseed oil was chosen as the oil for structural comparison, since Dilulin is synthesized from linseed oil. Figure 3 shows peaks at 4.1 and 4.3 ppm, which correspond to the methylene protons of the glycerol moiety for both oils. At 5.35 ppm are peaks for both

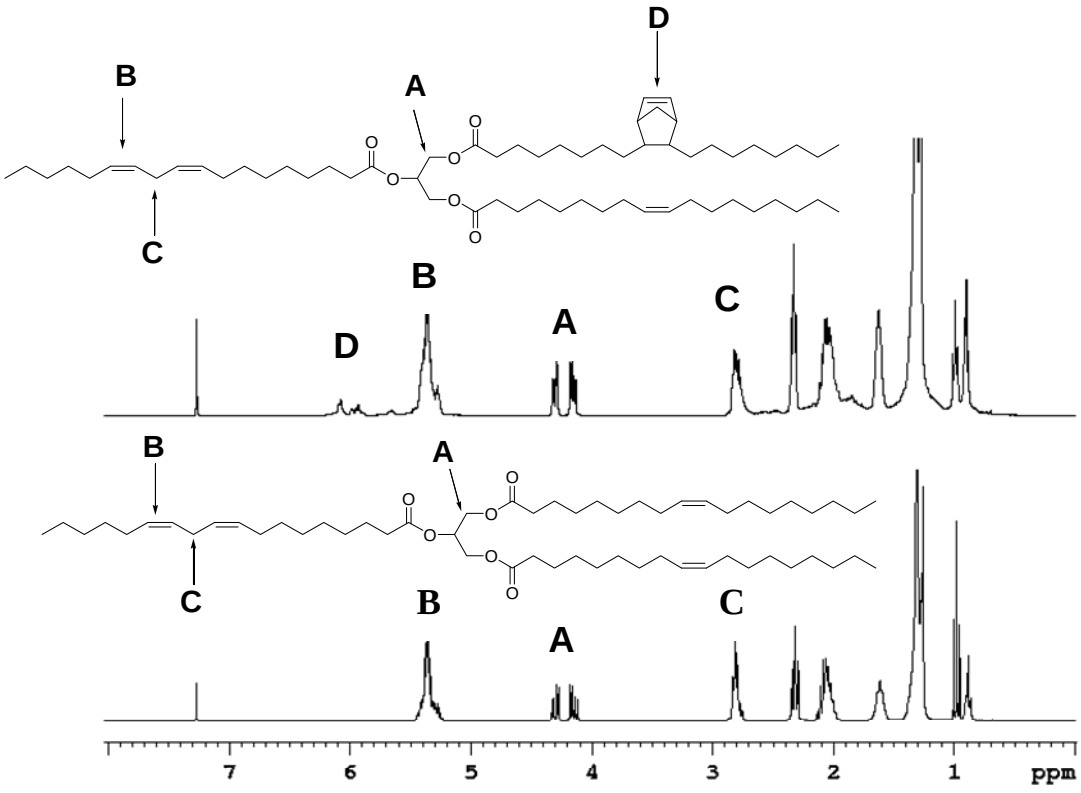

Figure 3. ^{1}H NMR Spectra of Pure Dilulin and Pure Linseed Oil

oils that correspond to both the vinylic protons in the fatty acid chains and the methine proton in the glycerol moiety. The peaks at 6.1 ppm and 6.2 ppm for Dilulin are due to a norbornene moiety. The integration of these peaks reveals an average of 1 norbornene per triglyceride. In actuality the norbornene number for any particular triglyceride may vary from 1-6 as was found in previous work with norbornylized oils, however molecules ranging from 3 to 6 norbornene moieties are quite low in number.[15] The small peak at 5.65 ppm is that of either the cyclopentene portion of the residual DCPD (proven from TLC) or that of an ene-type reaction (discussed later). Figure 4 shows the ^{13}C NMR spectra of Dilulin and regular linseed oil. Peaks that are characteristic of the norbornene moiety appear in the Dilulin spectrum at

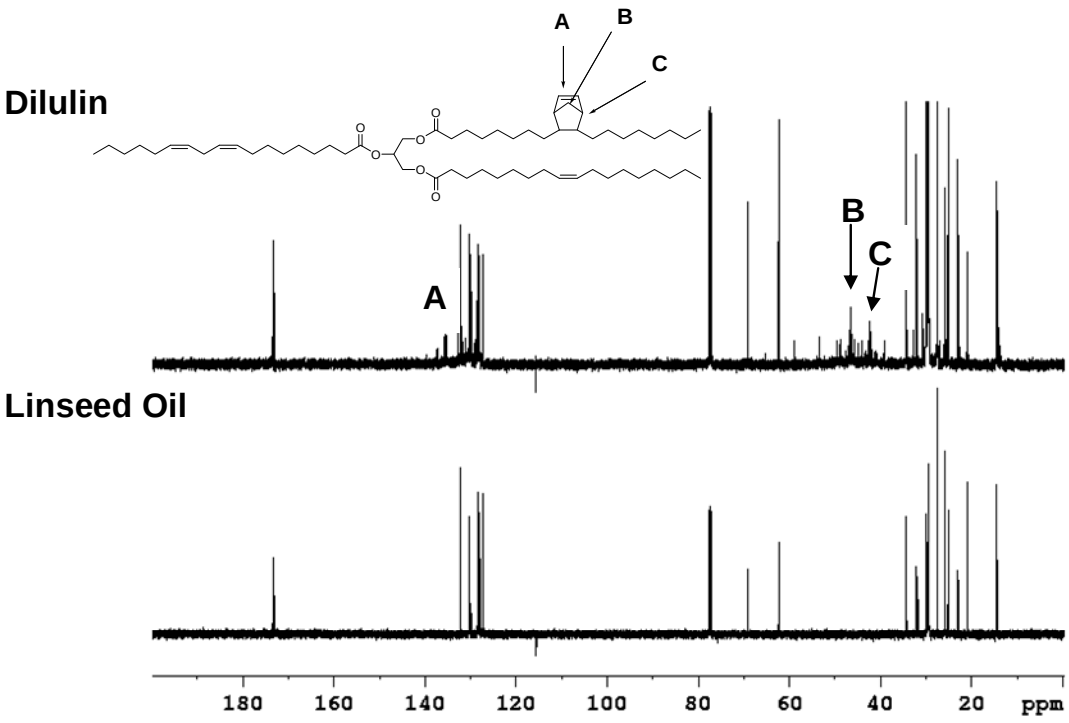

Figure 4. ^{13}C NMR Spectra of Pure Dilulin and Pure Linseed Oil

136 ppm (A) for the vinylic carbons and 48 ppm (B) for the methylene carbons of the ring. In addition to these peaks, a peak corresponding to the bridgehead carbon appears around 42 ppm (C).

Figure 5 shows the FT-IR spectra of both regular linseed oil and Dilulin. Evidence for incorporation of the norbornene unit is seen by the presence of a small peak at 1570 cm^{-1}. The purified Dilulin also has this peak, indicating that it is not due to residual DCPD. Most vegetable oils have naturally occurring cis double bonds. Regular linseed oil and Dilulin are no exception to this with a peak at 725 cm^{-1}. However, the Dilulin also indicates the presence of a trans double bond detected at approximately 970 cm^{-1}. We believe this is due to two possible isomerization routes. One route involves isomerization of the double bond by an

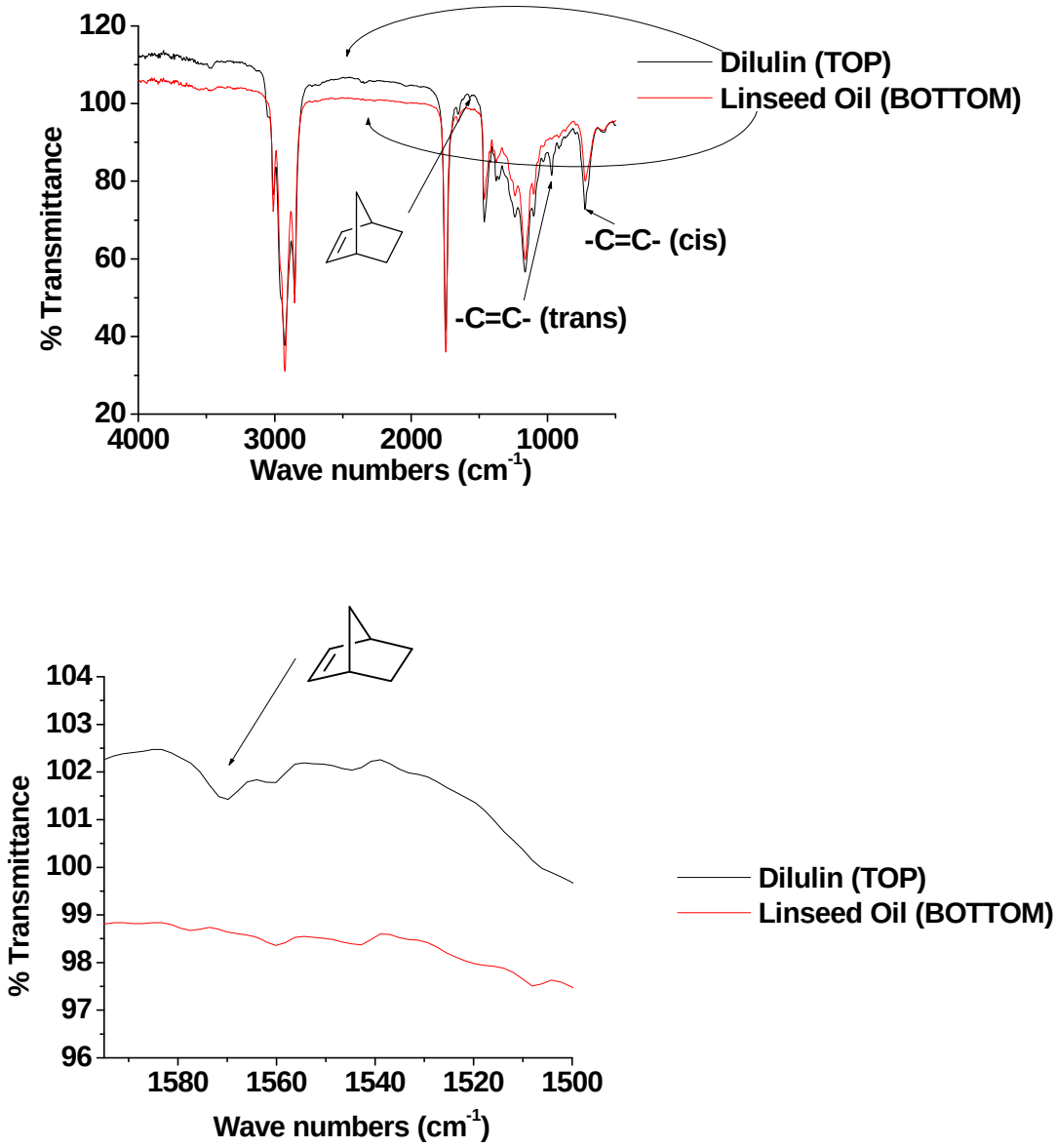

Figure 5. FT-IR Spectra of Pure Dilulin and Pure Linseed Oil (Top) and Enlargement of the Norbornene Region (Bottom)

ene-type reaction between the bis allylic hydrogens in the oil and cyclopentadiene (Figure 6) during the synthesis, which would allow for the formation of a trans double bond and a cyclopentene moiety. This is further evidenced in the ^{1}H NMR spectrum by a peak at 5.65

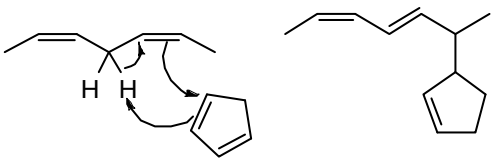

Figure 6. Ene Reaction between Cyclopentadiene and the Bis-Allylic Hydrogens

ppm (Figure 3) corresponding to a cyclopentene moiety. A similar reaction involving the bis allylic protons in a vegetable oil with maleic anhydride has been reported previously.[16] The second route may be a thermally related isomerization of the double bonds at the high temperature used to synthesize Dilulin. Both of these could be responsible for the trans double bond.

From these characterization techniques, we have determined that 1) Dilulin is a mixture of the desired oil containing the unsaturated norbornene-like moiety and DCPD or copolymers thereof; 2) there is an average of 1 bicyclic moiety per triglyceride; and 3) during the synthesis of Dilulin two possible isomerization routes occur; an ene-type reaction of the oil with cyclopentadiene introducing a cyclopentene group into the oil causing isomerization of the double bonds, and/or a thermally related isomerization of the double bonds in the triglyceride oil.

To verify that the Dilulin does have an unsaturated bicyclic moiety that can undergo ROMP, regular linseed oil and a 50:50 (wt %) mixture of regular linseed oil and DCPD were polymerized in the presence of 0.125 wt % Grubbs catalyst. Neither of these resulted in any desirable crosslinked thermoset. Rather, the pure linseed oil gave an oily substance and the 50:50 mixture also yielded an oily substance with a weak film on top. All of the Dilulin thermosets presented in this study, including the one comprised of pure Dilulin, resulted in

desirable crosslinked thermosets, proving that Dilulin does indeed possess an unsaturated bicyclic moiety capable of undergoing ROMP.

Optimization of Catalyst Concentration. The first step in this study was to determine the optimum concentration of catalyst. In our previous work utilizing the bicyclic castor oil (BCO) and cyclooctene, we found the best concentration of Grubb's second generation catalyst for all of the thermosets explored to be 0.5 wt %.[10] This, however, is a large concentration of catalyst and is a hindrance for scale-up. In this study, the concentration of catalyst was reduced as low as 0.03 wt % and studied up to 0.25 wt % while using the Dil50-DCPD50 composition. All of the concentrations employed did produce a crosslinked material. However, the sample that used 0.03 wt % catalyst was still quite oily after the curing sequence. Soxhlet extraction analysis of the resulting thermosets prepared using various concentrations of catalyst was employed to determine how effective each catalyst concentration was at producing a crosslinked thermoset. Table 1 shows the soluble portions obtained for each of the varying catalyst contents. At 45% soluble materials, the 0.03 wt % sample has the greatest soluble fraction, yet this value is actually lower than what it should

Table 1. Effect of Catalyst Concentration on the % Soluble Fraction

catalyst concentration	% sol	% insol
0.03 wt %	45	55
0.06 wt %	22	78
0.125 wt %	21	79
0.25 wt %	19	81

be, since the sample was quite oily and some of the residual surface oil was lost while weighing the sample. Table 1 reveals that as the catalyst concentration was increased from 0.06 wt % to 0.125 wt % to 0.25 wt %, the soluble fraction was 22%, 21% and 19%, respectively. A more detailed analysis of the compositions of these soluble fractions will be

discussed later. Figure 7 shows the ^{1}H NMR spectra of the soluble fractions with different catalyst concentrations. The sample with 0.03 wt % catalyst still possesses protons corresponding to the unsaturated bicyclic moiety, indicating this concentration of catalyst is too low to allow for efficient incorporation of Dilulin into the thermoset. All of the other

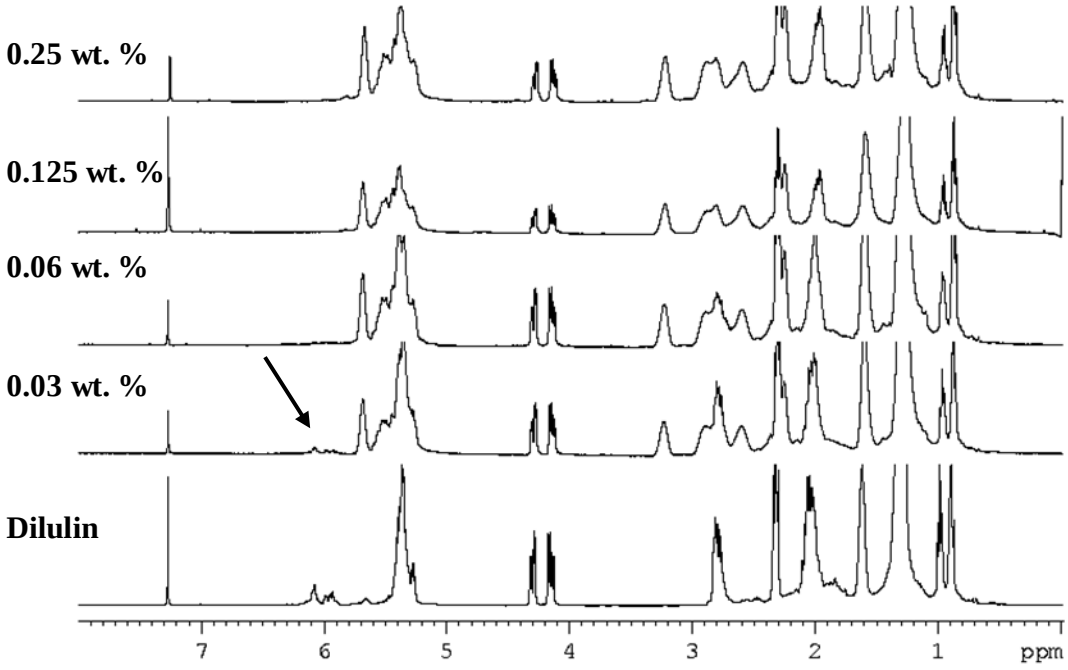

Figure 7. ^{1}H NMR of Different Catalyst Concentrations

samples with differing catalyst concentrations have undergone ring opening and incorporation of the unsaturated bicyclic moiety of the oil into the thermoset. With this data in hand, the optimum catalyst concentration chosen was 0.125 wt %. Even though the 0.06 wt % sample has roughly the same soluble portion as the 0.125 wt % and 0.25 wt % samples, this amount of catalyst failed to produce desirable thermosets when greater than 50 wt % of

the oil was used. Since the goal of this study was to examine the range of oil incorporation into the thermosets, 0.125 wt % catalyst was chosen as the "optimum" concentration.

Extraction Analysis. Table 2 shows the extraction analysis carried out on these Dilulin-DCPD thermosets. It can be seen that as the amount of oil increases the soluble fraction or unreacted component also increases from 21 wt % for the Dil50DCPD50 specimen to 28 wt % for the Dil100 specimen. Surprisingly, this is a rather small difference (approximately 7 wt %). Nonetheless, Dilulin's reactivity is lower than DCPD's. This is attributed to the fatty acid chains, which may hinder coordination between the catalyst and the norbornene moiety of the Dilulin. Figure 8 shows the ^{1}H NMR spectra of extracts from the thermosets along with the spectrum of pure Dilulin. The extracts look to be either oligomers of a Dilulin-DCPD copolymer, unreacted triglyceride oil, or both. These oligomers may indeed be cyclic in nature, as this is a common occurrence in ROMP polymerizations.[17]

Table 2. DMA, TGA and Extraction Data

Sample	T_g[a] (ºC)	Tan δ	25 ºC St Mod (MPa)	T_{10} (ºC)	T_{50} (ºC)	T_{max} (ºC)	% sol	% insol
Dil50DCPD50	36(64)	0.64	228	427(426)	461(461)	462(461)	21	79
Dil70DCPD30	-9(27)	0.67	6.35	414(385)	453(451)	462(457)	26	74
Dil90DCPD10	-30(-14)	0.75	1.88	362(348)	440(441)	459(457)	28	72
Dil100	-29(-4)	0.71	-	376(344)	438(437)	459(457)	28	72

[a] corresponds to the larger peak if phase separated

As the amount of DCPD in the feed ratio of the thermoset increases, the intensity of the peaks at 2.6 ppm, 2.8 ppm, 3.15 ppm, 5.45 ppm and 5.65 ppm, which correspond to oligomers containing DCPD, increase. Proof that the peaks correspond to oligomers or low molecular weight polymer is provided by the broadening of the peaks at 2.6 ppm, 2.8 ppm and 3.15 ppm, which usually indicates oligomer or polymer formation. The peak at 5.45 ppm

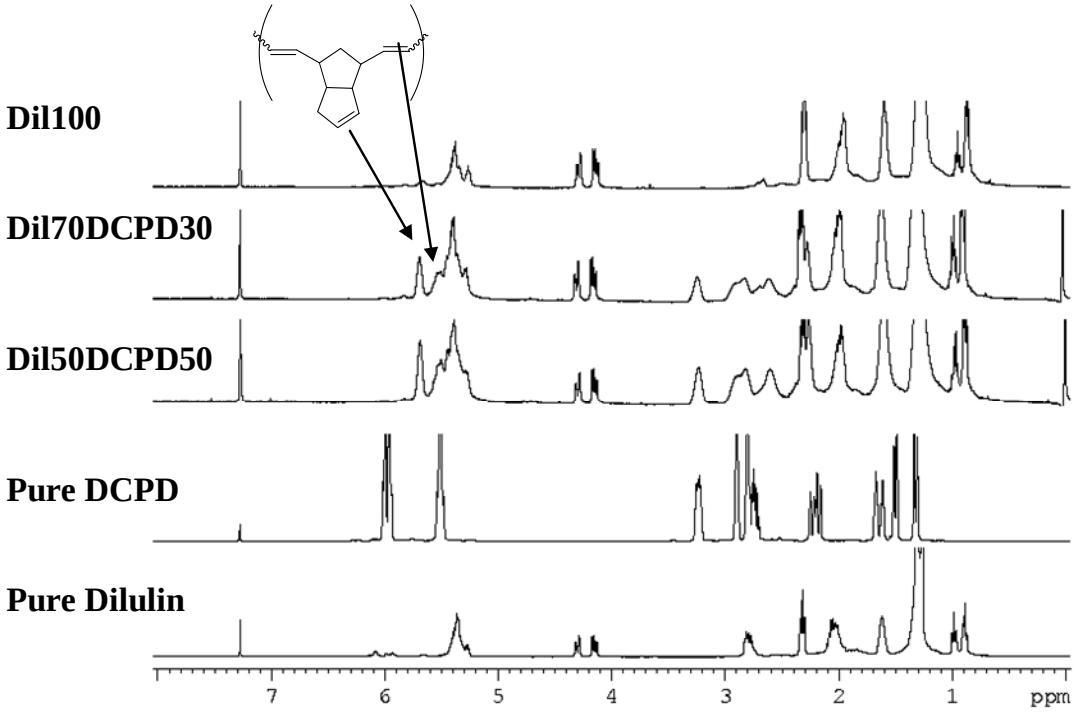

Figure 8. ^{1}H NMR Spectra of the Dilulin-DCPD Extracts

corresponds to the metathesized carbon-carbon double bond portion of the polymeric backbone. The peak at 5.65 ppm corresponds to the cyclopentenic vinylic hydrogens of the DCPD. This peak is fairly intense when DCPD is employed in the feed ratio. When no DCPD is used, as in the Dil100 sample, the extract looks to be mainly comprised of unreacted triglyceride oil. This is evidenced by the absence of a peak at 5.45 ppm, which indicates no oligomerization, along with the absence of norbornyl peaks at 6.1 ppm and 6.2 ppm. The small peak at 5.65 ppm can be attributed to the ene-type product mentioned earlier.

It is interesting that when $CDCl_3$ is added to the Dil50DCPD50, Dil70DCPD30 and Dil90DCPD10 soluble fractions, small needle-like materials appear. These materials are insoluble in common solvents at room temperature and are thought to be lightly crosslinked

oligomeric species. ^{13}C NMR analysis (not shown) revealed the structure of these materials to be similar to those of the insoluble crosslinked thermoset, which will be discussed later.

Generally speaking, these thermosets have a high amount of soluble material (nothing less than 20 % soluble). One possible reason for this is that the catalyst, which is highly active, may initially favor the formation of cyclic oligomers. Once significant polymer formation and crosslinking occurs, many of these oligomers may still exist, resulting in the high soluble fraction. Indeed, it is known that in the ROMP of cycloalkenes the product consists of a high molecular weight portion and a low molecular weight portion that is comprised of cyclic oligomers.[17] Also, it has been shown that in the ROMP of *endo*-dicyclopentadiene with certain reactive catalysts, the formation of cyclic oligomers occurs within minutes and decreases with time, whereas high molecular weight polymer is formed only slowly.[18] These previous findings are applicable to these Dilulin-DCPD thermosets and may help to explain such a high soluble fraction. Another reason for the high soluble fractions present in these materials may be cross metathesis between the double bonds in the fatty acid chains and the growing polymeric network. It has been shown that the Grubbs second generation catalyst is quite effective at the cross metathesis of internal olefins.[19] This could effectively reduce crosslinking and thus reduce incorporation of the Dilulin and DCPD into the thermoset.

Both FT-IR and solid state ^{13}C NMR spectroscopy have been carried out on the insoluble crosslinked portions that remain behind after the extraction process. The FT-IR spectra of the insoluble Dil50DCPD50 sample and Dil100 sample are shown in Figure 9. It can be seen that the peak corresponding to the norbornene moiety at 1570 cm^{-1} in both insoluble portions is gone, suggesting a ring opened product in the crosslinked thermoset.

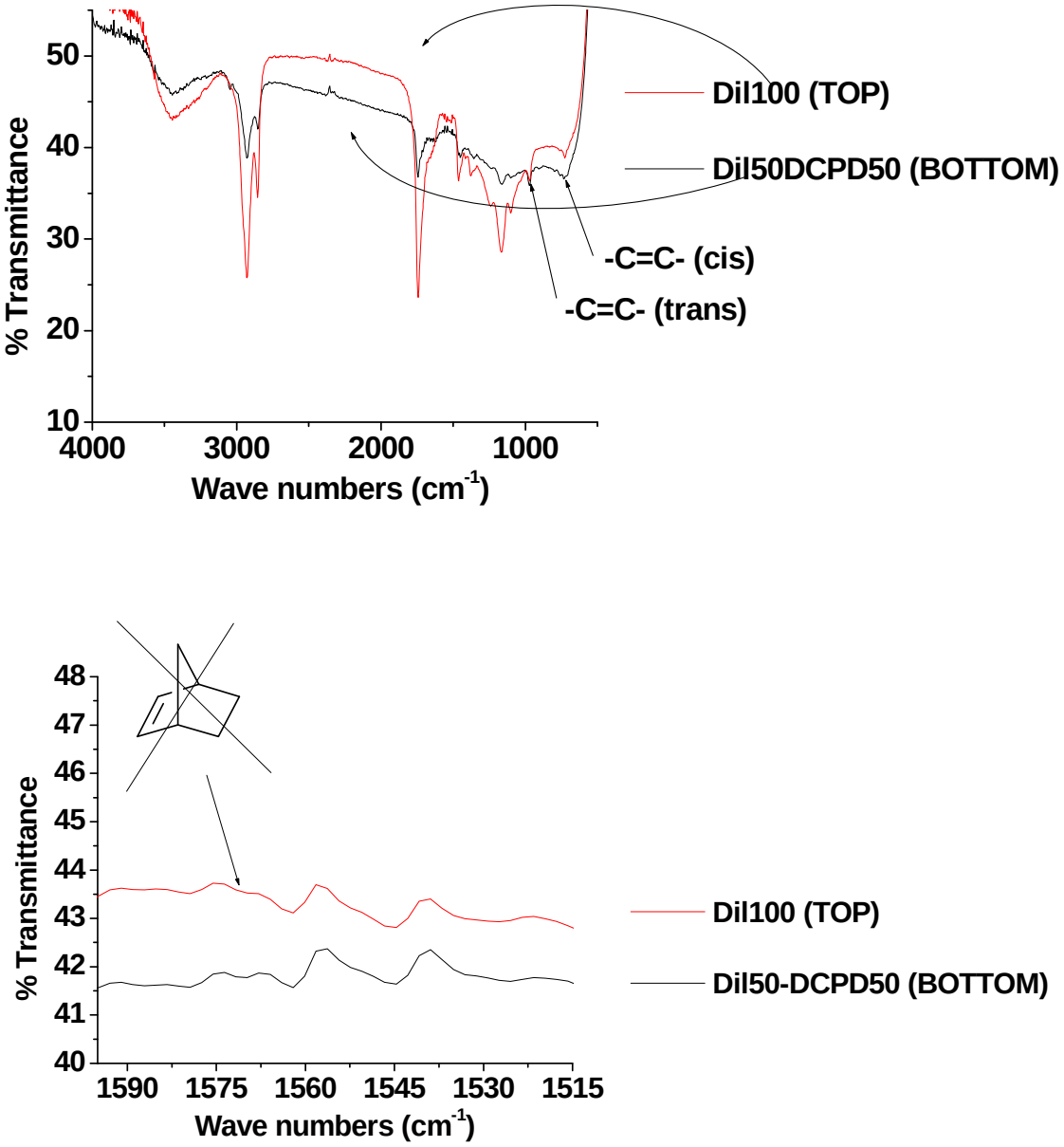

Figure 9. FT-IR Spectra of the Insoluble Portions of Dil50DCPD50 and Dil100 (Top) and enlargement of the Norbornene Region Indicating an Absence of Norbornene (Bottom)

Also both cis and trans double bonds can be seen around 725 cm^{-1} and 970 cm^{-1}, respectively. However, we cannot say with certainty whether the cis and trans peaks are due to the

metathesized carbon carbon double bonds or to the carbon carbon double bonds in the fatty acid side chains.

^{13}C NMR spectral analyses carried out on the insoluble portions of the Dil70DCPD30 and Dil100 samples have proven inconclusive as far as determining the cis and trans configurations in the thermoset. Figure 10 shows the presence of carbon carbon double bonds around 129-134 ppm (A) for both samples. But, because of the breadth of the peaks,

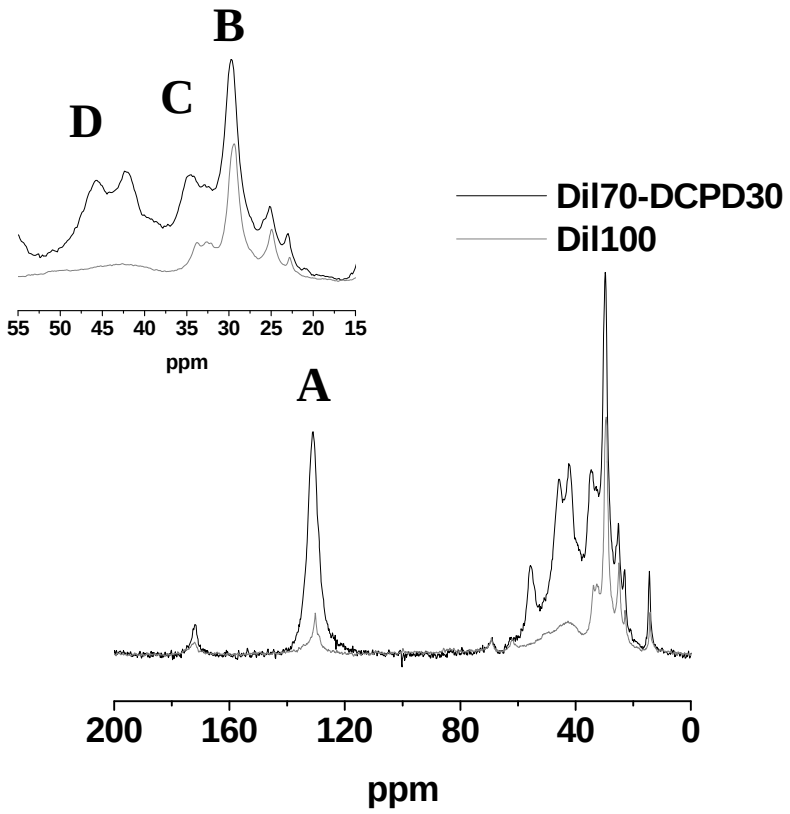

Figure 10. ^{13}C NMR Spectra of Dil70DCPD30 and Dil100

determining whether they are cis or trans is difficult. In addition, these olefinic peaks can either be from the metathesized carbon carbon double bonds or from the carbon carbon double bonds that occur naturally in the oil. If attention is directed towards other (non-

vinylic) peaks (B, C, D) in the ^{13}C NMR spectrum to aid in elucidation of the cis/trans configuration, one has the daunting task of determining what peaks are associated with the triglyceride itself or part of the DCPD portions. Given all of the various possibilities from ^{13}C NMR spectral analysis, along with the FT-IR analysis, coupled with previous literature showing poor stereoselectivity in the ROMP of DCPD using the Grubbs second generation catalyst,[20] unfortunately we cannot accurately determine what the cis/trans ratio of the polymeric backbone is.

Thus extraction analysis shows that the resulting thermosets are composed of 1) a soluble fraction that is mainly composed of oligomers of Dilulin and DCPD, triglyceride oil or both; and 2) a crosslinked polymeric network containing both monomers of Dilulin and DCPD (if it was used). The cis/trans configuration of the crosslinked network was unable to be elucidated, and it is assumed that it is rather random. The impact of Dilulin incorporation and the % soluble fraction will be looked at in the next section pertaining to DMA.

Dynamic Mechanical Analysis. Dynamic mechanical analysis (DMA) has been carried out on the polymeric samples using single cantilever and film/fiber tension modes. Both methods give similar T_g values, and for simplicity we will report only the single cantilever results. The T_g's were based of the maximum peak height of the tan δ curves. As seen in Table 2, the glass transition temperatures (T_g) decrease from 36 ºC to -29 ºC as the concentration of the oil in the sample increases. This is most easily explained by the increasing amount of unreacted oil (soluble fraction) that can plasticize or soften the thermoset, resulting in a lower T_g. In addition, with larger concentrations of oil incorporated into the final thermoset, a decrease in T_g can also occur, because of the increased number of fatty acid chains in the oil that can internally plasticize the thermoset.[21]

Figure 11 shows the DMA curves for the analyzed specimens. It can be seen that the Dil100 curve has a relatively narrow single peak. The Dil50DCPD50, Dil70DCPD30 and Dil90DCPD10 samples have broad curves with two peaks, which indicate phase separation. In these curves, the lower T_g peak corresponds to a more oil-rich phase and the higher T_g peak corresponds to a more DCPD-rich phase. In addition the tan δ values for the lower T_g peaks are greater than the higher T_g peaks, pointing to less stiffness and crosslinking in these oil-rich regions. As for the Dil100 sample, no phase separation was seen with the

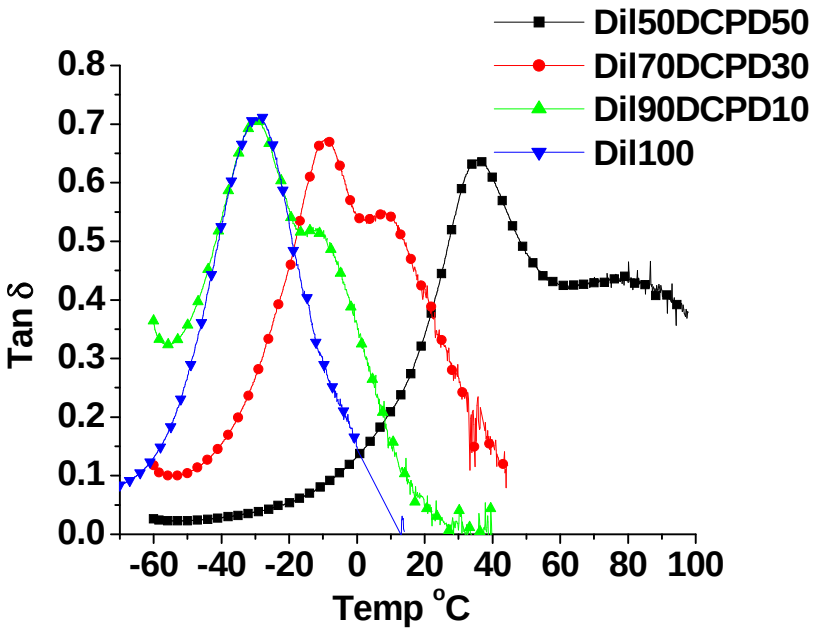

Figure 11. Tan Delta Curves For the Non Solvent-Extracted Samples

homopolymer of the thermoset. The phase separation is likely due to the differences in reactivity of the Dilulin and DCPD. The tan δ values for all of these samples range from 0.65 to 0.72. The Dil50DCPD50, Dil70DCPD30 and Dil90DCPD10 materials could be attractive

in damping applications, since their tan δ values are all above 0.3 and cover a temperature range of 60 ºC.[22]

Also in Table 2 are the storage modulus values at room temperature. The storage modulus of the Dil50DCPD50 sample is much higher than the other samples. This is attributed to the fact that at room temperature the Dil50DCPD50 sample is below its T_g and not in the rubbery plateau, as compared to the other samples, thus giving rise to a high storage modulus (Figure 12). The Dil50DCPD50 sample has not yet reached its rubbery

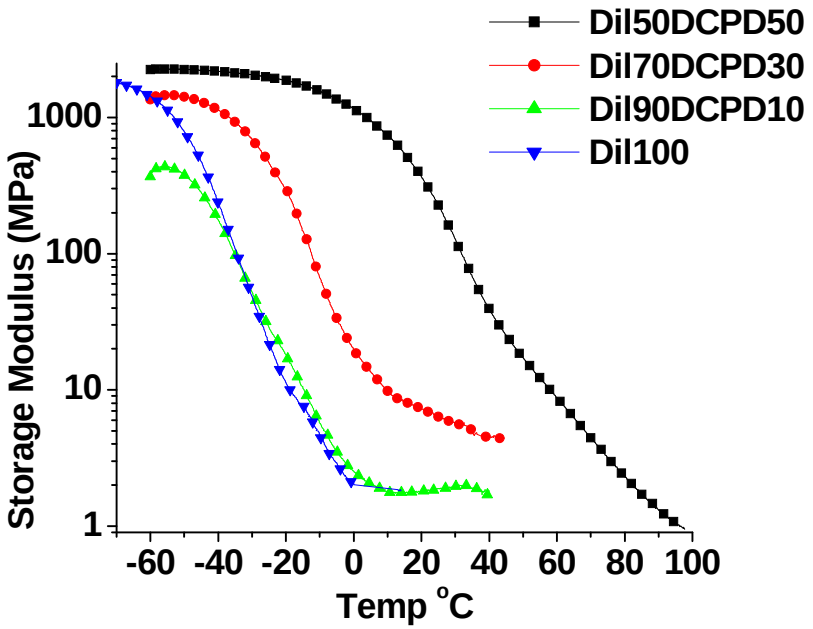

Figure 12. Storage Modulus Curves for the Non Solvent-Extracted Samples

plateau at 100 ºC, whereas the Dil70DCPD30 and Dil90DCPD10 samples have reached their rubbery plateaus around 10 ºC and then break around 40 ºC, indicating the weakness of these samples. The Dil100 sample, which broke before 20 ºC, has the consistency of gelatin and is quite weak.

We have also explored the effect of the soluble fraction as a plasticizer. In general, a plasticizer is usually a high boiling, oily organic liquid that is mixed with a polymer to impart softness or flexibility, which in turn lowers the T_g.[21] To measure the plasticizing effect of the oil in our system, samples were extracted in a soxhlet extractor for 24 h and then dried in a vacuum oven at 70 ºC overnight. The solvent-extracted samples, which possess cracks and small voids after the extraction process, are less flexible than their non solvent-extracted counterparts. The glass transition temperatures of these samples are shown in parentheses in Table 2. As one can see, the plasticized samples have a lower T_g than those with no plasticizer (solvent-extracted), which follows the expected trend. The Dil90DCPD10 and Dil100 samples still possess relatively low T_g's. This is due to both the higher content of the flexible triglyceride oil in the crosslinked polymer backbone, which contains fatty acid chains that plasticize (internally) the thermoset, and to the lower content of the rigid crosslinker DCPD.

In looking at Figure 13, it can be seen that the tan delta curves for the solvent-extracted samples seem to possess some of the phase separation seen in the non solvent-extracted samples. However, the differences in peak heights of the oil-rich and DCPD-rich portions in the tan δ curves of these two materials are quite different. This indicates removal of the soluble fraction and points to the possibility of plasticizer molecules (namely the unreacted triglyceride oil or oligomers thereof) becoming more entangled with the fatty acid side chains in the oil-rich regions of the thermoset. In effect, this enhances the tan δ values of the oil-rich regions in the non solvent-extracted samples, creating a larger difference in tan δ between the oil-rich and DCPD-rich regions.

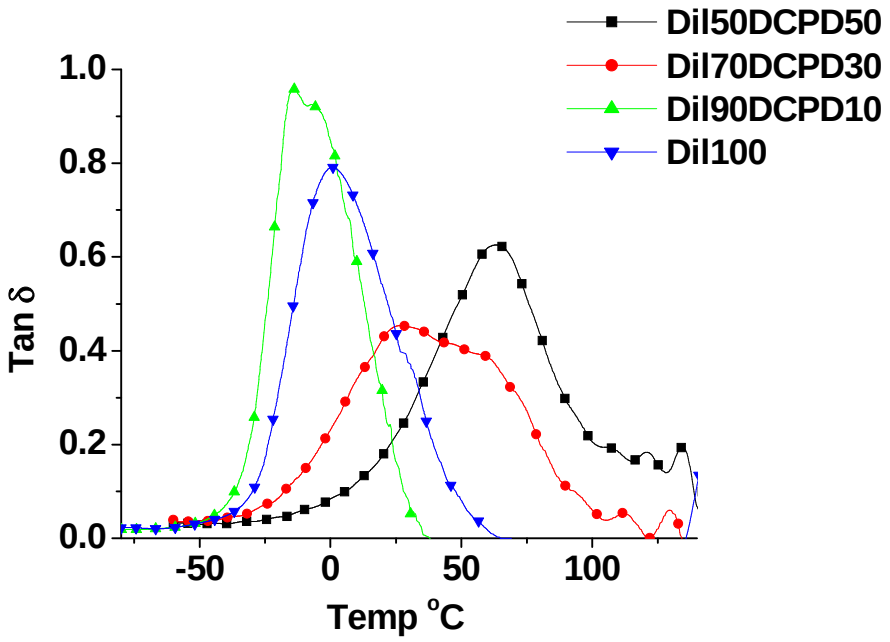

Figure 13. Tan Delta Curves for the Solvent-Extracted Samples

Thermogravimetric Analysis. Thermogravimetric analysis has been carried out on these thermosets. Figure 14 shows the degradation curves of the thermosets in air. A three stage degradation curve can be seen for the thermosets. The first stage from 200 ºC to 400 ºC is degradation of the triglyceride oil or free fatty acid components that remain in the crosslinked thermoset. The second stage (400 ºC to 500 ºC) is where maximum degradation occurs, and represents degradation of the crosslinked thermoset. The third stage (between 500 ºC and 650 ºC), consists of a short-lived plateau whose height in terms of weight %, is greater when greater amounts of DCPD are present in the thermoset. Degradation of the third stage is that of the char which remains behind.

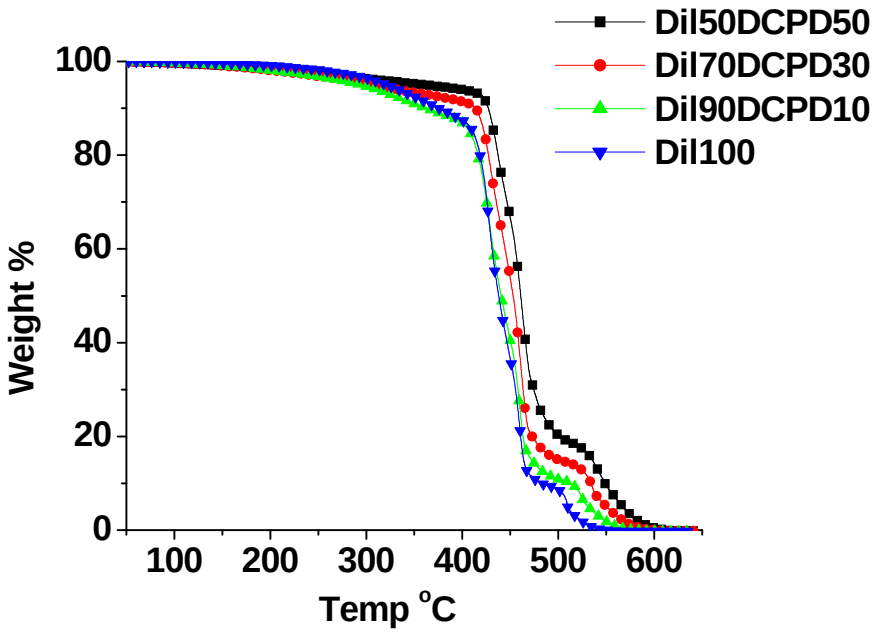

Figure 14. TGA Analysis of the Non Solvent-Extracted Samples

The T_{10} and T_{50} values (temperatures of 10 % and 50 % weight loss) have been determined in order to evaluate the thermal stability of the bulk polymer and the consistency of crosslinking in the bulk polymer, respectively.[23] Table 2 reveals that, with the exception of the Dil100 sample at T_{10}, all of the samples have decreasing T_{10} and T_{50} values with increasing amounts of oil and decreasing amounts of DCPD crosslinker. This trend is more pronounced in the T_{10} values for the Dil90DCPD10 and Dil100 samples, which have T_{10} values below 400 ºC. The reason for this is that the bulk polymer for these samples is greater in oil content. The oil portions of the backbone are not as thermally stable as those containing DCPD thereby giving a lower T_{10}. The T_{max} values are shown in Table 1 as well. All of these samples have roughly the same T_{max} values around 460 ºC. Without any valid method to test for this, we are assuming at this time that this is related to thermal crosslinking of the double

bonds in the fatty acid chains or metathesized carbon carbon double bonds, yielding roughly equal thermal stability among the samples in this region.

Thermogravimetric analysis has also been performed on the solvent-extracted thermosets. Figure 15 shows the same three stage degradation curves as in the non solvent-extracted samples. The solvent-extracted samples follow a trend similar to the non solvent-

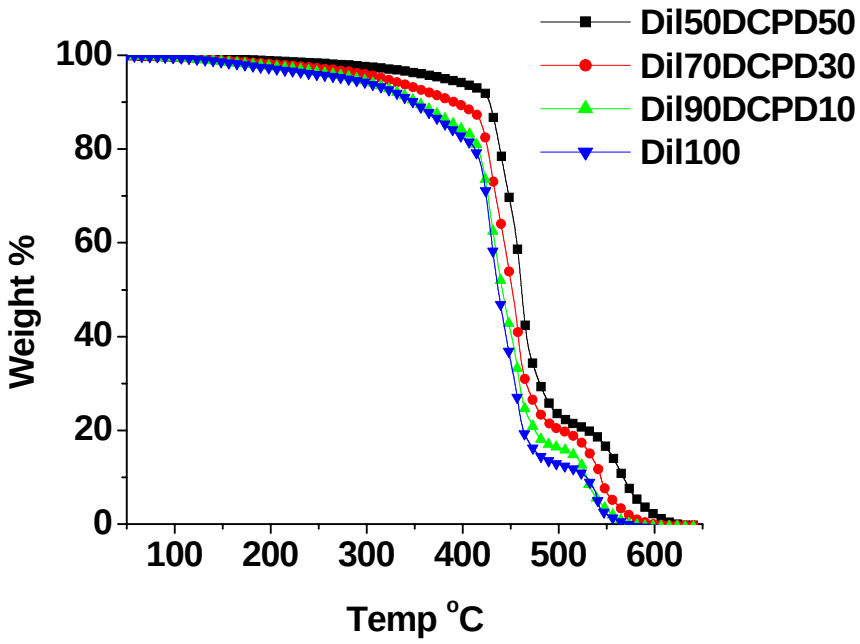

Figure 15. TGA Analysis of the Solvent-Extracted Samples

extracted samples in terms of the T_{max} values, in that all of the samples, regardless of the oil concentration, have similar values. Again, we attribute this to thermal crosslinking occurring during the temperature ramp of the thermogravimetric analysis. The T_{50} values decrease with decreasing DCPD crosslinker content, revealing less crosslinking in the bulk polymers that

contain increased amounts of oil. The T_{max} and T_{50} values for the solvent-extracted and non solvent-extracted samples are the same. However, a major difference between the solvent-extracted and non solvent-extracted samples is seen in the T_{10} values. The solvent-extracted T_{10} values are lower than the non solvent-extracted samples. A plausible reason for this is a synergism between the soluble fraction and the bulk polymer, which enhances the thermal stability of the non solvent-extracted thermosets in this temperature region. It has been stated that the stability of a polymeric matrix is related not only to the characteristics of the polymer, but also to the various interactions between the macromolecules and molecules[24] (i.e. the polymer and the plasticizer). Thus, a positive synergistic effect between the soluble fraction and the bulk polymer may exist in this temperature region, which delays the degradation of the bulk polymer, yielding the higher T_{10} with the non solvent-extracted sample.

Conclusion

Dilulin, a commercially available modified linseed oil was characterized and found have an average of 1 norbornene per triglyceride and to be approximately a 95:5 mixture of the desired oil and unreacted DCPD and/or oligomers of DCPD. Unique materials have been synthesized by the copolymerization Dilulin and dicyclopentadiene (DCPD and characterized. The materials contain anywhere from 50 to 100 % of the oil. The different oil concentrations are responsible for the wide range of properties, such as % soluble fraction, T_g, storage modulus and thermal stability among the samples. The % soluble fraction did increase somewhat as the oil concentration is increased. However, it has been found that the soluble fraction is relatively high for all of these samples. This is attributed to cyclic oligomerization, cross metathesis occurring in the unsaturated fatty acid side chains or both caused by the reactive catalyst. DMA analysis reveals that increasing the oil content and decreasing DCPD

content results in samples with lower T_g's. Solvent-extraction analysis reveals that the soluble fraction acts as a plasticizer, as do the fatty acid side chains incorporated into the thermoset that internally plasticize these materials. The samples have T_{max} values that are all relatively similar, which we feel are due to the added stability imparted by the double bonds remaining in the thermoset. The % soluble fraction looks to interact synergistically with the bulk polymer in the T_{10} region, as was shown with the greater T_{10} values for the non solvent-extracted samples. We look forward to continuing to work with these materials by improving oxidative stability with the use of additives and by further enhancing mechanical properties by using different reinforcing fibers and fillers.

Acknowledgements

The authors gratefully acknowledge Cargill for the generous donation of Dilulin. We would like to thank the United States Department of Educations GAANN fellowship financially supported this research. We are thankful to Dr. Michael Kessler from the materials science and engineering department at Iowa State University for his thoughtful discussions and use of his thermal analysis equipment. In addition we thank Mr. Tim Mauldin from the chemistry department at Iowa State University for his thoughtful insight into this work.

References

[1] Johnson, J. *Chem. Eng. News*. **2006**, *84*, 35, 13-17.

[2] Knoth, G. *J. Am. Oil Chem. Soc*. **2006**, *83*, 823-833.

[3] [3a] For a review, see: *Natural Fibers, Biopolymers, and Biocomposites*; Mohanty, A.K.; Misra, M.; Drzal, L.T.; Eds.; CRC Press Taylor and Francis, Boca Raton 2005;

[3b] Zhang, J.; Jiang, L.; Zhu, L.; Jane, J.; Mungara, P. *Biomacromolecules* **2006**, *7*, 1551-1561.

[4] Ermann, U., Friedt, W., Lang, S., Wilfried, L., Machmüller, G.; Metzger, J.O.; Rüsch gen Klaas, M.; Schäfer, H.J.; Schneider, M.P. *Angew. Chem. Int. Ed.* **2000**, *39*, 2206-2224.

[5] [5a] Petrović, Z.S.; Wei, Z.; Javni, I. *Biomacromolecules* **2005**, *6*, 713-719; [5b] Zlatanić, A.; Petrović, Z.S.; Dušek, K. *Biomacromolecules* **2002**, *3*, 1048-1056; [5c] Javni, I.; Zhang, W.; Petrovic, Z.S. *J. Polym. Environ.* **2004**, *12*, 123-129; [5d] Guo, A.; Zhang, W.; Petrovic, Z.S. *J. Mat. Sci*. **2006**, *41*, 4914- 4920.

[6] [6a] Cakmakli, B.; Hazer, B.; Tekin, I.O.; Kizgut, S.; Kosal, M.; Menceloglu, Y. *Macromol. Biosci*. **2004**, *4*, 649-655; [6b] LaScalla, J.; Wool, R.P. *Polymer* **2005**, *46*, 61-69.

[7] [7a] Li, F.; Larock, R.C. *J. Appl. Poly. Sci.* **2001**, *80*, 658-670; [7b] Andjelkovic, D.D.; Valverde, M.V.; Henna, P.H.; Li, F.; Larock, R.C. *Polymer* **2005**, *46*, 9674-9685; [7c] Andjelkovic, D.D.; Larock, R.C. *Biomacromolecules* **2006**, *7*, 927-936; [7d] Li, F.; Hasjim, J.; Larock, R.C. *J. Appl. Poly.Sci.* **2003**, *90*, 1830-1838.

[8] [8a] Henna, P.H.; Andjelkovic, D.D.; Kundu, P.P.; Larock, R.C. *J. Appl. Poly. Sci.* **2007**, *104*, 979-985; [8b] Valverde, M.V.; Andjelkovic, D.D.; Kundu, P.P.; Larock, R.C. *J. Appl. Poly. Sci.* **2008**, *107*, 423- 430.

[9] [9a] Li, F.; Larock, R.C. *Biomacromolecules* **2003**, *4*, 1018-1025; [9b] Kundu, P.P.; Larock, R.C. *Biomacromolecules* **2005**, *6*, 797-806.

[10] Henna, P.H.; Larock, R.C. *Macromol. Mater. Eng.* **2007**, *292*, 1201-1209.

[11] Harned, A.M., Zhang, M., Vedantham, P. Mukherjee, S., Herpel, R.H., Flynn, D.L., Hanson, P.R. *Aldrichimca Acta* **2005**, *38*, 3-16.

[12] [12a] Novak, B.M.; Grubbs, R.H. *J. Am. Oil. Chem. Soc.* **1988**, *110*, 960-961; [12b] Hillmyer, M.H.; Grubbs, R.H.; Laredo, R.H. *Macromolecules* **1995**, *28*, 6311-6316 [12c] Davidson, T.A.; Wagener, K.B.; Priddy, D.B. *Macromolecules* **1996**, *29*, 786-788; [12d] Bielawski, C.W.; Grubbs, R.H. *Prog.Polym. Sci*. **2007**, *32*, 1-29.

[13] Kodali, D. U.S. Patent 6,420,322, 2002.

[14] Jones, A.S.; Rule, J.D.; Moore, J.S.; White, S.R.; Sottos, N.R. *Chem. Mater.* **2006**, *18*, 1312-1317.

[15] Chen, J., Soucek, M.D., Simonsick, W.J., Celikay, R.W. *Polymer* **2002**, *43*, 5379-5389.

[16] Eren, T.; Kuesefoglu, S.H.; Wool, R.P. *J. Appl. Poly. Sci.* **2003**, *90*, 197-202.

[17] Ivan, K.J.; Mol, J.C. *Olefin Metathesis and Metathesis Polymerization*; Academic Press: San Diego, 1997; p 54.

[18] Pacreau, A.; Fontanille, M. *Makromol. Chem*. **1987**, *188*, 2585-2895.

[19] Lehman, S.E., Wagener, K.B. *Macromolecules* **2002**, *35*, 48.

[20] Schaubroeck, D.; Brughmans, S.; Vercaemst, C. *J. Mol. Catal. A.* **2006**, *254*, 180-185.

[21] Wilson, A.S. *Plasticizers: Principles and Practice*; University Press: Cambridge, 1995; pp 1, 206-207.

[22] Li, F., R.C. Larock, *Polym. Adv. Technol.* **2002**, *13*, 436-449.

[23] Li, F., Hanson, M.V., Larock, R.C. *Polymer*, **2001**, *42*, 1567-1579.

[24] Sreedhar, B., Chattopadhyay, D.K., Sri Hari Karunakar, M., Sastry, A.R.K. *J. Appl. Polym. Sci.* **2006**, *101*, 25-34.

CHAPTER 5. FABRICATION AND PROPERTIES OF VEGETABLE OIL-BASED GLASS FIBER COMPOSITES BY RING OPENING METHATHESIS POLYMERIZATION

A Paper to be Published in Macromolecular Materials and Engineering

Phillip H. Henna[†], Michael R. Kessler[‡] and Richard C. Larock[†*]

[†]*Department of Chemistry, Iowa State University, Ames, IA, 50011, USA*
[‡]*Department of Materials Science and Engineering, Iowa State University, Ames, IA, 50011, USA*

Abstract

Glass fiber biobased composites have been prepared by the ring opening metathesis polymerization (ROMP) of a commercially available vegetable oil, possessing an unsaturated bicyclic moiety, and dicyclopentadiene (DCPD). The composites and the corresponding resins have been characterized thermophysically and mechanically. The resins are yellow, transparent and vary from being hard and strong to soft and flexible. The composites are also yellow, but are translucent. The effect of DCPD and glass fiber concentrations has been analyzed. The glass transition temperatures for both the resins and the composites range from 18 °C to 82 °C, with higher glass transition temperatures for resins and composites with higher DCPD content. Glass fibers significantly improve the tensile modulus of the resin from 28.7 MPa to 168 MPa and the Young's modulus from 525.4 MPa to 1576 MPa. These biobased composites utilize only a limited amount of expensive petroleum-based monomers, while employing a renewable resource.

Introduction

Energy, environmental and societal concerns have increased the interest in utilizing renewable plant-based materials as feedstocks for polymeric materials, while reducing our dependence on a volatile and unstable petroleum market. Furthermore, many renewable plant-based materials are cheaper than petrochemicals.[1] In recent years, considerable attention has focused on vegetable oils and derivatives as monomers to produce biobased polymers.[2]

Vegetable oil monomers are quite amenable to many different polymerization techniques, including free radical,[3] step growth,[4] cationic[5] and ring opening metathesis polymerization (ROMP).[6] The resulting biobased polymers offer unique and promising properties encouraging the replacement of petrochemical-based materials in some applications. Some such applications, however, require the use of fiber reinforcement or other fillers to further enhance the mechanical properties.

Fiber-reinforced polymer (FRP) composites are typically comprised of discontinuous reinforcing fibers surrounded by a polymeric matrix, which binds with the reinforcing fibers so that the load is supported and transmitted through the material from fiber to fiber.[7] FRP composites find numerous applications in the aerospace, automotive, industrial, infrastructure, marine, military, and sports fields.[8] They have the advantage of being lightweight, possessing good mechanical properties, being resistant to corrosion, and having a low assembly cost.[9]

FRP composites can employ either thermoplastic or thermosetting resins. For thermoplastic FRP's, the molten polymer is blended with the fiber and molded into the desired shape at an elevated temperature. Thermosetting resins are more commonly used as

the polymeric matrix in FRP composites, since they are suitable for injection molding, because of their relatively low viscosity before cure. After the thermosetting resin is injected into a mold with the desired shape, the monomers are heated until crosslinking occurs, which entraps the fiber in the polymeric network.[10]

Vegetable oil-based thermosetting resins have recently been used to make composite materials. We have reported the cationic polymerization of regular and conjugated corn[11] and soybean[10] oil-based glass fiber composites, and conjugated soybean oil[12] and conjugated corn oil[13] clay nanocomposites. More recently, we have employed spent germ, a by-product from ethanol production, as a filler in a tung oil-based composite.[14] Others have reported glass fiber-reinforced soy-based polyurethanes,[15] natural- and glass-fiber reinforced soybean phosphate ester polyurethanes,[16] and acrylated epoxidized soybean oil composites comprised of either butyrated kraft lignin[17] or natural fiber.[9,18]

Dilulin is a commercially available oil from Cargill prepared by a high temperature, high pressure Diels - Alder reaction between linseed oil and dicyclopentadiene (DCPD)

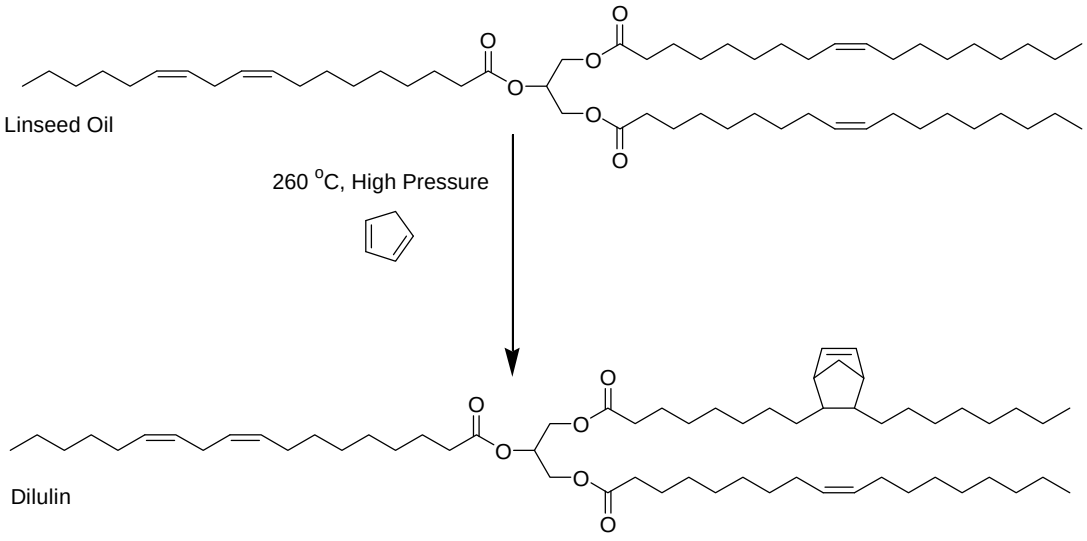

Figure 1. Synthesis and Structure of Dilulin

(Figure 1).[19] Dilulin appears to be a 95:5 mixture of the modified oil, possessing an average of one bicyclic moiety per triglyceride, and DCPD oligomers.[6b] We have reported the ROMP of Dilulin with DCPD (Figure 2) and other strained crosslinkers[20] to produce unique thermosetting resins. Utilizing DCPD, soft and flexible resins have been prepared, with sample flexibility increasing as the Dilulin content increased from 50 wt. % up to 100 wt. %

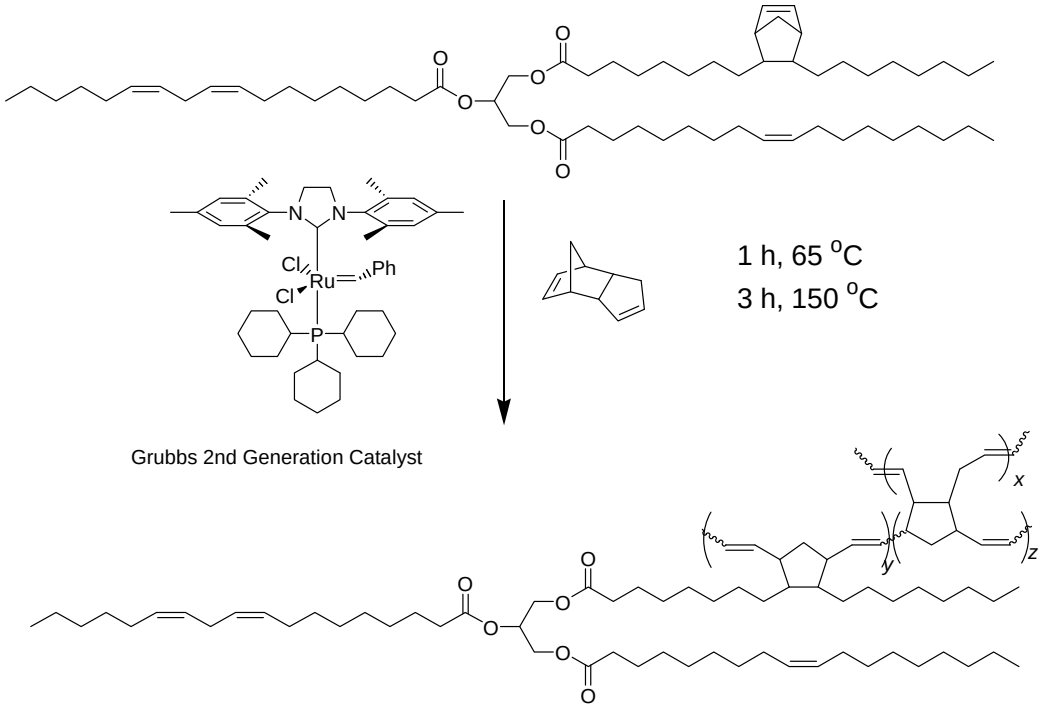

Figure 2. ROMP of Dilulin and DCPD

oil.[6b] Herein, we report the fabrication and thermal and mechanical testing of short glass fiber mat composites utilizing a Dilulin-DCPD resin. Differing ratios of Dilulin to DCPD have been explored, as has variation in the glass fiber content.

Experimental

Materials. The Dilulin was a gift from Cargill (Minneapolis, MN), which was used as received and stored in a refrigerator. Dicyclopentadiene (95%) was obtained from ACROS

(Geel, Belgium) and used as received. Grubbs second generation catalyst was obtained from Sigma Aldrich (Milwaukee, WI) and recrystallized by a procedure similar to that found in the literature[21] to allow better dissolution in the resin. Reagent grade methylene chloride, stabilized with amylene, was obtained from Fisher (Fair Lawn, NJ) and used as received. PTFE release agent (MS-122DF) was obtained from Miller-Stephenson Chemical Co. (Morton Grove, IL). The short glass fiber mat was a gift from Creative Composites (Brooklyn, IA).

Fabrication of Dilulin-DCPD Resins and Composites. The resins have been prepared on an 80 g scale. To a 100 mL glass beaker was added the appropriate amount (30 to 60 wt. %.) of Dilulin. To this was added the appropriate amount (in wt. %) of DCPD. The two monomers were stirred together at a high RPM in a fume hood. Then 0.125 wt. % (based upon the entire resin mixture) of the catalyst was added slowly portion-wise to the stirring monomer. After all of the catalyst was added, the mixture was allowed to stir for a few minutes and then poured into a glass mold, which consisted of two 6 inch (length) by 4 inch (width) glass plates, clamped and separated by a 1/8 inch rubber gasket. The mold was then placed in a programmable oven (Yamato Scientific America; San Francisco, CA) and cured for 1 h at 65 °C and post-cured 3 h at 150 °C. The nomenclature used is as follows: Dilulin is referred to as Dil and dicyclopentadiene is referred to as DCPD. For example, a resin containing 40 wt. % Dilulin and 60 wt. % DCPD is designated Dil40-DCPD60.

The composites have been prepared by cutting the short glass fiber chopped strand mat into 6 inch (length) by 5 1/4 inch (width) sheets. The sheets of glass fiber were then placed into a PTFE-coated 6 inch by 6 inch steel mold, containing two 6 inch (length) x 3/8 inch (width) x 1/8 inch (thick) spacers on opposite sites. The uncured resin (140 g) was

poured onto the glass fiber to ensure complete wetting. The top of the mold (also PTFE-coated) was then put in place and the mold placed into a pre-heated press (Carver; Wabash, IN) at 65 °C. Enough pressure was applied to allow some resin to be expelled out of the crevasses of the mold. When gelation onset was observed, the pressure was increased to 325 psi. This temperature and pressure were maintained for 1 h. The mold was then removed from the press and post-cured under atmospheric pressure in an oven for 3 h. After post-cure, the composite was allowed to cool and then weighed to determine the wt. % of glass fiber. In this study, when the resin composition of the composite was changed, a constant glass fiber loading of approximately 40 wt. % was used. The nomenclature employed for a composite with a resin composition of 60 wt. % Dilulin and 40 wt. % DCPD is Dil60-DCPD40c.

Soxhlet Extraction. Soxhlet extraction has been carried out on the pure resins and composites. Typically a 2.5 g specimen has been placed into a cellulose thimble and refluxed in methylene chloride at a temperature of 60 °C. After extraction, the insoluble portion was dried in a vacuum oven overnight at 70 °C and then weighed.

SEM. SEM analysis has been carried out using a Hitachi S-2460 N (Japan) variable pressure electron microscope at an accelerating voltage of 20 kV under a helium environment of 60 Pa to examine the morphology of the fracture surfaces of the composites after tensile testing

Dynamic Mechanical Analysis. Dynamic mechanical analysis (DMA) has been carried out on a Q800 DMA (TA Instruments; New Castle, DE) instrument in a three point bending mode with an amplitude of 25 μm, a preload force of 0.0100 N, and a force track of 150 %. Specimens were cut into rectangular shapes with a geometry of 20 mm x 10 mm x 1.8 mm (length x width x thickness). Each specimen was cooled to -60 °C and held isothermally at that temperature for 3 min. The sample was then heated at 3 °C/min to 250 °C.

Tensile Tests. Tensile tests were performed at 25 °C, according to ASTM standard D638, using an Instron universal testing machine (model 4502) at a crosshead speed of 5 mm/min. The dogbone-shaped test specimen (type I specimen ASTM D638) had a gauge section with a length of 57 mm, a width of 12.5 mm, and a thickness of 3 mm.

Results and Discussion

Extraction Analysis of the Resins. The pure thermosetting resins prepared varied from 40 wt. % (Dil60-DCPD40) up to 70 wt. % (Dil30-DCPD70) DCPD. All of the thermosetting resins are transparent with a yellow tint. As the concentration of DCPD increases in the feed ratio, the resins go from being soft and weak to quite hard and strong. Entries 1-4 in Table 1 show the soxhlet extraction analysis of these thermosetting resins. The soluble portion decreases from 17 wt. % to 10 wt. % as the DCPD concentration increases from 40 wt. % to 70 wt. %. These extracts are mixtures of oil, dicyclopentadiene oligomers, and unreacted

Table 1.

Entry	Composition	wt. % GF	T_g (ºC)	υ_e (mol/m^3)	25 ºC E' (MPa)	Soluble Fraction (%)	Insoluble Fraction (%)
1	Dil60-DCPD40	-	21	99	10	17	83
2	Dil50-DCPD50	-	39	198	187	16	84
3	Dil40-DCPD60	-	58	204	799	14	86
4	Dil30-DCPD70	-	76	382	1769	10	90
5	Dil60-DCPD40c	40	18	-	228	21	79
6	Dil50-DCPD50c	40	37	-	2380	21	79
7	Dil40-DCPD60c	40	58	-	6899	21	79
8	Dil30-DCPD70c	40	82	-	6384	20	80
9	Dil30-DCPD70c	32	83	-	6166	19	81
10	Dil30-DCPD70c	43	82	-	6384	20	80
11	Dil30-DCPD70c	56	84	-	8519	20	80

triglyceride oil[6b] (^{1}H NMR spectrum not shown). The soluble portion appears to act as a plasticizer, which softens the resin. The plasticizer (soluble portion) and the increased

amount of the flexible triglyceride monomer, containing fatty acid side chains that internally plasticize the resin, are responsible for the increased flexibility of the thermosetting resin with increasing Dilulin content. [22,23]

Thermophysical Properties of the Resins. Dynamic mechanical analysis (DMA) of both the pure resins and the composites using 3-point bending mode testing was used to obtain the storage moduli and loss factors (tan δ) as a function of temperature. The glass transition temperatures (T_g) were taken as the maximum peak height of the tan δ curve. Entries 1-4 in Table 1 and Figure 3 show the T_g's of the pure resins. As the concentration of DCPD increases in the crosslinked thermosets, the T_g increases substantially from 21 ºC to 76 ºC,

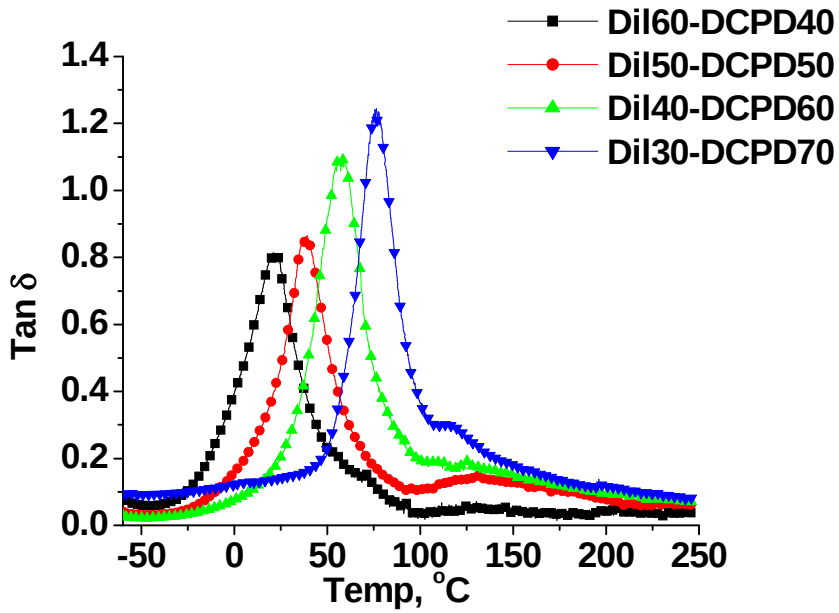

Figure 3. Tan δ Curves for the Pure Resins

due to the increased degree of crosslinking and crosslinking density (Table 1) provided by DCPD.[24] The experimental crosslinking densities (υ_e) have been calculated at 100 ºC above

the T_g in the rubbery plateau of the storage modulus curve using the following equation:

$$E' = 3\upsilon_e RT$$

where E' is the storage modulus in Pa, υ_e is the crosslink density, R is the gas constant and T is the absolute temperature in K.[25] Also the increased flexible triglyceride incorporation and the slightly greater soluble fraction in the resins possessing more oil leads to a plasticizing effect, softening the resins and hence lowering the T_g. The tan δ curves are much taller and narrower when more DCPD is used, indicating that these resins result in a more homogeneous network.[26] This is interesting, since crosslinking usually broadens the tan δ curve. However, it appears that the Dilulin, with its randomly placed norbornene groups in the fatty acid chains, causes a rather heterogeneous network in the backbone. In addition, some of the tan δ curves with less DCPD have a smaller peak or shoulder at higher temperatures. This points to phase separation in these resins.

Table 1 (entries 1-4) also shows the room temperature storage modulus (E') values for these resins. As the DCPD content of the resin increases, the room temperature storage modulus values increase from 10 to 1769 MPa. Since the storage modulus is a measure of the stiffness of a sample,[27] it is expected that samples possessing less flexible triglyceride oil and more rigid DCPD crosslinker would have higher storage modulus values than those samples with higher amounts of oil and less crosslinker. Figure 4 shows the storage modulus curves for these resins. There is a substantial decrease in storage modulus between 0 ºC and

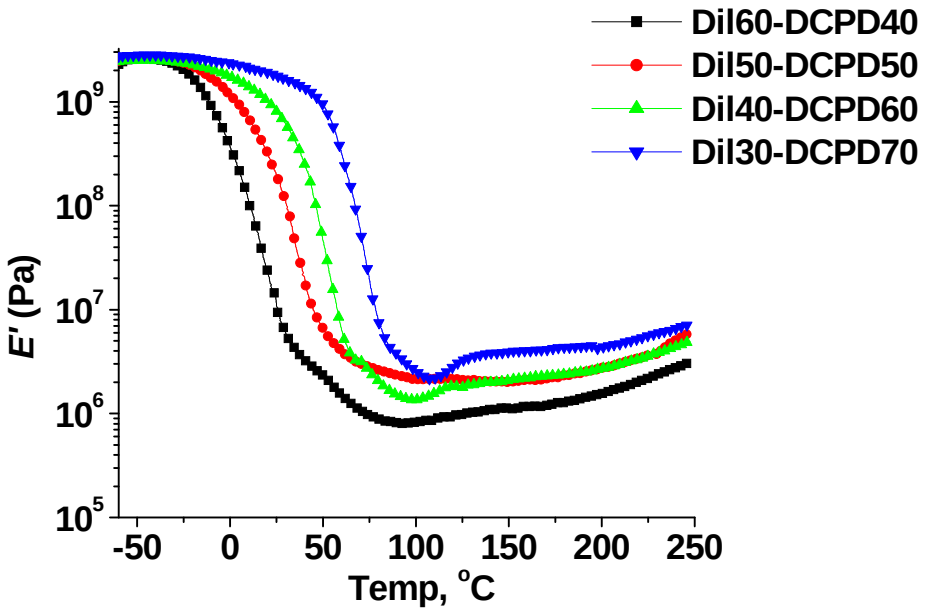

Figure 4. Storage Modulus Curves for the Pure Resins

75 ºC that is indicative of the primary relaxation (Tα) peak related to energy dissipation. This is also shown in Figure 3 with the tan δ peaks passing though a maximum in this region. The rubbery plateau modulus increases with increasing DCPD content as evidenced in Figure 4. This can be explained by the fact that resins with more DCPD have fewer free dangling side chains in the polymer network and a lower molecular weight between crosslinks (M_c), providing a more rigid material.[26]

Mechanical Testing of the Resin. The mechanical properties of the pure resins are shown in entries 1-4 in Table 2. The ultimate tensile strengths (σ_{max}) for these resins increase from 0.5 MPa to 29 MPa as the DCPD content increases and the sample decreases in flexibility. The value of 29 MPa for the Dil30DCPD70 sample is similar to the σ_{max} for some high density polyethylene specimens.[28] Figure 5 shows the stress vs. strain curves for all of the

samples. The Dil30-DCPD70 sample has a yield point and looks to be the only hard sample. The other

Table 2.

Entry	Composition	wt. % GF	σ_{max} (MPa)	*E* (MPa)	% ε_b	Toughness (MPa)
1	Dil60-DCPD40	-	0.5 ± 0.1	0.91 ± 0.1	138 ± 12	0.4 ± 0.1
2	Dil50-DCPD50	-	1.0 ± 0.1	27 ± 5	132 ± 15	1.1 ± 0.2
3	Dil40-DCPD60	-	7.0 ± 0.1	68 ± 11	156.0± 0.1	8.1 ± 0.1
4	Dil30-DCPD70	-	29.0 ± 0.3	525 ± 45	35 ± 7	7 ± 1
5	Dil60-DCPD40c	40	29.0 ± 0.1	680 ± 169	14 ± 1	2.7 ± 0.3
6	Dil50-DCPD50c	40	46 ± 4	615 ± 98	16 ± 2	4 ± 1
7	Dil40-DCPD60c	40	68 ± 37	1061 ± 209	10 ± 1	5 ± 1
8	Dil30-DCPD70c	40	145 ± 7	1510 ± 94	12 ± 2	8 ± 1
9	32 wt % GF	32	91 ± 7	1071 ± 92	10.0 ± 0.2	5.0 ± 0.3
10	43 wt % GF	43	148 ± 4	1545 ± 61	12 ± 2	8 ± 1
11	56 wt % GF	56	168 ± 7	1576 ± 46	12 ± 1	10 ± 1

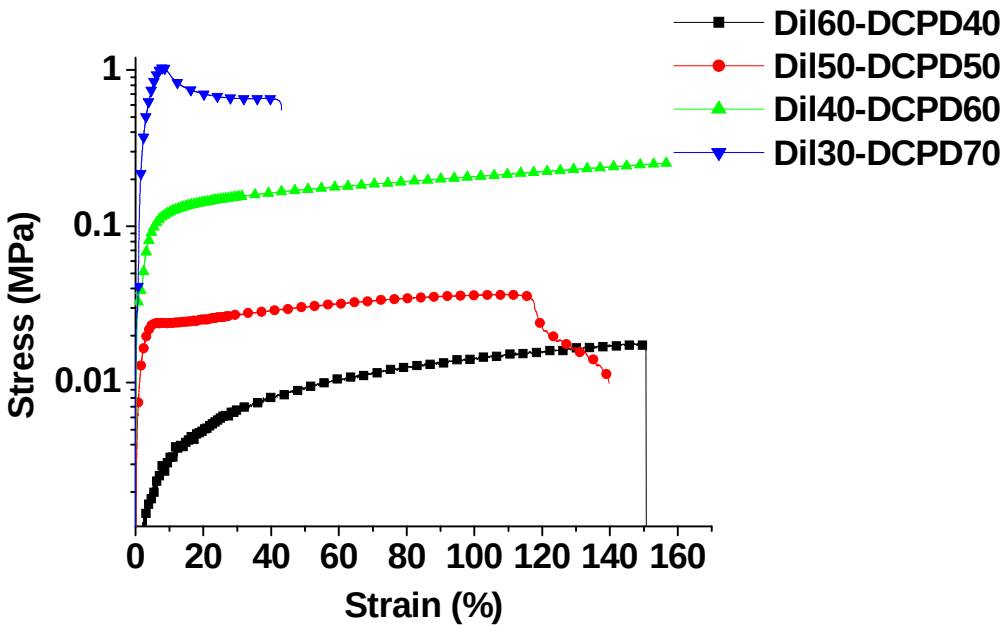

Figure 5. Stress vs. Strain Curves for the Pure Resins

samples behave as soft materials, which explains why the Young's modulus (*E*) for these thermosetting resins decreases substantially from 525 to 0.9 when decreasing the DCPD content from the Dil30-DCPD70 composition to the Dil60-DCPD40 composition. This is expected, since hard and strong samples (Dil30-DCPD70) have higher modulus (elastic deformation) values than soft and weak samples (Dil60-DCPD40), which have low modulus values. The samples with 40 and 50 wt. % oil lie in between, yet have relatively low Young's modulus values.

The percent elongation at break (ε_b) values given in Table 2 for entries 1-4 show that the hard and strong (Dil30-DCPD70) resin extends to about 35% its original length before breaking. The other samples containing 40 to 60 wt. % Dilulin have greater ε_b values, due to less DCPD crosslinker, which inhibits polymeric chain movement. The 40 wt. % Dilulin sample did not break, and the value in the % ε_b column is how far the sample extended before the instrument stopped testing. The toughness (defined as the area under the stress-strain curve) does not follow any general trend from resin to resin. However, the resins with more DCPD have a greater toughness than those samples with less DCPD (6.7 MPa for Dil30-DCPD70 versus 0.42 MPa for Dil60-DCPD40). This points to the increased crosslinking ability of DCPD, which helps to resist fracture and improve toughness.

Extraction Analysis of the Composites. The incorporation of chopped strand glass fiber (GF) into the various resins results in composites having an opaque yellow color. As the concentration of DCPD decreases in the resin, the composite becomes less stiff with the Dil60-DCPD40c composite possessing considerable flexibility. The composites show a decrease in the insoluble portion (Table 1, entries 5-8), indicating that the presence of glass fiber did hinder the polymerization and crosslinking of the resins. The latter interpretation is

supported by data for composites where a greater concentration of DCPD has been used. Interestingly, all of the resins with different crosslinker content have approximately the same insoluble portion of around 80%. Variation of GF using the same resin results in composites with the same insoluble portion (approximately 80%) as shown in entries 9-11 in Table 1.

Thermophysical Properties of the Composites. Figure 6 and entries 5-8 in Table 1 show the increase in T_g from 18 ºC to 82 ºC for composites with approximately 40 wt. % GF as the concentration of DCPD in the resin increases from Dil60-DCPD40c to Dil30-DCPD70c. This was expected, since a similar trend was seen in the pure resin. In addition to this, the Dil50-DCPD50c and Dil60-DCPD40c composites have shoulder peaks on the tan δ curves, indicating some phase separation. Also seen is an increase in room temperature storage modulus values from 228 MPa to 6384 MPa with increased amounts of DCPD, which was also observed earlier with the pure resins. The slight increase in storage modulus value in

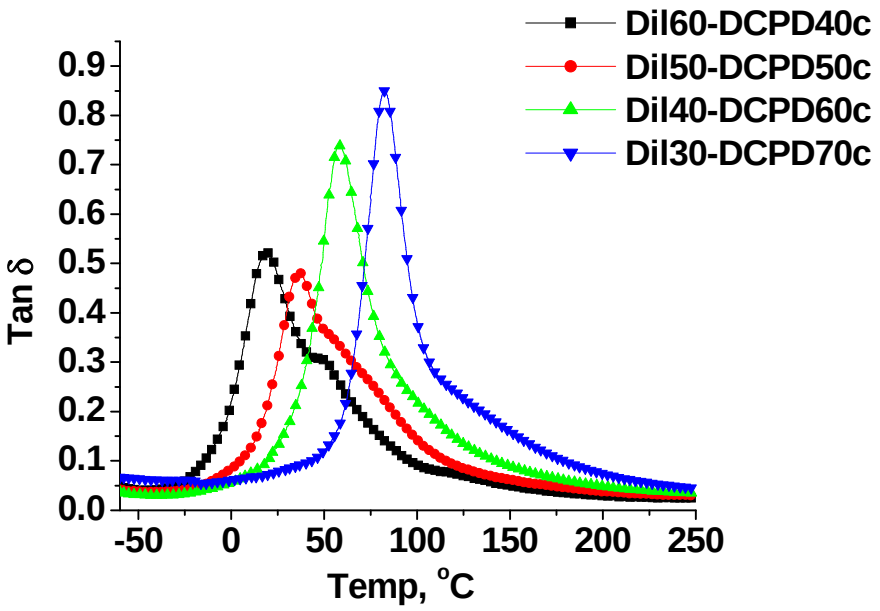

Figure 6. Tan δ Values for Composites with a GF Loading of Approximately 40 wt. %

going from the Dil40-DCPD60c composite to the Dil30-DCPD70c composite is so small that we attempt no explanation. The storage modulus curves for the composites (Figure 7) also go through the same dramatic decrease between 0 ºC and 75 ºC and have the same trend in the rubbery plateau as was seen with the pure resins.

Mechanical Properties of the Composites. Entries 5-8 in Table 2 show the mechanical properties of these composites with different Dilulin concentrations and a constant glass fiber content of 40 wt. %. The σ_{max} values increase from 29 MPa to 145 MPa with increasing content of DCPD as expected due to the greater content of the more rigid DCPD crosslinker incorporated into the thermoset, less oil in the backbone of the polymeric matrix, and less of the plasticizing soluble fraction – all of which result in a softer composite. With the exception of the 60 wt. % sample, *E* values increase with increasing DCPD content (680

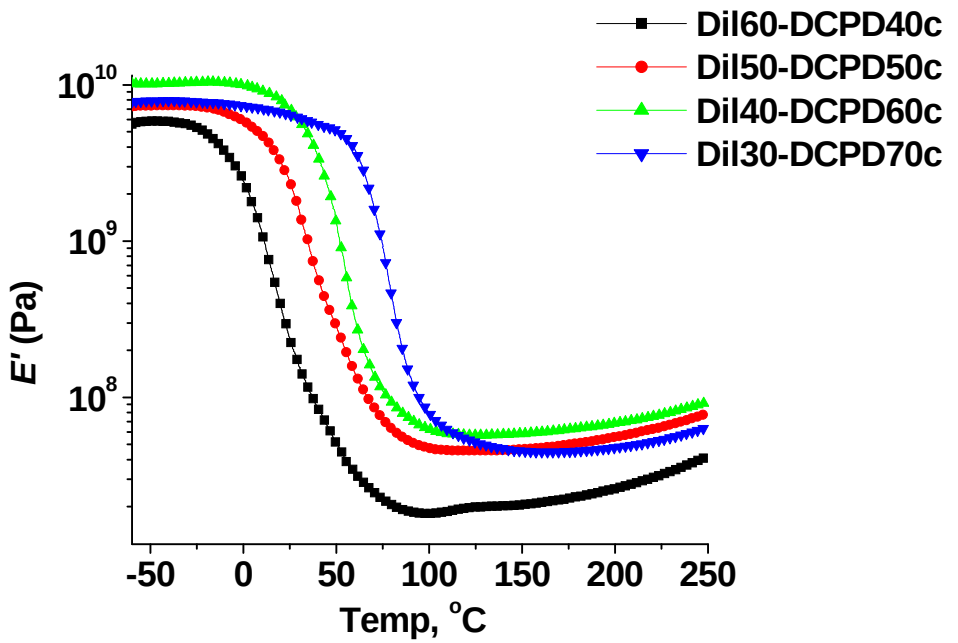

Figure 7. Storage Moduli for Composites with a GF Loading of Approximately 40 wt. %

MPa with the Dil60-DCPD40 composite to 1510 MPa with the Dil30-DCPD70 composite). The Dil60-DCPD40 composite does have a margin of error that may place it in line with the expected trend. As mentioned previously, the hard and strong Dil30-DCPD70 resin gives a higher modulus value than the softer resins with 40 wt. % or more of the oil.

There is no real trend in the ε_b values for these samples. However, they only differ by a small amount. This indicates that increasing the oil content does not impact the ε_b value when GF is used. The toughness of these samples increases from 2.7 MPa to 7.6 MPa with increasing amounts of DCPD. Again composites with more DCPD crosslinker are better at resisting fracture.

Morphology Analysis of the Composites. Figure 8 shows the SEM images for the Dil30-DCPD70c and Dil60-DCPD40c composites, which both contain approximately 40 wt. % glass fiber (GF). It is evident that the composites consist of two phases, a polymer matrix phase and a glass fiber phase. The resin appears to have penetrated between and wetted the fibers as shown with the striations (images A and D) in the resin where glass fibers were before tensile testing and fracture. However, the images show a weak adhesion between the polymer matrix and glass fibers, as evidenced by the absence of resin on the clean surface of the glass fibers. Image A (Dil30-DCPD70c) has many small broken fiber fragments scattered about on the fracture surface. This points to the greater degree of crosslinking with this resin, which may prevent the fiber from pulling out of the polymer matrix causing the fiber to break apart. There are little to none of these broken fragments present when the resin is less crosslinked (Dil60-DCPD40c), as shown in image D. Images C and F are cut away views of the composite. It can be seen that the polymer matrix in the less crosslinked Dil60-DCPD40c

composite (image F) has a fracture and is weaker, whereas the higher crosslinked Dil30-DCPD70c polymer matrix (image C) does not have any fracture in the matrix phase.

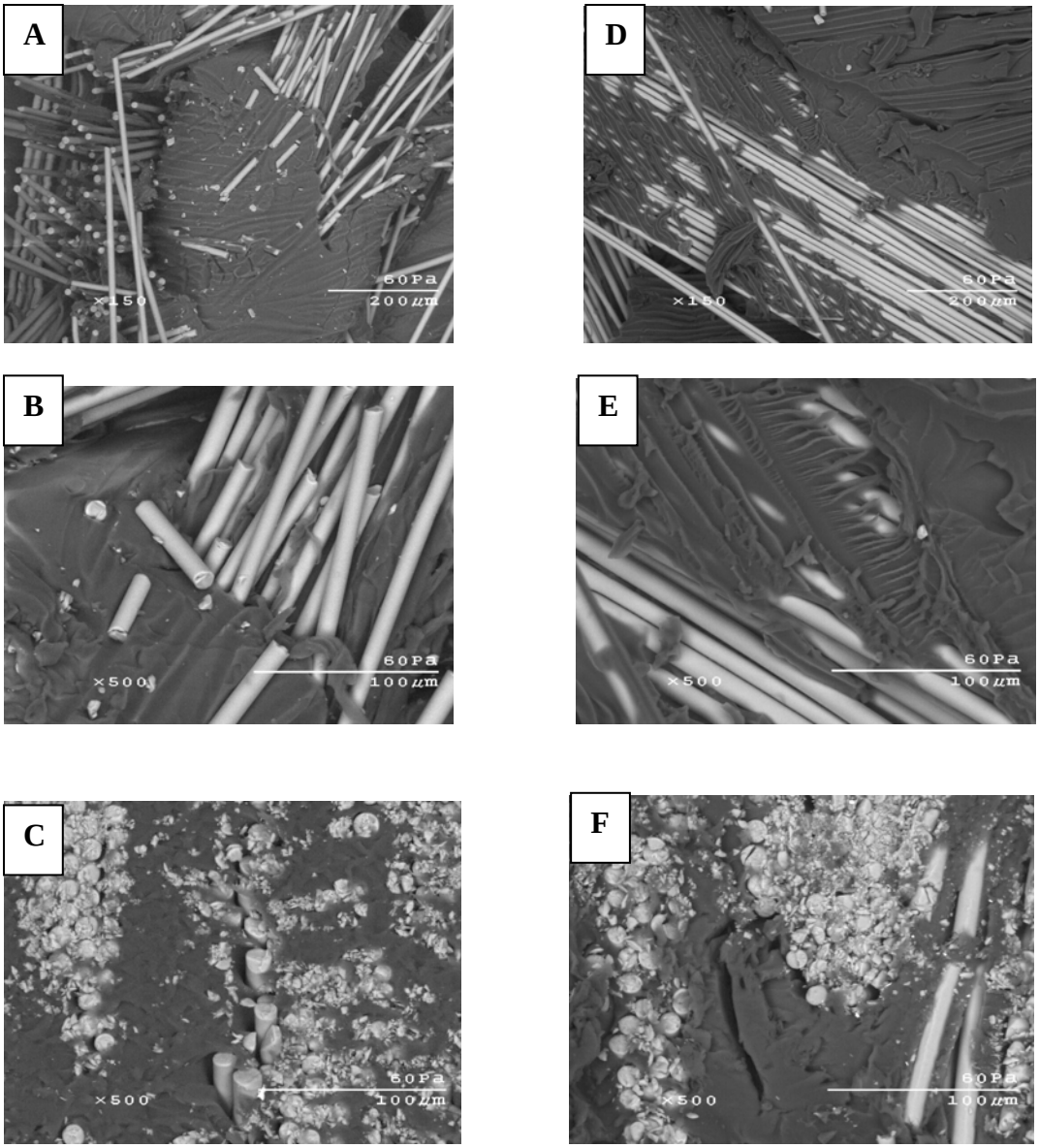

Figure 8. SEM Images of the Dil30-DCPD70c fracture surface (A, 150 x; B, 500 x) and cut surface (C, 500 x) and the Dil60-DCPD40c fracture surface (D, 150 x; E, 500 x) and cut surface (f, 500 x).

Comparison of the Thermophysical Properties for the Pure Resins and Composites. In comparing the T_g's of the resins to the composites (Table 1), it can be seen that the incorporation of GF does not increase the T_g to any significant extent for any of the resins. However, the tan δ values do decrease in value with GF incorporation. This is expected, because incorporation of GF increases the stiffness of the specimen, while at the same time reducing the concentration of the polymer matrix portion of the sample.

Incorporation of the GF creates a much more rigid and stiff sample when compared to the pure resin. The result of this is increased room temperature storage modulus values as shown in Table 1. The sample with 60 wt. % oil had about a 20 fold increase in room temperature storage modulus (10.21 MPa to 228 MPa). When looking at the rubbery plateau region at 175 °C (Figures 4 and 7), it can be seen that the storage modulus values increase by an order of magnitude for the composites, indicating that the GF reduces the deformability of the composites.[10] Generally speaking, these thermophysical properties follow what is expected when comparing composites to the corresponding resins.

Comparison of the Mechanical Properties for the Pure Resins and Composites. The incorporation of glass fiber into the resins substantially increases the σ_{max} values. In each of the different resins, incorporation of 40 wt. % glass fiber resulted in much stronger materials (28.7 to 145.2 MPa for the Dil30-DCPD70 system). Even the Dil60-DCPD40c composite, which had a rather low σ_{max} value, saw a 61 fold increase in σ_{max}. Figure 9 shows this increase in σ_{max} for the composites when compared to the resins. Figure 9 also shows the increase in σ_{max} as the DCPD concentration is increased for both the pure resins and composites.

The Young's modulus (*E*) also increases with incorporation of glass fiber. This was expected, since glass fiber imparts stiffness and rigidity to the material, resulting in such an improvement. Figure 10 shows the increase in *E* for the GF composites, when compared to

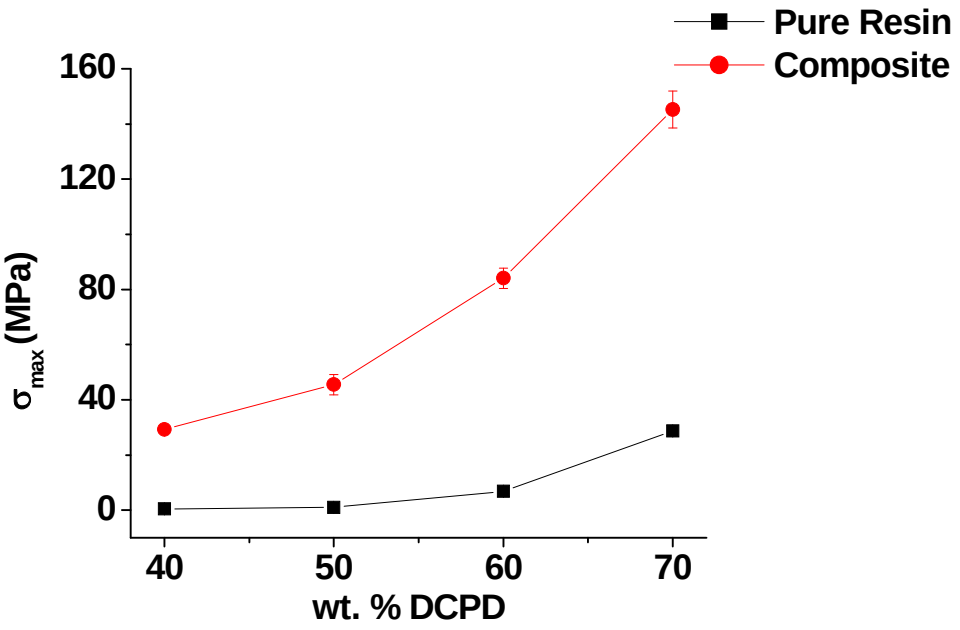

Figure 9.Tensile Strength Comparison for the Pure Resins and Composites at 40 wt. % GF

the pure resins. The effect of glass fiber incorporation on *E* is quite large for the Dil50-DCPD50c to Dil30-DCPD70c composites, and dramatic for the Dil60-DCPD40c composite, which saw a 74,625 % increase in *E*.

The percent elongation at break (ε_b) decreases with the incorporation of glass fiber (Figure 11). This was especially seen with the samples containing 40 wt. % to 60 wt. % of DCPD, where decreases in % ε_b of 147 % are seen. There is hardly any correlation between toughness and glass fiber content other than the fact that the Dil50-DCPD50c and Dil60-

DCPD40c composites seem to have their toughness improved more with the presence of glass fiber than the Dil30-DCPD70c and Dil40-DCPD60c composites. The presence of the

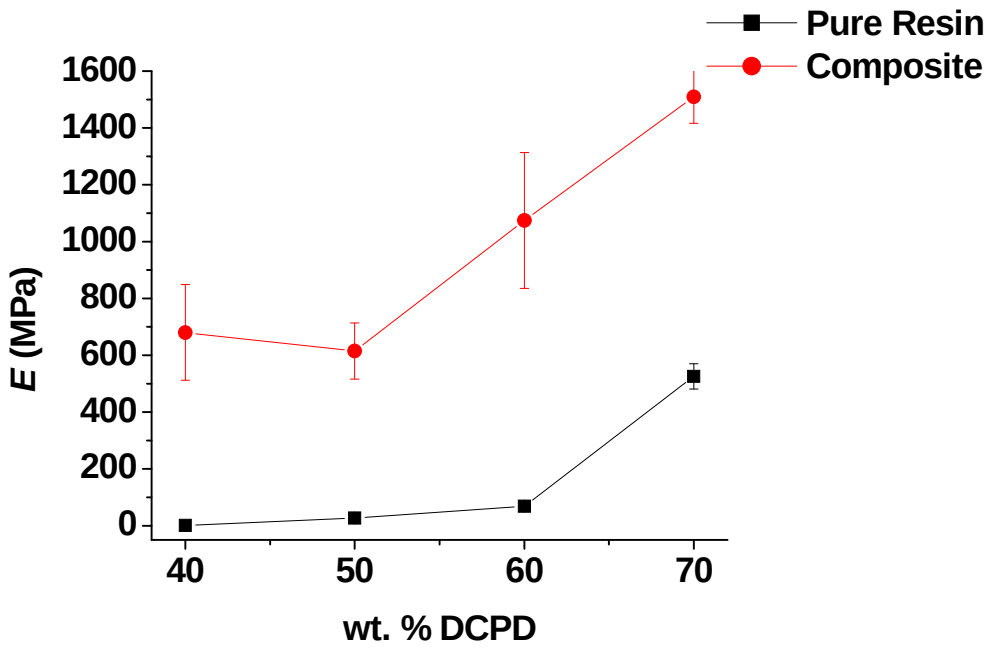

Figure 10. Young's Modulus Comparison for the Pure Resins and Composites at 40 wt. % GF

glass fiber in the Dilulin rich Dil50-DCPD50c and Dil60-DCPD40c composites helps to transfer the load from the weaker resin to the stronger GF, reducing crack propagation and ultimately fracture.[29]

Thermophysical Properties at Various Glass Fiber Loadings. It can be seen in Table 1, entries 9-11, that the GF content does not impact the T_g of the composite. However, a small decrease in the tan δ can be seen with the composite that has 56 wt. % GF, as shown in Figure 12. As the GF content is increased, less resin is incorporated in the final material and

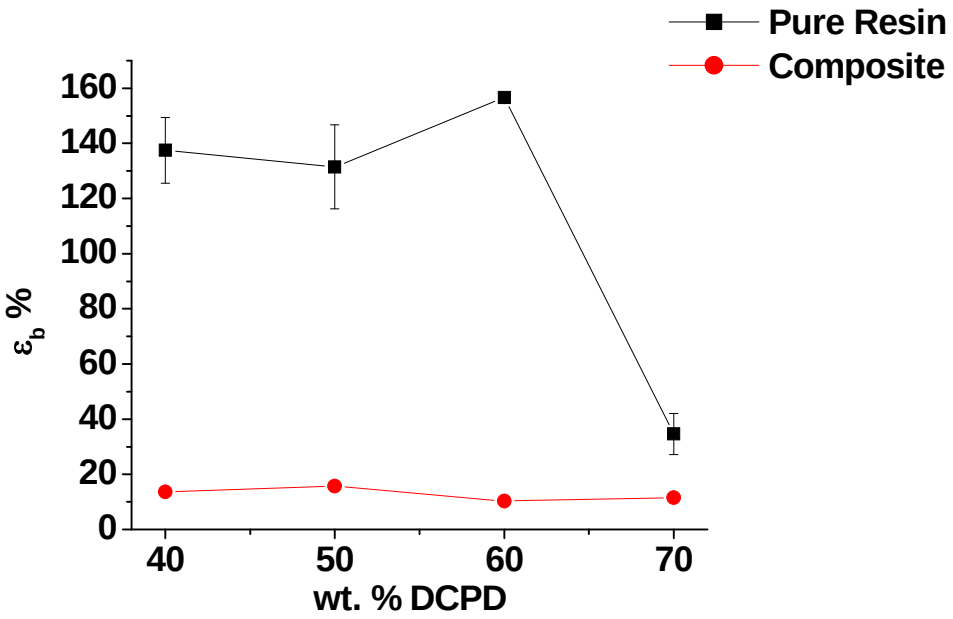

Figure 11. Percent Elongation at Break Comparison for the Pure Resins and Composites at 40 wt. % GF

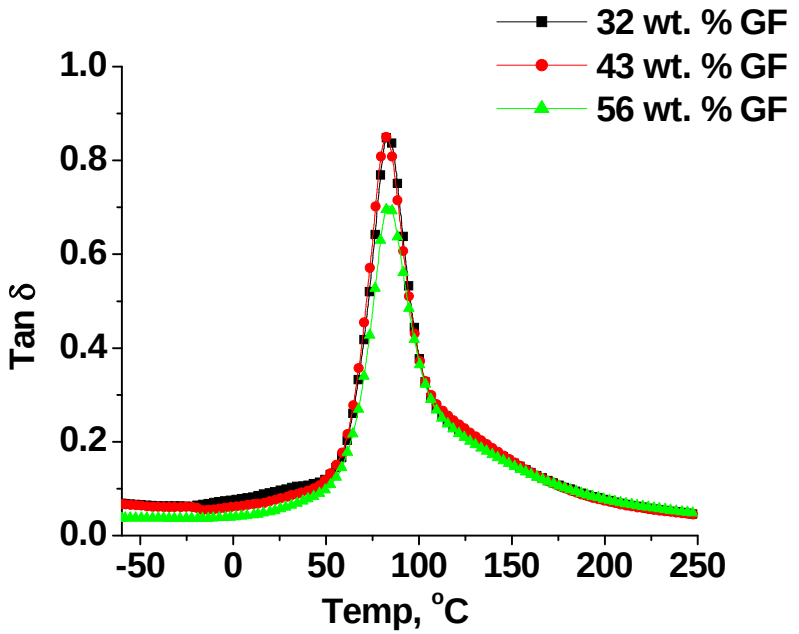

Figure 12. Tan δ Curves for Various GF Loadings

less segmental mobility results, giving the lower tan δ value. Storage modulus values at room temperature show a dependence on the GF content as shown in Table 1, entries 9-11. As the GF content is increased, so to does the storage modulus value. This points to the added rigidity that more GF adds, giving way to reduced flexibility. Figure 13 shows the storage modulus curves for various glass fiber loadings. The greater the GF loading, the greater the storage modulus in the rubbery plateau region, due to the greater stiffness of the GF.

Mechanical Properties at Various Glass Fiber Loadings. The effect of glass fiber content has been explored using the resin containing 30 wt. % oil. A low (32 wt. %), medium (43 wt. %) and high (56 wt. %) amount of glass fiber (GF) incorporation has been explored. Table 2, entries 9-11, and Figure 14 show that increasing the amount of glass fiber in the resins results in an increase in σ_{max} values, with the more resin rich 32 wt. % GF composite

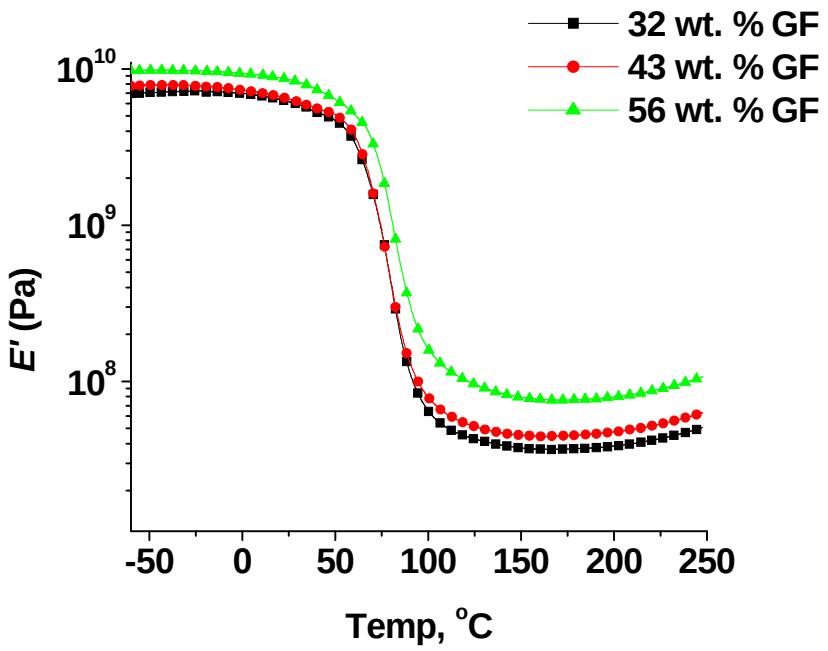

Figure 13. Storage Moduli of Composites with Various GF Loadings

having a σ_{max} value of 91.4 MPa and the 56 wt. % GF composite having a σ_{max} value of 168 MPa. The *E* values have also been examined and found to increase with increasing GF content (Table 2, entries 9-11, and Figure 15). The values of *E* are greater though when the

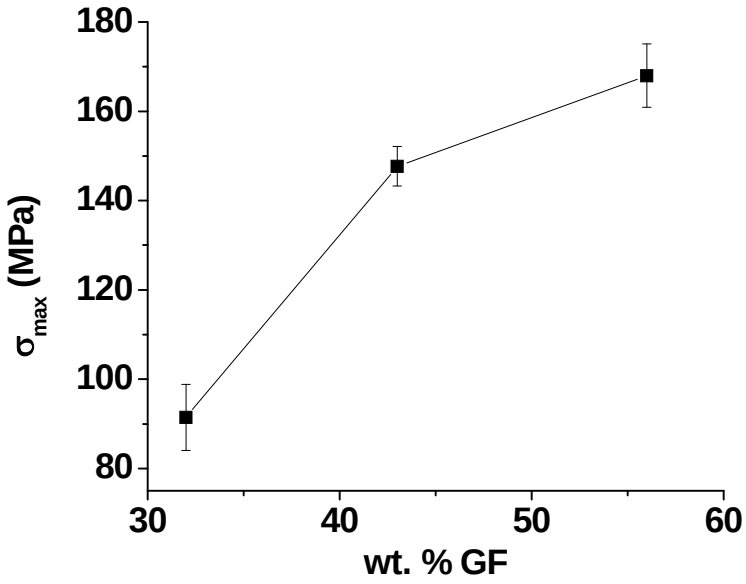

Figure 14. Tensile Strength at Various GF Loadings Using the Dil30-DCPD70 Resin

composite has 43 wt. % or more GF. When 32 wt. % GF is used, the composite is richer in resin, rather than GF, giving the lower *E* value.

Percent elongation at break (ε_b) values slightly increased from 9.5 to 12.1 % when increasing the GF content, which was unexpected. However, we view this increase as negligible and insufficient to claim that increased GF content causes increased % ε_b. Figure 16 shows how toughness, on the other hand, did increase significantly with increasing GF content (4.5 to 9.8 MPa). With more GF present, the propensity of the composite to fracture can be reduced, attributing to the increased toughness. [30]

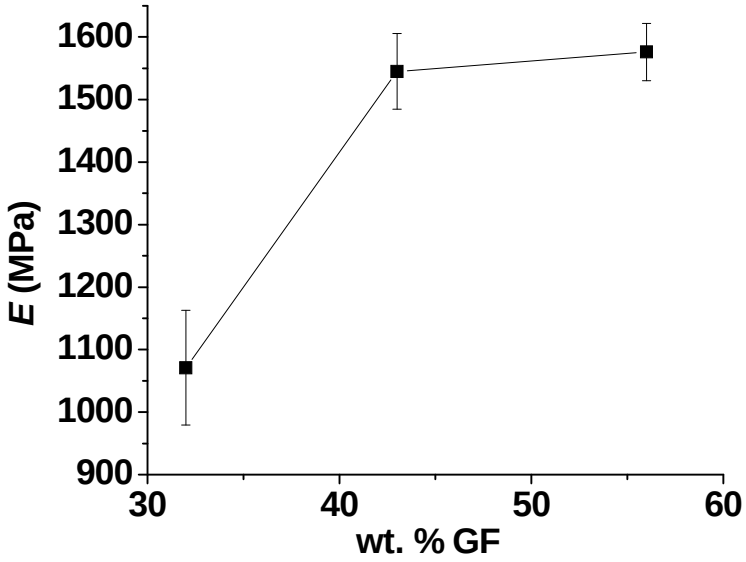

Figure 15. Young's Modulus at Various GF Loadings Using the Dil30-DCPD70 Resin

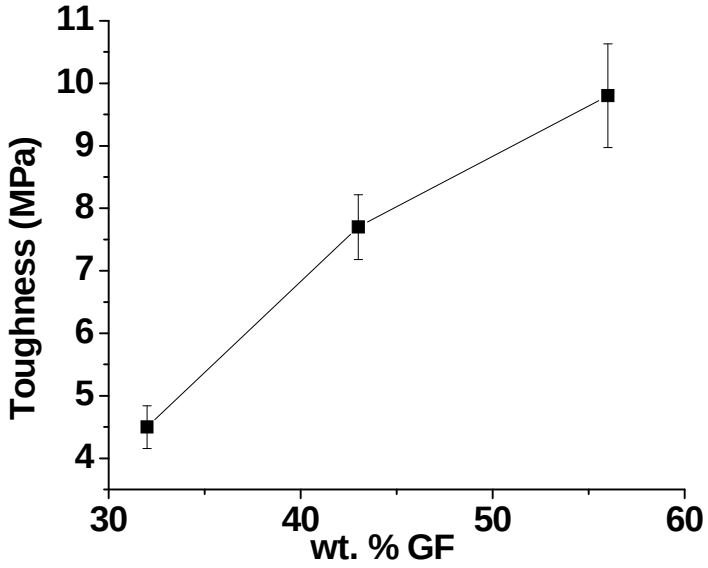

Figure 16. Toughness at Various GF Loadings Using the Dil30-DCPD70 Resin

Calculations have also been carried out to see how the moduli (from tensile testing) of the composites with varying GF content compared with different theoretical models. The upper and lower bounds are estimated using the rule of mixtures (iso-strain)[31] (equation 1) and the inverse rule of mixtures (iso-stress) (equation 2).[32]

The rule of mixtures (ROM) equation for determining the theoretical composite modulus (E_c) is

$$E_c = E_f V_f + E_m(1 - V_f) \qquad (1)$$

where E_f is the fiber modulus, E_m is the matrix modulus, and V_f is the fiber volume fraction. The inverse of the rule of mixtures (ROM) is given by the equation

$$E_c = \left[\frac{V_f}{E_f} + \frac{(1 - V_f)}{E_m}\right]^{-1} \qquad (2)$$

where E_f is the fiber modulus, E_m is the matrix modulus, and V_f is the fiber volume fraction. Both of these equations, however, represent a rather idealized situation. Therefore, the Halpin-Tsai equation (3) for randomly oriented fibers and the Cox equation (6) for non-aligned short fibers have also been plotted.[33] The Halpin-Tsai expression is given by

$$\frac{E_c}{E_m} = \frac{3}{8}\left[\frac{1 + \xi\eta_L V_f}{1 - \eta_L V_f}\right] + \frac{5}{8}\left[\frac{1 + 2\eta_T V_f}{1 - \eta_T V_f}\right] \qquad (3)$$

where ξ is $2l/D$ for the fiber

and $\eta_L = \dfrac{E_f / E_m - 1}{E_f / E_m + \xi}$ (4)

and $\eta_T = \dfrac{E_f / E_m - 1}{E_f / E_m + 2}$ (5)

The Cox equation for non-aligned fibers is given by

$$E_c = \eta_o \eta_1 E_f V_f + E_m(1 - V_f) \quad (6)$$

where $\eta_1 = 1 - \dfrac{\mathrm{Tanh}(a \cdot l / D)}{a \cdot l / D}$ (7)

and $a = \sqrt{\dfrac{-3E_m}{2E_f \ln V_f}}$ (8)

The factor η_o is an efficiency factor and has a value of 1/5 for randomly oriented fibers.

It can be seen from Figure 17 that the composites prepared in this work with different glass fiber loadings fall short of both the Halpin-Tsai and Cox models. We feel this is mainly due to the poor interaction between fiber and resin shown earlier in the SEM images in Figure 8, which results in low load transfer between fibers and much less reinforcement than predicted by the models.

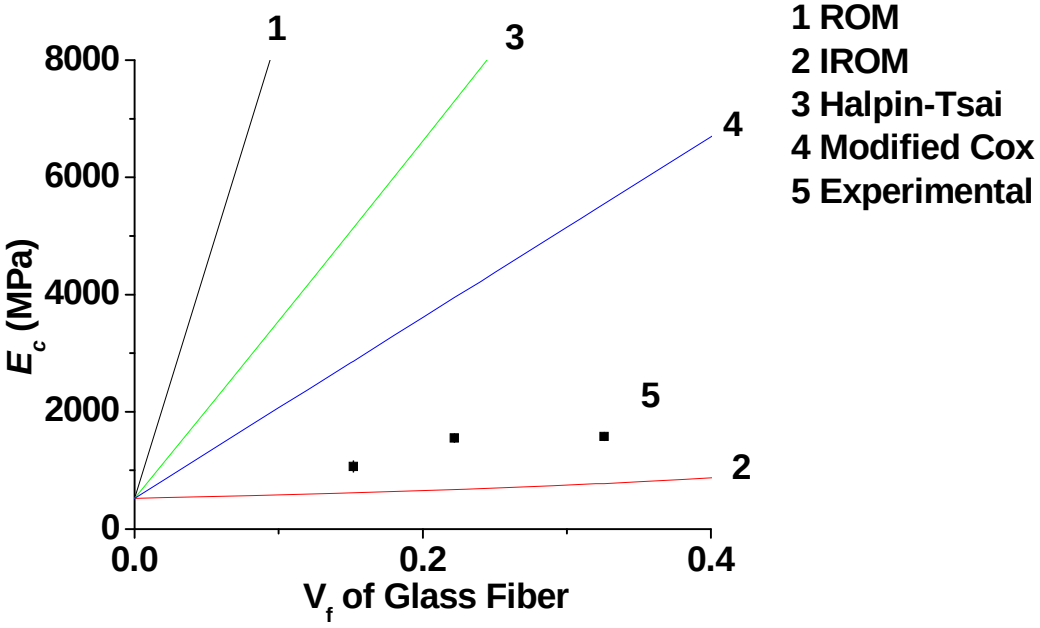

Figure 17. Theoretical Models for the Dil30-DCPD70 composites at various GF loadings

Thermogravimetric Analysis. Figure 18 shows the TGA curves for the pure resins in air. All of the curves have a similar 3 stage degradation. All of the resins are thermally stable up to 200 ºC. The first region of degradation, between 200 ºC and 400 ºC, represents degradation of the soluble materials. Hence, it can be seen that samples with less soluble fraction do not loose as much mass in this region as do samples with more soluble fraction. The second stage is between 400 ºC and 500 ºC and represents degradation of the bulk polymer, also known as T_{max}.[34] The third stage (between 500 ºC and 650 ºC) consists of a short lived plateau whose height in terms of wt. % is greater when greater amounts of DCPD are present in the thermoset. Degradation of the third stage is that of the char, which remains behind.

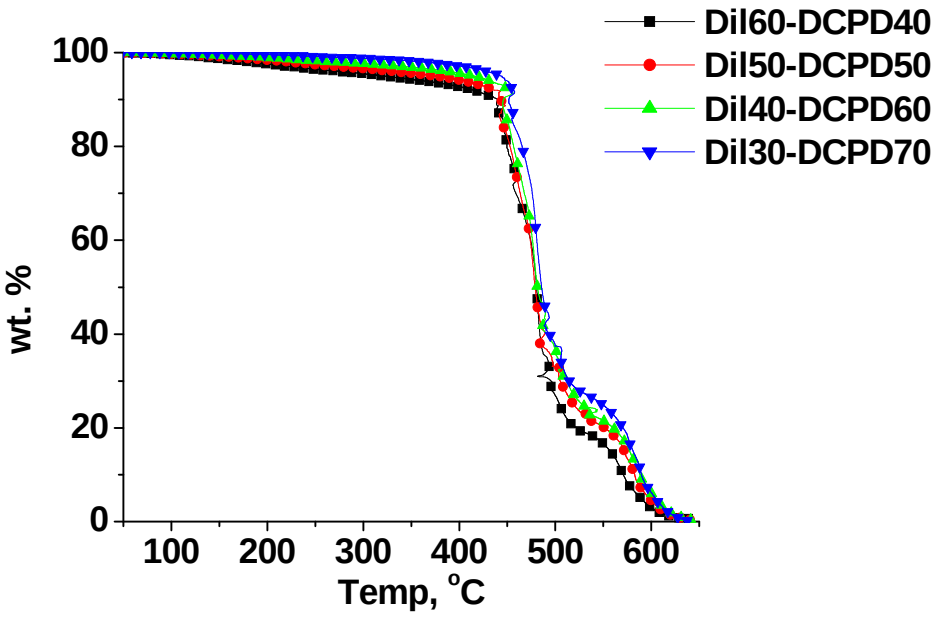

Figure 18. Thermal Degradation of the Pure Resins

Figure 19 shows that the composites with varied resin compositions also follow a similar degradation to that of the pure resins. This indicates poor adhesion between resin and glass fiber, which has been established by SEM analysis. The presence of GF does not seem to influence the degradation mechanism. The degradation curves for the composites with different GF loadings are similar to those of the composites (figure not shown).

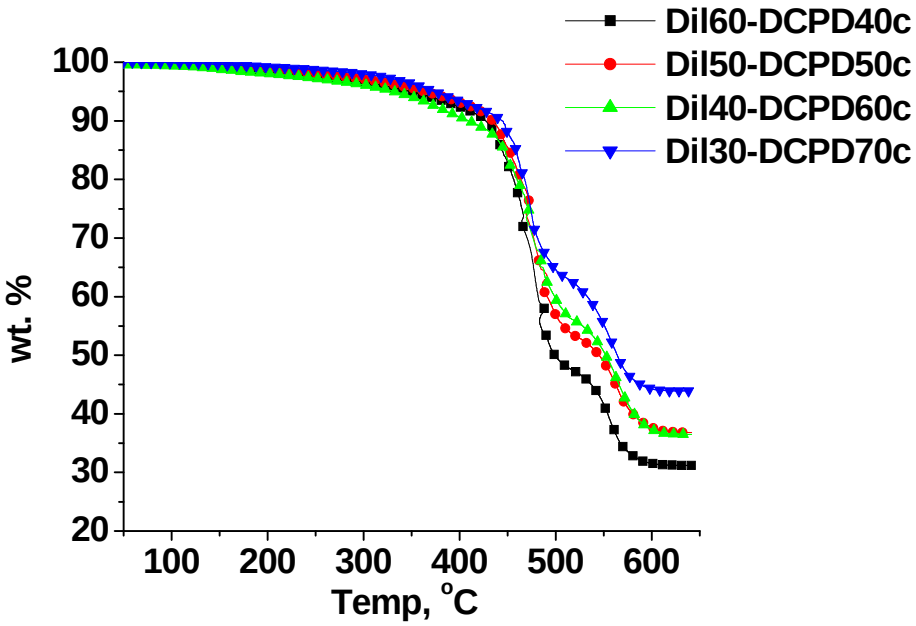

Figure 19. Thermal Degradation of the Composites with 40 wt. % GF

Conclusions

A commercially available modified vegetable oil, Dilulin, has been successfully copolymerized with DCPD in the presence of GF to make promising composites. SEM analysis of the surface morphology has revealed a weak adhesion between the fiber and the polymeric matrix. The thermophysical and mechanical properties of the resins and their corresponding composites have been compared. Both are found to increase in T_g, E', σ_{max}, E

and toughness as the DCPD content is increased. The GF content did not impact the T_g values, but did increase the E' values as shown in the room temperature values and the E' curves. The presence of 40 wt. % GF improved the mechanical properties when compared to the corresponding pure resins. As an example, the σ_{max} and E values for the Dil30-DCPD70 resin increased from 28.7 MPa to 145.5 MPa and from 525.4 MPa to 1510 MPa, respectively. The percent elongation at break (ε_b) was found to decrease in the presence of the glass fiber. Increasing the amount of GF in the Dil30-DCPD70 system from 32 wt. % to 56 wt. % resulted in σ_{max} increasing from 91.4 MPa to 168 MPa and the E value increasing from 1071 MPa to 1576 MPa. The toughness also increased with increasing GF content due to the ability of the GF to inhibit crack propagation and fracture. Thermogravimetric analysis of these resins revealed that the presence of GF did not alter the degradation mechanism of the polymeric matrix. Both the resins and the composites underwent maximum degradation (T_{max}) between 400 °C and 500 °C. Theoretical models, such as the Halpin-Tsai and Cox equations, for random short fibers further illustrate the weak interaction between resin and fiber as is illustrated with the high predicted E values. We shall examine the use of coupling agents to improve the GF/resin interaction. In addition, other glass fiber architectures will be explored with this resin system.

Acknowledgments

We would like to thank the Department of Education's GAANN fellowship for financially supporting this research and Cargill for the donation of Dilulin. We also thank Dr. Michael Kessler from the Materials Science and Engineering Department at Iowa State University for the use of his thermal analysis equipment and useful discussions. The authors also wish to thank the machine shop in the Chemistry Department at Iowa State University

for cutting the samples into the needed geometries. We would also like to thank Dr. Jay-Lin Jane from the Department of Food Science and Human Nutrition at Iowa State University for use of the Instron for mechanical testing. In addition, we thank Warren Straszheim from the Materials Science and Engineering Department at Iowa State University for performing the SEM analysis. We also extend a thank you to Craig Shore from Creative Composites for the donation of the short glass fiber mat.

References

[1] H. Uyama, M. Kuwabara, T. Tsujimoto, S. Kobayashi, *Biomacromolecules* **2003**, *4*, 211-215.

[2] "*Feedstocks for the Future: Renewables for the Production of Chemicals and Materials*", ACS Symposium Series 921; J.J. Bozell, M.K. Patel, Eds.; American Chemical Society: Washington D.C., 2006.

[3] [3a] J. Ku, R.P. Wool, *Polymer* **2005**, *46*, 71-80; [3b] M. Mosiewicki, M.I. Aranguren, J. Borrajo, *J. Appl. Polym. Sci.* **2005**, *97*, 825-836; [3c] M. Valverde, D. Andjelkovic, P.P. Kundu, R.C. Larock, *J. Appl. Polym. Sci.* **2008**, *107*, 423-430; [3d] P.H. Henna, D.D. Andjelkovic, P.P. Kundu, R.C. Larock, *J. Appl. Polym. Sci.* **2007**, *104*, 979-985.

[4] [4a] G. Lligadas, J.C. Ronda, M. Galià, V. Cadiz, *Biomacromolecules* **2007**, *8*, 686-692; [4b] Z. S Petrović, W. Zhang, A. Zlatanić, C. C. Lava, M. Ilavský, *J. Polym. Environ.* **2002**, *10*, 5-12.

[5] [5a] F. Li, R.C. Larock, *J. Appl. Polym. Sci.* **2001**, *80*, 658-670; [5b] F. Li, M.V. Hanson, R.C. Larock, *Polymer* **2002**, *42*, 156-1579; [5c] D.D. Andjelkovic, R.C. Larock, *Biomacromolecules* **2006**, *7*, 927-936; [5d] D.D. Andjelkovic, M. Valverde,

P. Henna, F. Li, R.C. Larock, *Polymer* **2005**, *46*, 9674-9685.

[6] [6a] P.H. Henna, R.C. Larock, *Macromol. Mater. Eng*. **2007**, *292*, 1201-1209; [6b] P.H. Henna, R.C. Larock, manuscript in preparation.

[7] N. Shahid, R.G. Willate, A.R. Barron, *Compos. Sci. Technol*. **2005**, *65*, 2250-2258.

[8] J. Nickel, U. Riedel, *Materials Today* **2003**, *6*, 44-48.

[9] S.N. Khot, J.J. LaScala, E. Can, S.S. Morye, G.I. Williams, G.R. Palmese, S.H. Kusefoglu, R.P. Wool, *J. Appl. Polym. Sci.* **2001**, *82*, 703-723.

[10] Y. Lu, R.C. Larock, *Macromol. Mater. Eng.* **2007**, *292*, 1085-1094.

[11] Y. Lu, R.C. Larock, *J. Appl. Polym. Sci.* **2006**, *102*, 3345-3353.

[12] Y. Lu, R.C. Larock, *Biomacromolecules* **2006**, *7*, 2692-2700.

[13] Y. Lu, R.C. Larock, *Macromol. Mater. Eng.* **2007**, *292*, 863-872.

[14] D.P. Pfister, J.R. Baker, P.H. Henna, Y. Lu, R.C. Larock, *J. Appl. Polym. Sci.* **2008**, *108*, 3618-3625.

[15] S. Husić, I. Javni, Z.S. Petrović, *Compos. Sci. Technol.* **2005**, *65*, 19-25.

[16] [16a] J.P. Latere Dwan'Isa, A.K. Mohanty, M. Misra, L.T. Drzal, *J. Mater. Res.* **2004**, *39*, 2081-2087; [16b] J.P. Latere Dwan'Isa, A.K. Mohanty, M. Misra, L.T. Drzal, *J. Mater. Res.* **2004**, *39*, 1887-1890.

[17] W. Thielemans, R. P. Wool, *Compos: Part A*, **2004**, *35*, 327-338.

[18] A. O'Donnell, M.A. Dweib, R.P. Wool, *Compos. Sci. Technol.* **2004**, *64*, 1135-1145.

[19] D.R. Kodali, **2002** U.S. Pat 6,420,322.

[20] [20a] P.H. Henna, R.C. Larock, manuscript in preparation; [20b] T.C. Mauldin, K. Haman, X. Sheng, P. Henna, R.C. Larock, M.R. Kessler, manuscript in preparation.

[21] A.S. Jones, J.D. Rule, J.S. Moore, S.R. White, N.R. Sottos, *Chem. Mater.* **2006**, *18*, 1312-1317.

[22] A. Zlantic, Z.S. Petrovic, K. Dusek, *Biomacromolecules* **2002**, *3*, 1048-1056.

[23] A.S. Wilson, "*Plasticizers: Principles and Practice*". University Press, Cambridge 1995.

[24] S.L. Rosen, "*Fundamental Properties of Polymeric Materials*", 2nd Edition, John Wiley and Sons, New York 1993.

[25] [25a]P.J. Flory, "*Principles of Polymer Chemistry*", Cornell University Press, Ithaca 1953; [25b] I.M. Ward, "*Mechanical Properties of Solid Polymers*", Wiley Interscience, New York 1971.

[26] T.W. Pechar, G.L. Wilkes, B. Zhou, N. Luo, *J. Appl. Polym. Sci.* **2007**, *106*, 2350-2362.

[27] K.P. Menard, "*Dynamic Mechanical Analysis: A Practical Introduction*", CRC Press, Boca Raton 1999.

[28] A.M. Howatson, P.G. Lund, J.D. Todd, "*Engineering Tables and Data*", Chapman and Hall, London 1991.

[29] T. A. Osswald, G. Menges, "*Materials Science of Polymers for Engineers*", Hanser, Cincinnati 2003.

[30] A. Pegoretti, T. Ricco, *Composites: Part A* **2002**, *33*, 1539-1547.

[31] W.D. Callister, "*Materials Science and Engineering: An Introduction*", Wiley, New York 2003.

[32] W.K. Goertzen, M.R. Kessler *Compos. Part A* **2008**, *39*, 761-768.

[33] J.N. Colemant, U. Khan, W.J. Blau, Y.K. Gun'Ko *Carbon* **2006**, *44*, 1624-1652.

[34] F. Li, M.V. Hanson, R.C. Larock, *Polymer* **2001**, *42*, 1567-1579.

CHAPTER 6. GENERAL CONCLUSIONS AND OUTLOOK

This dissertation focuses on the synthesis and characterization of novel thermosetting resins derived from vegetable oils. The versatility of vegetable oils as monomers is not only seen in the properties of the different resins, varying from hard and strong to flexible and rubbery, but by the fact that they tolerate free radical and ring opening metathesis polymerization (ROMP) conditions. These vegetable oil-based materials are of considerable interest in the polymer industry. Potential applications for these vegetable oil-based materials include paneling, coatings, exterior body panels for automobiles, furniture parts and noise and vibration damping materials.

In Chapter 2, the industrially friendly free radical polymerization of conjugated linseed oil (C_{100}) with acrylonitrile (AN) and divinylbenzene (DVB) is discussed. The resulting materials are typical of a terpolymerization in that two components, C_{100} and AN, are present in larger amounts and one component (DVB) is present in a much smaller amount. By fine tuning the ratios of the monomers, materials with a range of properties can be prepared, the most promising of which contain 40 to 50 wt % oil.

Chapter 3 explores the ROMP of a functionalized castor oil with cyclooctene. The initial focus in that chapter is on the synthesis and characterization of the bicyclic castor oil (BCO). The rest of the chapter looks at catalyst optimization and characterization of the resins. These resins are transparent with a sand-like hue, possess low glass transition temperatures and are rubbery above ambient temperatures. In addition, analysis shows that the soluble fraction of these thermosets does play a role as a plasticizer.

Chapter 4 looks at the ROMP of Dilulin (Dil), a commercially available oil possessing an unsaturated bicyclic moiety, and dicyclopentadiene (DCPD). A thorough characterization determined the number and type of unsaturated bicyclic moieties per triglyceride. Themosetting Dil-DCPD copolymers range from slightly glassy in nature to flexible and rubbery and have a wide range of properties. These materials are transparent and possess a yellow color. Furthermore, preparation of a 100% vegetable oil-based resin utilizing only Dilulin, albeit mechanically quite weak, is described in this chapter. The advantage of this resin system is the use of cheap DCPD and the low catalyst loading.

The focus of Chapter 5 is applying the resin chemistry developed and optimized in Chapter 4 to make glass fiber composites. Variations in the DCPD crosslinker concentration at constant glass fiber (GF) loading and the GF loading at constant DCPD crosslinker concentration are explored. The incorporation of GF improves the mechanical properties when compared to the pure resins. Theoretical models calculated for these composites, however, point to weak interaction between the fiber and the resin. Gelation times for these composites are found to be on the order of 10 minutes.

The area of biobased materials is growing and looks to have a promising future in the commercial sector. The free radical and ROMP methodologies presented in this dissertation provide effective routes to produce biobased polymeric materials. However, current issues associated with these methodologies need to be addressed in order for their implementation on a commercial scale. For the free radical polymerization of vegetable oils, cure times need to be drastically reduced to even be considered viable for commercial applications. The gelation time of this system is on the order of hours, rather than the seconds or minutes desirable for industry. One possibility to reduce the gel time is to carry out solution

polymerization of the vegetable oil and other monomers to a certain conversion. After removal of solvent, the biobased prepolymer could be combined with additional monomer and initiator, and then polymerized in bulk. The higher molecular weight prepolymer with a presumably greater viscosity should help to lower gel time and ultimately the cure time, making this methodology more appealing to industry. In addition to this, another issue that plagues these thermosets is the use of acrylonitrile. This monomer has serious health affects that raise concerns, so reducing or eliminating this monomer all together will minimize the undesirable health effects associated with using it. Acrylonitrile also shrinks substantially when polymerized, causing unwanted cracking in the resin. This problem occurs with the C_{100}Lin thermosets. The use of other comonomers that do not shrink as much could be explored to see if they produce desirable materials that will not crack during production.

The ROMP of vegetable oils also has some avenues that need to be explored further. Cure times, although much shorter than for the free radical resins, still need to be shortened, as do the gel times. This may best be solved by a more thorough study of the cure sequences used. Another promising area of study is the use of other catalyst systems. The Grubbs 1st and 2nd generation catalysts, although quite versatile and robust, are expensive. Tungsten catalysts that are cheaper, yet appear to be just as versatile, robust and stable as the Grubbs catalysts, need to be looked into. Various other cyclic strained unsaturated monomers, such as cyclooctadiene, norbornadiene, or more elaborate crosslinkers, need to be explored as well. The high soluble fraction with the Dilulin resins needs to be addressed. Reducing this may lie in optimization of the cure sequence that was touched upon previously. Another key issue is oxidation of the resulting ROMP materials. Since the cured ROMP resins still possess regions of unsaturation after ring opening that are vulnerable to oxidation, it will be

necessary to look into employing additives with these resins before cure that will inhibit such oxidation. As for the composite materials, the use of coupling agents to improve fiber and resin interaction needs to be explored. Also other types of fibers, such as continuous glass fiber or natural flax fiber, should be examined. Agricultural by-products, such as DDGS, spent germ, and corn stover, are other types of fillers that should be studied in ROMP-based composite materials.

ACKNOWLEDGEMENTS

I would like to thank Dr. Richard C. Larock for his support, and for allowing me the privilege of carrying out research in his group. He is truly a great professor and a genuinely nice person. I also want to thank my committee for their guidance throughout the years. Dr. Verkade taught a great special topics class on industrial chemistry that was insightful. Dr. Zhao dutifully led fellow students and me through a challenging, but worthwhile course in physical organic chemistry. Dr. Mallapragada was very generous in letting our group use her thermal analysis equipment throughout the years, making much of our research possible. Dr. Schmidt-Rohr also provided insight and made time whenever I needed him.

I also need to thank all of my fellow labmates throughout the years. In particular Dr. Dejan Andjelkovic, Dr. Yongshang Lu, Marlen Valverde, Dan Pfister, Rafael Quirino, and Ying Xia for their insight and support. I especially want to extend an additional thanks to Dr. Yongshang Lu who provided excellent guidance through challenges in my research, and to Dr. Dejan Andjelkovic who helped me get started in this area of research.

In addition, I want to thank my parents for all that they have provided me with. I appreciate everything that they have done. I also want to thank Kristine for her unending support and sacrifices throughout the years.